



THE HONG KONG
POLYTECHNIC UNIVERSITY

香港理工大學

Pao Yue-kong Library
包玉剛圖書館

Copyright Undertaking

This thesis is protected by copyright, with all rights reserved.

By reading and using the thesis, the reader understands and agrees to the following terms:

1. The reader will abide by the rules and legal ordinances governing copyright regarding the use of the thesis.
2. The reader will use the thesis for the purpose of research or private study only and not for distribution or further reproduction or any other purpose.
3. The reader agrees to indemnify and hold the University harmless from and against any loss, damage, cost, liability or expenses arising from copyright infringement or unauthorized usage.

If you have reasons to believe that any materials in this thesis are deemed not suitable to be distributed in this form, or a copyright owner having difficulty with the material being included in our database, please contact lbsys@polyu.edu.hk providing details. The Library will look into your claim and consider taking remedial action upon receipt of the written requests.

**Development of Microplate-Based Biosensors for
High-Throughput Measurements**

A Thesis

forward to

Department of Applied Biology and Chemical Technology

in

Partial Fulfillment of the Requirements

for

the Degree of Doctor of Philosophy

at

The Hong Kong Polytechnic University

by

PANG Hei Leung

March, 2006



Pao Yue-kong Library
PolyU · Hong Kong

Declaration

I hereby declare that this thesis is my own work and that, to the best of my knowledge and belief, it reproduces no material previously published or written, nor material that has been accepted for the award of any other degree or diploma, except where due acknowledgement has been made in the text.

PANG Hei Leung

March, 2006

Acknowledgments

I would like to sincerely thank my supervisors Dr. C. H. Yeung and Prof. K. Y. Wong for their supervision, guidance, encouragement, valuable advice and discussion throughout the course of my work, and for their valuable comments on the draft of this thesis. Their novel ideas and devoted attitude in research have made my study a rewarding experience. Prof. K. Y. Wong is gratefully acknowledged for arranging my study leave at McGill University in 2005. In addition, I am also grateful to Dr. Larry M. C. Chow for his support in yeast studies and many fruitful discussions.

I would also like to thank all my postgraduate colleagues, Dr. N. Y. Kwok, Dr. C. M. Chan, Dr. P. Guo, Dr. K. C. Cheung, Dr. K. C. Chan, Dr. K. P. Ho, Dr. W. L. Wong, Mr. C. Y. Tang, Mr. K. M. Lam and Mr. W. H. Chung for their suggestions, encouragement and generous help.

I am also greatly indebted to my family and friends for their support and encouragement throughout my entire study. The technical staff of the Department of Applied Biology and Chemical Technology are thanked for their technical

assistance.

Last, but not least, I would like to acknowledge the Research Committee of the Hong Kong Polytechnic University for the award of a research studentship and a tuition scholarship in 2001-2006 and for the traveling grant supporting my conference presentation in the 228th ACS National Meeting held in Philadelphia in August, 2004.

Abstract of thesis entitled “Development of Microplate-Based Biosensors for High-Throughput Measurements”

Submitted by PANG Hei Leung

for the Degree of Doctor of Philosophy

at The Hong Kong Polytechnic University

in March, 2006.

Abstract

Nowadays, the increasing number of samples in environmental analysis, biomedical studies and drug screening requires the chemists to analyse a large number of samples within a short time without raising the cost of analysis of each sample. The standard microtiter plate (or microplate) is a 96-well container with small operating volume (total volume: 360µl for each well) and the flat clear bottom is suitable for optical measurement. The microtiter plate is a convenient platform to be modified as high-throughput biosensors for small sample analysis. In this project, microplate-based biosensors for dissolved oxygen measurement, toxicity tests, biochemical oxygen demand (BOD) determination and carbohydrate-protein interaction studies have been developed.

ORMOSIL (organically modified silicate) optical oxygen sensors on microtiter plates have been developed via a simple, convenient and low-cost method. The ORMOSIL high-throughput oxygen sensors prepared from tetramethoxysilane (TMOS) and dimethoxy dimethylsilane (DiMe-DMOS) with tris(4,7-diphenyl-1,10-phenanthroline)ruthenium(II), $[\text{Ru}(\text{dpp})_3]^{2+}$, as the sensing dye were coated onto the well bottom surface of a 96-well polystyrene microtiter plate to

give a high-throughput system for dissolved oxygen measurement. The ORMOSIL high-throughput oxygen sensors adhere on the well bottom surface strongly and give linear Stern-Volmer calibration plots with high sensitivity and long term stability.

The applicability of this ORMOSIL high-throughput oxygen sensor platform for cell-based toxicity assays has been studied. The toxicity of two antimalarial drugs chloroquine and quinacrine on a yeast model (*Saccharomyces cerevisiae*) for studying drug resistance was evaluated by measuring their effect on the respiration rate (dissolved oxygen consumption rate) of yeasts which was monitored by the ORMOSIL oxygen sensor. The IC₅₀ values (concentration of a drug that exhibits 50% respiration inhibition) of the drugs obtained by ORMOSIL oxygen sensor were found to be in good agreement with those determined by conventional optical density (OD₅₉₅) method.

In addition, ORMOSIL high-throughput oxygen sensors in combination with aerobic assimilatory microorganisms can also serve as biosensors for BOD determination. The BOD biosensor was constructed by coating a microbial film on top of the ORMOSIL oxygen sensing film. The microbial film was fabricated by immobilizing a bacterial species, *Stenotrophomonas maltophilia*, in

sol-gel-poly(vinyl alcohol) matrix. The results obtained with the BOD biosensor were in agreement with those of the conventional BOD₅ method for different wastewater samples.

A simple, convenient, low-cost and high-throughput microplate-based carbohydrate sensor has been constructed for carbohydrate-protein interaction study. The high-throughput carbohydrate sensor was constructed by covalent immobilization of aminated carbohydrate onto TESPI-ORMOSIL film (TESPI = 3-(triethoxysilyl)propyl isocyanate) on a microtiter plate. The TESPI-ORMOSIL film was prepared by coating a layer of 3-(triethoxysilyl)propyl isocyanate (TESPI) onto a transparent ORMOSIL film. The application of the high-throughput carbohydrate sensors in studying carbohydrate-protein interaction has been demonstrated by the well established carbohydrate-lectin system. The results show that this microplate-based carbohydrate microarray sensor is practical for high-throughput analysis of carbohydrate-protein interactions.

List of Abbreviation

Anti-ConA	Anti- <i>Concanavalin A</i> (i.e. antibody)
BOD	Biochemical oxygen demand
bpy	2,2'-bipyridyl
BSA	Bovine serum albumin
ConA	<i>Concanavalin A</i>
CQ	Chloroquine
DiMe-DMOS	Dimethoxy dimethylsilane
DO	Dissolved oxygen
dpp	4,7-diphenyl-1,10-phenanthroline
EC	<i>Erythrina cristagalli</i>
FITC-ConA	Fluorescein-labeled <i>Concanavalin A</i>
FITC-EC	Fluorescein-labeled <i>Erythrina cristagalli</i>
GGA	Glucose-glutamic acid
I	Luminescence intensities in the presence of oxygen
I (%)	Percentage inhibition
I ₀	Luminescence intensities in the absence of oxygen

I_0/I_{100}	Quenching ratio
IC_{50}	Drug concentration which produced 50% inhibition of growth rate or lectin binding
K_{SV}	Stern-Volmer constant
LED	Light emitting diode
MTMS	Methyltrimethoxysilane
OD	Optical density
OECD	Organization for Economic Co-operation and Development
ORMOSIL	Organically modified silicate
PBS	Phosphate buffered saline
PVA	Polyvinyl alcohol
Q_{DO}	Quenching response
QNC	Quinacrine
TESPI	3-(triethoxysilyl)propyl isocyanate
TMOS	Tetramethyl orthosilicate (or tetramethoxysilane)

Table of Content

Declaration	ii
Acknowledgements	iii
Abstract	vi
List of Abbreviation	ix
Table of Content	xi
Chapter 1 Introduction	1
1.1 Background	2
1.2 High-Throughput Luminescence-Based Oxygen Sensors	5
1.2.1 Luminescence-based oxygen sensors	6
1.2.2 Solid supports for optical oxygen sensors fabrication	13
1.2.3 Sol-gel-based optical oxygen sensors	19
1.2.4 High-throughput oxygen sensors	23
1.3 Biosensors Based on Optical Sensing of Oxygen	26
1.3.1 Biochemical oxygen demand (BOD) biosensors	28
1.3.2 Applications of microplates with optical oxygen sensors	32
1.4 High-Throughput Luminescence-Based Biosensors for Studying	35

Carbohydrate-Protein Interaction	
1.4.1	Carbohydrate-lectin interactions 35
1.4.2	Recent development on high-throughput carbohydrate sensors 40
	for carbohydrate-protein interaction studies
1.5	Aims and Objectives of this Project 55
Chapter 2	Fabrication and Evaluation of 58
	[Ru(dpp)₃]²⁺-Entrapped Organically Modified
	Silicate (ORMOSIL) Oxygen Sensing Films on
	Polystyrene Microtiter Plate
2.1	Introduction 59
2.2	Experimental Section 62
2.3	Results and Discussion 68
2.3.1	Optimization of the oxygen sensing film 68
2.3.2	Stern-Volmer plots 84
2.3.3	Leaching of ruthenium complex from ORMOSIL films 89
2.3.4	Stability of the ORMOSIL films 92
2.4	Concluding Remarks 96

Chapter 3	Application of the $[\text{Ru}(\text{dpp})_3]^{2+}$-Entrapped Organically Modified Silicate (ORMOSIL) Oxygen Sensing Films on Microtiter Plate for IC_{50} Determination of Drugs on a Heterologous Yeast Model	97
3.1	Introduction	98
3.2	Experimental Section	100
3.3	Results and Discussion	109
3.3.1	Determination of IC_{50} values of antimalarial drugs by measurement of dissolved oxygen concentration	109
3.3.2	Comparison of IC_{50} values determined by optical oxygen sensors and conventional optical density (OD_{595}) method	126
3.4	Concluding Remarks	130
Chapter 4	A High-Throughput Biosensor Based on $[\text{Ru}(\text{dpp})_3]^{2+}$-Entrapped Organically Modified Silicate (ORMOSIL) Oxygen Sensing Films on Microtiter Plate for Multi-Sample Determination of Biochemical Oxygen Demand (BOD)	131

4.1	Introduction	132
4.2	Experimental Section	134
4.3	Results and Discussion	141
4.3.1	Optimization of microbial film	141
4.3.2	Calibration of BOD biosensor	143
4.3.3	Effects of pH and temperature	148
4.3.4	Influence of heavy metal ions on BOD	151
4.3.5	Comparison of BOD values obtained by BOD biosensor and BOD ₅ method	153
4.3.6	Stability and service life	156
4.4	Concluding Remarks	158
Chapter 5	Organically Modified Silicate (ORMOSIL) Films on Microtiter Plate for the Construction of Carbohydrate Microarrays	159
5.1	Introduction	160
5.2	Experimental Section	162
5.3	Results and Discussion	172
5.3.1	Carbohydrate-lectin interactions	172

5.3.1.1	Lectin-binding patterns	172
5.3.1.2	The effect of carbohydrate concentration used in immobilization on lectin-binding	176
5.3.2	Inhibition on carbohydrate-lectin binding	178
5.4	Concluding Remarks	181
Chapter 6	Conclusions	182
References		188

Chapter 1

Introduction

1.1 Background

The increasing number of samples in environmental analysis, biomolecular studies and drug screening requires chemists / biologists to analyse a large number of samples within a short period of time without raising the cost of analysis of each sample. With the ever increasing number of samples and the limited availability of cells and expensive biochemicals, there is a need to develop economic, time-saving and fully automated equipment with highly sensitive detection devices (high-throughput systems) for multi-sample analyses with small sample volumes. In these high-throughput systems, multiple parameters such as oxygen concentration, pH, etc. are often required to be determined at the same time within the same device. These high-throughput systems serve the purpose of screening hundreds to thousands of potential drug candidates against a biological target within a short period of time in the pharmaceutical industry. In high-throughput screening, microtiter plate is the most simple and convenient device. The first microtiter plate was introduced by Gyula Takatsy in 1955 which marked the beginning of miniaturization of sample handling [1]. A microtiter plate is often made of plastic (mostly polystyrene) which contains up to 1536 sample wells for multi-sample analysis. Commercially available microtiter plates have 6, 24, 96, 384 or 1536 sample wells arranged in a

rectangular matrix. A 96-well microtiter plate is shown in Figure 1.1. Most of the microtiter plates have a flat clear bottom which allows optical measurement of absorbance and / or fluorescence through the well bottom. Nowadays, microplate readers are essential equipment in most biochemical or even chemical laboratories and they find their wide applications in toxicity tests, enzymatic assays, clinical assays, proteomics study and drug screening.

In this thesis, modification of microtiter plates for various high-throughput applications will be described. Specifically, microtiter plates are modified as high-throughput dissolved oxygen sensors, BOD biosensors and carbohydrate sensors. The background of each of the sensors studied in this dissertation will be discussed in the following sections.



Figure 1.1 A black 96-well microtiter plate with flat clear bottom for fluorescence measurement.

1.2 High-Throughput Luminescence-Based Oxygen Sensors

Oxygen is one of the most important gases in our living environment. It plays a key role in the biological system and ecosystem. The amount of dissolved oxygen (DO) in rivers and oceans is an indicator of water quality. The higher the DO concentration, the lower is the concentration of organic pollutants. Oxygen consumption by microorganisms and aerobic cells is an important indicator on their metabolic activity and state of growth. Monitoring and measurement of dissolved oxygen concentration in cell cultures is thus of interest for drug screening, cell cultivation, toxicity tests and environmental analysis. Conventionally, the electrochemical Clark-type electrodes [2, 3] are used for oxygen concentration determination. However, this method has several disadvantages. The Clark electrode suffers from electrical interference (electrode fouling) and requires constant supply of oxygen as the electrode consumes oxygen during measurement [4-10]. Besides, the electrode surface tends to be poisoned by contaminants such as proteins, hydrogen sulfide, halocarbon anesthetics and organic compounds [6, 10, 11]. To overcome these disadvantages, optical sensing technique for oxygen detection and monitoring have been developed since the late sixties [11-24]. Advantages of optical oxygen sensors over conventional electrochemical oxygen sensors include nil

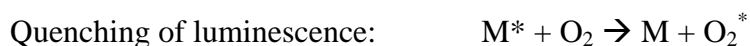
oxygen consumption, no requirement for reference, robustness, low cost and ease of miniaturization.

1.2.1 Luminescence-based oxygen sensors

The principle of optical oxygen sensing is based on the dynamic luminescence quenching of luminescent dyes by oxygen. Luminescence is a process that emits photons ($h\nu$) and can be classified as either fluorescence or phosphorescence according to the spin state of the excited state. Fluorescence is a short-lived emission from the excited singlet state (S^*) to singlet ground state (S_0) with the electrons spin paired (i.e. with no change of the multiplicity). Since this radiative relaxation (emission) is spin allowed, its decay time is short, usually about 10^{-9} to 10^{-7} s. On the other hand, the excited molecule in singlet state can change its spin multiplicity through intersystem crossing to the lowest excited triplet state (T^*). When radiative relaxation occurs from T^* to S_0 , that is phosphorescence. This transition is a forbidden transition, thus phosphorescence is a long-lived emission with decay time about 10^{-5} to 10 s. Besides, as the energy of the triplet state is less than that of the singlet state, phosphorescence occurs at longer wavelengths than fluorescence. Furthermore, lifetime of the triplet excited state is much longer than

that of the singlet excited state and they are more susceptible to interact with other molecules. Such interactions are known as quenching (i.e. deactivation of an excited state). A substance that accelerates the decay of an excited state to a lower excited or ground state is called a quencher; oxygen molecule (O_2) is an effective quencher because of its triplet ground-state nature.

The oxygen molecule has two unpaired electrons in two different π^* anti-bonding orbitals which result in a triplet ground state (T_0). It is reactive to chemical species because relatively little energy is needed to convert the oxygen molecule from the triplet ground state to the lowest excited singlet state. However, this conversion is spin forbidden through light absorption. The quenching of luminescence of the excited complex by oxygen molecule is a very effective process because it is a spin-allowed process.



Luminescence quenching can be expressed as the change in the emission intensity in the presence of different concentrations of quencher. The Stern-Volmer equation [25] relates the emission intensity and oxygen (quencher) concentration together in homogeneous systems:

$$I_0/I = 1 + K_{SV}[O_2] \quad (1.1)$$

where I_0 and I are the emission intensities in the absence of oxygen and presence of oxygen respectively, K_{SV} is the Stern-Volmer quenching constant and $[O_2]$ is the concentration of oxygen.

In the development of oxygen-sensitive dyes, polycyclic aromatic hydrocarbons (PAHs) and transition metal complexes are most commonly used. In the early 1930's, Kautsky et al. reported that the luminescence of organic dyes such as tryptaflavine, benzoflavine, euchrysin 3R, rheonine 3A, rhoduline yellow, safranin, chlorophyll and hematoporphyrin were quenched by oxygen [26, 27]. After that, Bergman constructed the first prototype device for oxygen monitoring using polycyclic aromatic hydrocarbons (PAHs) fluoranthene as sensing dye in 1968 [12]. Then a variety of PAHs such as pyrenebutyric acid (PBA) [28], perylene dibutyrate [14], decacyclene, 1,12-benzoperylene, diphenylanthracene [29], pyrene [13] and pyrene derivatives [30] were tested as sensing materials. A fiber optic probe for *in vivo* measurement of oxygen partial pressure by adsorbing perylene dibutyrate on amberlite resin beads was described by Peterson et al. in 1984 [14].

Even though strong quenching by oxygen was observed in PAHs, they exhibit absorbance maximum in the ultraviolet region with small Stoke's shift. They are also relatively photochemically unstable and suffer interference from water and halocarbon anesthetics [14, 31, 32]. As a result, the light source and instrumentation are relatively expensive.

Apart from PAHs, oxygen-sensitive luminescent transition metal complexes have become more popular for optical oxygen sensors. They are attractive for oxygen sensing because of their high luminescent quantum yield, long excited-state lifetime, large Stoke's shift, strong absorption in the visible (blue-green) region and high thermostability and photostability. In this way, a low cost light source such as blue light-emitting diode (LED) and a simple cut-off filter can be used. Among various luminescent metal complexes, platinum(II) dyes, palladium(II) dyes and ruthenium(II) diimine complexes have received the most attention for oxygen sensing [33, 34].

A number of platinum and palladium dyes have been used in oxygen sensing, these include the platinum dimer tetrakis(pyrophosphito) diplatinate(II) $[\text{Pt}_2(\text{pop})_4]^{4-}$ (pop = $\text{P}_2\text{O}_5\text{H}_2^{2-}$) [35, 36], dicyanoplatinium(II) complexes $[\text{Pt}(\text{dpp})(\text{CN})_2]$ and

[Pt(dtbp)(CN)₂] (dpp = 4,7-diphenyl-1-10-phenanthroline, dtbp = 4,4'-di-*tert*-butyl-2,2'-bipyridine) [37] and platinum / palladium porphyrins. Among them, platinum and palladium porphyrins were found to have very characteristic strong long-wave phosphorescence with visible light excitation at room temperature and long excited-state lifetimes (sub-millisecond). They included platinum or palladium porphyrins of octaethylporphyrin (OEP), tetra(pentafluorophenyl)porphyrin (TFPP), octaethylporphine ketone (OEPK), *meso*-tetraphenylporphyrin (TPP), *meso*-tetra(2,6-dichlorophenyl)porphyrin (TDCPP), *meso*-tetra[3,5-bis(trifluoromethyl)phenyl]porphyrin (TFMPP), *meso*-tetramesityl- β -octabromoporphyrin (Br₈TMP), tetrabenzporphyrin (TBP), *meso*-tetrakis(4-*N*-methylpyridyl) porphyrin (TMPyP) and *meso*-tetrakis(4-*N,N,N*-trimethylaminophenyl) porphyrin (TTMAPP) and Pd-*meso*-tetra-(4-carboxyphenyl)-porphyrin (Pd-TCPP) [21, 23, 38-49]. The best known example is an oxygen-sensitive paint for continuous mapping of aerodynamic pressure on aircrafts using Pt(OEP) developed by Kavandi et al. [39]. However, most common platinum porphyrins such as Pt(OEP) degrade after extended exposure to UV light [50]. To overcome this problem, researchers have spent much effort in the development of new phosphorescent platinum porphyrins. Wong and co-workers reported that platinum porphyrins with halogen substituents on the

porphyrin macrocycles are more stable towards photochemical degradation [43]. New platinum complexes of octaethylporphine-ketone (Pt-OEPK) were synthesized by Papkovsky et al. and were immobilized in polystyrene as oxygen sensing probes [44]. These platinum ketone-porphyrins exhibit higher photochemical stability, quantum yield, larger Stoke's shift (compared to Pt-OEP) and better compatibility with semiconductor optoelectronics (e.g. LED) than other platinum porphyrins [44]. Koo et al. developed fluorescent nanosensors for real-time measurements of dissolved oxygen inside live cells by incorporating Pt(OEP) and Pt(OEPK) into organically modified silicate (ORMOSIL) nanoparticles [23].

Apart from platinum / palladium porphyrins, ruthenium diimine complexes are another class of attractive oxygen-sensitive dyes. Ruthenium complexes show intense visible light absorption that simplifies sensor design and expands the variety of excitation sources available. They also tend to be thermally, chemically and photochemically robust which extend the sensor service life [51]. Among various ruthenium diimine complexes, ruthenium complexes with the ligands 2,2'-bipyridyl (bpy), 1,10-phenanthroline (phen) and 4,7-diphenyl-1,10-phenanthroline (dpp) have received much attention [11, 16, 17, 19, 22, 24, 52-94]. These dyes have high quantum yields of luminescence, long excited-state lifetime, intense visible light

absorptions and high photochemical stabilities. The first fiber-optic oxygen sensor based on $[\text{Ru}(\text{bpy})_3]^{2+}$ was reported by Wolfbeis and co-workers in 1986 [52]. $[\text{Ru}(\text{bpy})_3]^{2+}$ was adsorbed on kieselgel particles and dispersed into the silicone polymer which was brought onto the surface of a glass slide or the distal end of a fiber optic. This sensor offers high sensitivity and specificity for oxygen and has favorable analytical wavelengths (excitation maximum: 460 nm, emission maximum: 610 nm).

After extensive studies of the photophysics and photochemistry of ruthenium diimine complexes immobilized in polymer films [11, 55, 56, 64, 95, 96], Demas and coworkers found that $[\text{Ru}(\text{dpp})_3]^{2+}$ is the most attractive sensing dye. It is due to its large Stoke's shift (emission well-separated from excitation; excitation maximum: 460 nm, emission maximum: 610 nm), high quantum yield (~ 0.5), long excited-state lifetime ($> 5 \mu\text{s}$) and large quenching constant. Demas and co-worker developed a thin film sensor for the determination of oxygen in both gaseous and liquid samples by immobilizing $[\text{Ru}(\text{dpp})_3]^{2+}$ in silicone rubber [11]. They applied this sensor for monitoring oxygen concentration in breathing studies. Besides, Wong and co-workers have also found that the optical characteristics of $[\text{Ru}(\text{dpp})_3]^{2+}$ depend on the concentration of ruthenium dye and the solvent used in the preparation of the

silicone rubber oxygen sensing film [17]. Recently, Demas's group have constructed a portable solid-state oxygen sensor by casting a sol-gel film containing $[\text{Ru}(\text{dpp})_3]^{2+}$ onto the surface of a blue light emitting diode (LED) for the determination of gaseous and dissolved oxygen [97]. Wolfbeis and co-workers have developed a fiber optic oxygen microsensor tip (tip diameters: 5-10 μm) for the measurement of oxygen gradients in a freshwater sediment core by casting a ORMOSIL film with $[\text{Ru}(\text{dpp})_3]^{2+}$ onto the fiber optic tip [82]. Another luminescence-based fiber optic oxygen sensor for *in situ* measurement of oxygen consumption from intact mouse hearts was described by Zhao et al. [98]. In addition, a hand-held optical sensor for dissolved oxygen measurement was developed by Choi and co-workers [99]. This hand-held oxygen sensor was fabricated by dispersing $[\text{Ru}(\text{dpp})_3]^{2+}$ absorbed silica gel particles in silicone rubber and coated onto a 580 nm long-pass filter. The $[\text{Ru}(\text{dpp})_3]^{2+}$ dye was excited by a blue LED and the emission intensity was captured by a silicon photodiode.

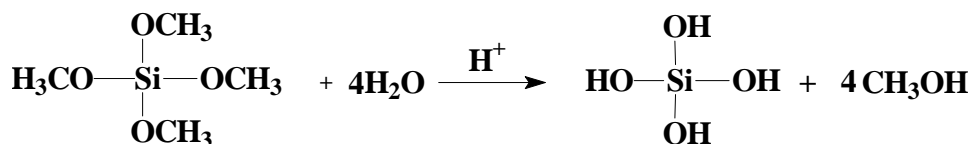
1.2.2 Solid supports for optical oxygen sensors fabrication

In order to prevent any reactions occurring between the luminescent dye and species other than oxygen in the measuring environment, luminescent dyes are

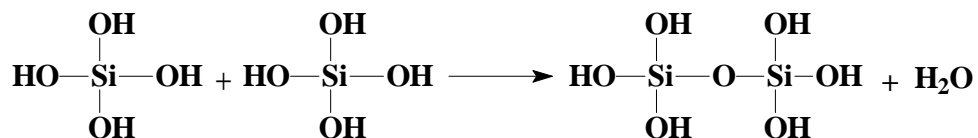
usually immobilized in an appropriate gas permeable polymeric materials, such as silicone rubber [9, 11, 17, 37, 41, 55, 67, 76, 99, 100], polystyrene [40, 45, 66, 101-103], poly(vinyl chloride) [45, 100, 104], polymethylmethacrylate [47, 104-106], ion-exchange polymers [21], fluoropolymers [91, 107-112], cellulose acetate butyrate [47, 106] and sol-gel derived materials [19, 22, 24, 46, 57, 69, 75, 82, 84, 87, 93, 94, 100, 113-122]. The gas permeable polymer matrix acts as a rigid solid support which also provides protection for the sensing dyes and discriminates the entrance of analyte molecules to the sensing film. For the choice of polymer, it is necessary to consider the structural property, stability, optical property, chemical inertness and permeability to oxygen. For example, the strong hydrophobic nature of silicone rubber can lead to solubility problems with ionic inorganic complexes such as $[\text{Ru}(\text{dpp})_3]^{2+}$ which display poor solubility in silicone rubber [67]. On the other hand, poly(vinyl chloride), polymethylmethacrylate and cellulose acetate butyrate films are usually plasticized with dioctyl phthalate or tributyl phosphate to improve oxygen permeability and response [8, 47]. However, these plasticizers can leach out from the polymers and are a potential source of contamination. Recently, interest in the application of sol-gel for sensor fabrication is increasing as sol-gel materials have distinct advantages over the aforementioned polymers. The sol-gel process is a low temperature (room temperature) process and provides materials with

high homogeneity and purity. Typical desirable properties of sol-gel materials include high surface area, tunable porosity, complete transparency from visible light to the near ultra-violet, tunable shapes, relatively low cost and good chemical, photochemical and thermal stability [19, 82, 94, 115, 123-125].

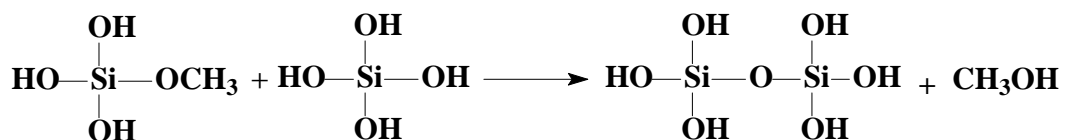
The sol-gel process is a versatile solution process for making advanced materials, including glass-like or ceramic materials and organic-inorganic hybrids. In general, the sol-gel process involves the transition of a solution system from a liquid “sol” (colloidal suspension of small particles) into a solid “gel” phase (rigid porous network) [126] and this transition includes three steps: hydrolysis, condensation and polycondensation. For the preparation of sol-gel materials, the most popular precursor is liquid silicon alkoxide such as tetramethoxysilane (TMOS). This precursor undergoes hydrolysis by mixing with water in the presence of acid catalyst. The hydrolysis reaction is shown below which results in the formation of silanol groups (Si-OH):



Next, the silanol groups of hydrolyzed TMOS will undergo condensation to give an oligomer:



and / or

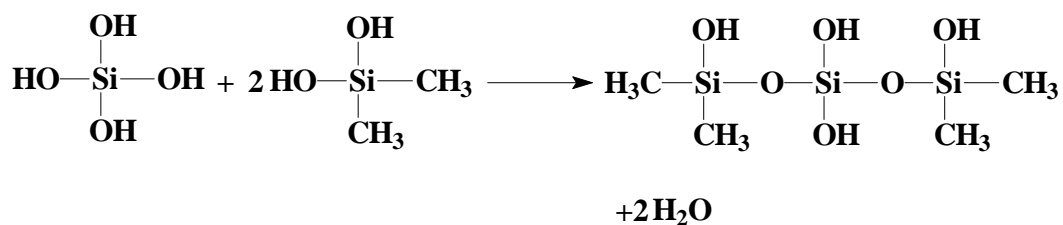


Finally, networks of Si-O-Si linkages undergo subsequent polycondensation to form a three-dimensional silica network. The sol-gel can be cast into desired forms by allowing the sol-gel solution to solidify in an appropriately shaped vessel, e.g. vial [124]. Optical oxygen sensors in forms of thin films, small particles, or fiber optics can also be made using the sol-gel method. However, the sensitivity of sol-gel oxygen sensors based on pure precursor (silicon alkoxide) is rather poor in aqueous systems due to its poor oxygen permeability [82, 122].

Therefore, another group of precursors, organically modified silicate

(ORMOSIL), was introduced which resulted in better properties than those prepared solely from TMOS. ORMOSILs are inorganic-organic hybrid materials in which organic fragments are built into the silicon-oxide network [127]. The ORMOSIL precursors are usually substituted with nonhydrolyzable alkyl group(s) which act as a network modifier that terminates the silicate networks and provides the desired properties for a range of applications. The ORMOSIL precursors commonly used are methyltriethoxysilane (MTEOS) [19, 116, 128-130], ethyltriethoxysilane (ETEOS) [130], methyltrimethoxysilane (MTMOS) [75, 94, 115, 129, 131], phenyltrimethoxysilane (Ph-TMOS) [131-135], dimethoxy dimethylsilane (DiMe-DMOS) [88, 131], diethoxydimethylsilane (DEDMS) [136, 137] and diphenyldimethoxysilane (DiPh-DMOS) [131]. ORMOSIL materials provide advantages such as high flexibility, high surface area and low shrinkage over inorganic gels which help to prevent cracking, increase hydrophobicity and improve film adhesion to its support [117, 123]. The addition of alkyl group increases the hydrophobicity and porosity of the matrix, resulting in an improved linearity of Stern-Volmer plot and sensitivity of the oxygen sensor [22-24, 88]. Besides, ORMOSIL-based oxygen sensing films avoid the penetration of water into the matrix and enhance the diffusion of gases (i.e. partition co-efficient) [82, 123]. For example, when silicon alkoxide is mixed with ORMOSIL, the condensation reaction

will be terminated by the presence of nonhydrolyzable alkyl groups.



As the alkyl groups can terminate the condensation process, the degree of cross-linking is reduced resulting in an improvement in brittleness and porosity of the films. During polycondensation, the strength of the gel (viscosity) will be increased. The ORMOSIL film is obtained finally after the drying process, after the solvents (water and alcohol) have been removed from the interconnected pore network and a sol-gel film with three-dimensional network is formed.

In addition, monomers (precursors) containing an easily derivatized moiety such as amino-, vinyl-, epoxy-, or mercapto- group can be used to prepare readily derivatized sol-gels. These can be subsequently used as covalent anchors for specific chelating agents, redox mediators, or photometric reagents [123].

For the fabrication of oxygen sensors, the oxygen-sensitive dye is usually added to the “sol” solution and then dried as “gel”. In the sol-gel film, dyes are entrapped inside the pores of the matrix and analytes such as oxygen gas are usually small enough to diffuse into these pores and interact with the sensing dyes.

1.2.3 Sol-gel-based optical oxygen sensors

For the development of optical oxygen sensors, a widely used approach is the immobilization (entrapment) of oxygen-sensitive dye into a suitable matrix followed by interconnection of this solid (i.e. film) to a transducer [126]. Sol-gel derived materials are comparatively better than many organic polymers as matrix for immobilization because of their higher stability, optical transparency, flexibility and gas permeability [123, 138, 139].

The application of sol-gel materials in optical oxygen sensing has gained a lot of attention recently [18, 19, 22-24, 46, 57, 61, 62, 69, 71, 73-75, 81-83, 87, 88, 93, 94, 97, 113-118, 121, 140-150]. Liu et al. first reported the optical fiber oxygen sensors fabricated by immobilizing platinum octaethylporphine (PtOEP) in different sol-gel coatings and studied the oxygen permeability of the sol-gel coatings [140].

After that, extensive work in the development of sol-gel-based optical oxygen sensors have been carried out by MacCraith's group. They first fabricated an optical oxygen sensor by coating an optical fiber with a cage-like structure sol-gel (TEOS) film in which $[\text{Ru}(\text{dpp})_3]^{2+}$ was entrapped [57]. At a later stage, they also developed a LED-based oxygen sensor [69]. In that sensor, the length of the fiber optic had been enlarged and a low cost, stable blue LED was used as the excitation light source. Later, they developed ORMOSIL oxygen sensing film coated on glass slide for dissolved oxygen measurement [19]. The organically modified precursor MTEOS was used to improve the surface hydrophobicity of the sensing film and the sensitivity was increased by a factor of more than 3.5. On the other hand, Murtagh and Shahriari also studied the effects of organic modification on the behavior of ORMOSIL oxygen sensors based on $[\text{Ru}(\text{dpp})_3]^{2+}$ [75]. They concluded that the improved sensitivity of ORMOSIL films could be attributed to the increasing oxygen diffusivity in the more hydrophobic organically modified silicate (ORMOSIL). One year later, McCulloch and Uttamchandani described a highly miniaturized sol-gel-based fiber optic oxygen sensor [118]. This technology is based on the use of submicron fiber optic tips (0.1 – 1 μm) with $[\text{Ru}(\text{phen})_3]^{2+}$ immobilized in TEOS sol-gel on the end surface.

The first sol-gel-based optical nanosensor, or sol-gel probe encapsulated by biologically localized embedding (PEBBLE) for real-time measurement of subcellular molecular oxygen was reported by Xu et al. in 2001 [121]. The spherical sol-gel PEBBLE sensors were made by the incorporation of $[\text{Ru}(\text{dpp})_3]^{2+}$ into TEOS spheres of radii 50 to 300 nm. The sol-gel PEBBLEs were inserted in rat C6 glioma cells for real-time intracellular oxygen analysis. Furthermore, another PEBBLE nanosensor (average diameter: about 120 nm) was developed by Koo et al. for dissolved oxygen measurement using organically modified silicate nanoparticles as a matrix to entrap the oxygen-sensitive dyes Pt(OEP) or Pt(OEPK) [23]. The ORMOSIL nanoparticles were prepared via a sol-gel-based process, which included the formation of core particles with phenyltrimethoxysilane (Ph-TMOS) followed by the formation of a coating layer with methyltrimethoxysilane (MTMOS). PEBBLEs were injected in rat C6 glioma cells to monitor the *in vitro* intracellular changes of dissolved oxygen. On the other hand, oxygen-sensitive sol-gel particles (160 – 200 mesh) for oxygen monitoring in organic solvents have been prepared by Garcia et al. by mixing TEOS, TMOS and MTMOS-based materials with $[\text{Ru}(\text{bpy})_3]^{2+}$ [94].

Apart from sensitivity, ease of calibration is another important parameter for

an ideal oxygen sensor. When oxygen-sensitive dyes are immobilized in a polymeric matrix (heterogeneous microenvironment), the Stern-Volmer equation (1.1) generally will not be obeyed and the plot will become nonlinear with downward curvature [10, 11, 19, 36, 55, 57, 64, 73, 75, 79, 81-83, 86, 88, 93, 97, 116, 117, 119, 121, 129, 140, 144, 151-153]. Several models have been proposed and factors such as oxygen solubility in polymer, adsorption of gas in polymer microcavities and microheterogeneity of the dye molecules inside the polymer environment were suggested to account for the nonlinearity of the calibration curve [36, 95, 151]. The nonlinear Stern-Volmer plot prevents a simple two-point calibration for these oxygen sensors. Recently, several researchers discovered that a linear Stern-Volmer plot could be obtained for certain oxygen sensors made of ORMOSIL materials [22, 24, 88]. This promising finding opens a door to simple two-point calibration of optical oxygen sensors [22, 24] and it further encourages the development of sol-gel-based optical oxygen sensors in the scientific community.

1.2.4 High-throughput oxygen sensors

There is a rapid increase of interest in multi-analyte and multi-sample sensing in environmental analysis as well as in high-throughput screening of drugs and the technology for high-throughput screening is evolving rapidly [154]. Modification of microtiter plates is a common way to fabricate sensors for high-throughput specific analysis. Wodnicka et al. firstly developed a fluorescent “Oxygen BioSensor” using microtiter plates as the high-throughput platform for real-time dissolved oxygen measurement [155]. This oxygen sensor was fabricated by adsorbing $[\text{Ru}(\text{dpp})_3]^{2+}$ onto silica gel and then immobilized into water-based silicone rubber applied onto the bottom of microtiter plate. Later, this oxygen sensor was commercialized by Becton Dickinson (Franklin Lakes, USA) as BD™ Oxygen Biosensor System [156]. The BD™ Oxygen Biosensor System allows instantaneous detection of oxygen levels without the need for additional reagents or steps. Another similar commercially available oxygen measuring plate is the OxoPlate® from Precision Sensing Gmb (Regensburg, Germany). The OxoPlate® was fabricated by immobilizing small polystyrene particles incorporated with platinum porphyrin at the bottom of microtiter plate. In both types of oxygen biosensors, the oxygen calibration curves are nonlinear.

Wolfbeis and co-workers have further modified the microtiter plate as optical sensors for multi-analyte sensing of oxygen, temperature, pH and carbon dioxide [157]. They prepared different sensing films by mixing the dyes with polystyrene and then spread onto a transparent polyester support. After evaporation of solvent, the optical sensing films were punched into spots (7 mm i.d.) and fixed to the bottom of microtiter plate wells. The luminescence was measured through the transparent bottom of the microtiter plate by a CCD camera. The microtiter plate equipped with sensor spots is capable of mapping different parameters and analyte gradients simultaneously.

Bright and Cho [85] reported a simple integrated array format that uses 36 microwells machined directly onto a LED surface of 5 mm diameter. To illustrate the potential of this approach, they filled individual microwell with a sol-gel material doped with $[\text{Ru}(\text{dpp})_3]^{2+}$. The LED optical output was used to excite the $[\text{Ru}(\text{dpp})_3]^{2+}$ immobilized within the microwell-entrapped sol-gel directly. They termed this new sensor scheme an optical sensor array and integrated light source (OSAILS).

Bright and co-workers also described a photonically based chemical-responsive sensor array (CRSA) with a radioluminescent (RL) light source for multielemental sensing [150]. The RL light source comprised of a strontium-90 (^{90}Sr) radionuclide plastic scintillator in which a blue light (λ_{max} 435 nm) was generated which excites the analyte-responsive luminophores within the CRSA. A 5 x 5 multielement array of the size 18 mm x 18 mm was used for oxygen sensing. The sensor array was prepared by coating $[\text{Ru}(\text{dpp})_3]^{2+}$ -doped sol-gel with a 200 μm diameter solid tungsten pin onto a glass microscope cover slip.

1.3 Biosensors Based on Optical Sensing of Oxygen

As oxygen is an important physiological parameter, measuring oxygen concentration together with an appropriate biological component is a convenient way to fabricate biosensors. The use of optical oxygen sensors allows the fabrication of biosensors for high-throughput analysis and multi-analyte determination with cells and their effectors [158].

Wolfbeis and co-workers were the first to report the use of an optical oxygen sensor for the determination of glucose concentration. In this biosensor, glucose oxidase (GO_x) was immobilized on an oxygen sensing film prepared by entrapping $[\text{Ru}(\text{phen})_3]^{2+}$ -adsorbed silica gel into silicone matrix. In between the enzyme layer and the oxygen sensing film, a layer of carbon black was used to prevent optical interference from ambient light and sample. The decrease in oxygen concentration during the enzymatic oxidation of glucose by GO_x gives an indirect indication of glucose concentration. Later on, Rosenzweig and Kopelman miniaturized the fiber optic glucose biosensor to micrometer scale [159, 160]. The fabrication of this biosensor was based on a methodology first suggested by Li and Walt [161]. In that micrometer sized biosensor, glucose oxidase was immobilized in an acrylamide

polymer in contact with the oxygen sensing layer in which $[\text{Ru}(\text{phen})_3]^{2+}$ was the sensing material. On the other hand, Papkovsky and co-workers reported a flow-through glucose biosensor system [162], in which the sensor membrane was positioned in a compact integrated flow-through cell. The GO_x was immobilized either directly on an oxygen sensor membrane or in controlled-pore glass in a microcolumn reactor. The biosensor can be used in real-time continuous monitoring of glucose concentration. More recently, Wang et al. reported the use of BD™ Oxygen Biosensor System (OBS) for high-throughput detection of non-human primate and human islets oxygen consumption rates in response to different glucose concentrations [163]. The oxygen consumption rates of islets were measured by the OBS in the microwells where islets were cultured with different glucose concentrations and the dissolved oxygen concentrations were monitored kinetically. This high-throughput methodology provided an *in vitro* means to rapidly and robustly assess the functional viability of an islet preparation prior to clinical transplantation.

1.3.1 Biochemical oxygen demand (BOD) biosensors

The amount of municipal and industrial effluents is increasing as the world's population and industrialization grow. This results in an increase of organic matters in wastewater and freshwater. Therefore, rapid analysis and monitoring of pollutants are important for environmental protection [164]. Biochemical oxygen demand (BOD) is an important and widely used parameter in the measurement of biodegradable organic compounds and pollutants in water. It can be used to evaluate the efficiency of wastewater treatment processes. BOD is a measure of the quantity of dissolved oxygen (mg l^{-1}) consumed by microorganisms during the decomposition of organic matters in aqueous samples. The 5-day BOD test (BOD_5) is a conventional method adopted by the American Public Health Association and has been the standard method since 1936 [165]. To determine the BOD_5 for a wastewater sample, the water sample was first diluted with water containing a mixture of minerals and nutrients and a small quantity of microorganisms. The dissolved oxygen (DO) concentration of the sample is determined immediately by a DO probe or by Winkler titration, and the diluted samples are then incubated in dark at 20°C for 5 days. The uptake of organic wastes by microorganisms as food for growth and reproduction would consume the oxygen present in the sample. At the

end of the incubation period, the residual DO is determined. The BOD of wastewater samples can be calculated by equation 1.2.

$$\text{BOD}_5 \text{ (mg l}^{-1}\text{)} = [(\text{DO}_{\text{init}} - \text{DO}_{\text{final}}) - R(\text{S}_{\text{init}} - \text{S}_{\text{final}})] / F \quad (1.2)$$

where

- DO_{init} = initial dissolved oxygen concentration;
- DO_{final} = final dissolved oxygen concentration (after 5 days' incubation);
- S_{init} = initial dissolved oxygen concentration in seed control before incubation;
- S_{final} = final dissolved oxygen concentration in seed control (after 5 days' incubation);
- R = seed volume ratio (v/v), seed in each sample to seed in seed control; and
- F = dilution factor, expressed as a decimal.

The ratio F can be calculated by equation 1.3:

$$F = \text{volume of sample} / \text{total volume (sample and dilution water)} \quad (1.3)$$

Even though BOD_5 is a good indicator of the concentration of organic matters in water, the conventional BOD_5 test involves cumbersome procedures and a 5-day incubation period and requires substantial experience and skill of the operator to get reproducible results, and is unsuitable for on-line monitoring of organic pollutants [166]. Therefore, optical microbial BOD sensors have been developed for remote, rapid, reliable and reproducible determination of BOD.

The principle of the optical BOD biosensor is based on the measurement of oxygen uptake by microorganisms as a result of the biodegradation of metabolizable organic matters. When the microorganisms degrade the biodegradable organic matters, their respiration rate increase which results in the consumption of dissolved oxygen from the sample solution. The rate of oxygen uptake (oxygen consumption rate), which is measured or monitored using an optical oxygen sensor, is proportional to the concentration of the organic substances.

The first optical BOD biosensor for BOD determination was described by Wolfbies and co-workers in 1994 [167]. The BOD biosensor was constructed by coating different layers onto the tip of an optical fiber. The layers are placed in order on an optically transparent gas-impermeable polyester support. The first layer on the polyester support was an oxygen sensing layer prepared by dispersing $[\text{Ru}(\text{dpp})_3]^{2+}$ in plasticized poly(vinyl chloride). A microbial layer with the yeast *Trichosporon cutaneum* in polyvinyl alcohol was then placed on top of the oxygen sensing layer. Finally, the microbial layer was covered by a substrate- permeable polycarbonate membrane to retain the yeast cells. The BOD values estimated by this new biosensor correlated well with those determined by the conventional BOD₅

method.

In the same year, a scanning optical BOD sensor has also been developed by Wong and co-workers [60]. The sensing element is a silicone rubber film entrapped with $[\text{Ru}(\text{dpp})_3]^{2+}$. The sensing films were attached to the bottom of transparent glass vials in which dissolved oxygen was measured. A scanner head with four blue LEDs as the excitation light source and a fiber optic connected to the PMT detector was used to collect the signal from the sensing film inside the BOD vials. Therefore, one optical scanner can be used to monitor the dissolved-oxygen concentration in a number of vials in one batch. The main advantage of this sensor is its capability of measuring several of BOD samples within the same period of time. This sensor has been further improved with immobilized microbial films recently [166]. The oxygen sensing film and the microbial film were immobilized on the bottom of glass sample vials. The microorganisms were immobilized in a sol-gel composite material of silica and poly(vinyl alcohol)-grafted-poly(vinylpyridine) on the oxygen sensing film. The BOD values were determined from the rate of oxygen consumption by the microorganisms and correlated well with the results of the conventional 5-day BOD test.

An optical fiber biosensor was developed for the measurement of low BOD values by Karube and co-workers [168]. This BOD sensor used a commercial optical oxygen sensor as a transducer which measured the luminescence quenching by oxygen. Good correlation was obtained between the sensor responses and BOD₅ values.

Wong and co-workers described an ORMOSIL-based fiber-optical microbial sensor for determination of BOD in 2003 [169]. In this BOD sensor system, the sensing film consisted of a [Ru(dpp)₃]²⁺-entrapped ORMOSIL layer and a microbial layer with microorganisms immobilized in a PVA/sol-gel matrix. The BOD measurement was performed in a batch mode in which the BOD sensing film was placed the bottom in an air tight detection cell and the oxygen consumption by the microorganisms was monitored by the change in luminescence intensity. The results showed a linear relationship between the rate of change of luminescence intensity and the BOD values.

1.3.2 Applications of microplates with optical oxygen sensors

Since the level of dissolved oxygen in an assay medium correlates to the

number and viability of the cells in the medium, microtiter plates with optical oxygen sensors are ideal for monitoring cell viability and proliferation. The technology is particularly well suited to investigate cells' kinetic responses to proliferative or toxic stimuli such as drugs [155]. For example, the BD™ Oxygen Biosensor System has been used to determine IC₅₀ values of toxic substances on living cells by monitoring the change in dissolved oxygen concentration in the presence of various concentration of toxic substances [155]. In addition, John et al. reported the use of microtiter plate integrated with optical dissolved oxygen sensors for microbial cultivation monitoring [90]. Recently, other applications such as determination of microorganism growth rates [170, 171], characterization of antibacterial compounds [172], quantitative analysis of metabolic network [173], cell viability assays [174], cell culture medium optimization [175] and cytotoxicity assays [176] have been reported.

Papkovsky's research group has used another approach to fabricate optical oxygen sensors on microtiter plates. They inserted a disposable phosphorescent oxygen sensing membrane into the microwells of microtiter plates to monitor the respiration of yeast cells [177]. The oxygen sensing membrane was prepared by adsorbing the oxygen-sensitive dye, Pt(OEPK), in a mixture of polystyrene and ethyl

acetate on a filter membrane which was then cut into disks of the same diameter as the microwells and inserted into the microwells. However, such disposable sensor cannot be reused and liquids can be easily trapped between the sensing membrane and the bottom of the well. They have also described water-soluble oxygen probes in microtiter plate for dissolved oxygen determination and cell viability screening assay [178]. The oxygen probe (PtCP-BSA) was prepared by labeling bovine serum albumin (BSA) with oxygen-sensitive platinum porphyrin derivative (PtCP).

1.4 High-Throughput Luminescence-Based Biosensors for Studying Carbohydrate-Protein Interaction

1.4.1 Carbohydrate-lectin interactions

Carbohydrate-protein interactions that involve specific protein-linked oligosaccharides and their complementary binding proteins are known to be directly involved in numerous important biological processes. These interactions take place in cells, on the cell surface, in the extracellular matrix or in secretions. They participate in the folding of nascent proteins in the endoplasmic reticulum, the targeting of newly synthesized lysosomal enzymes to their correct destination, the recruitment and activation of cells in mechanisms of inflammation, and the adhesion of microbes to host cells [179]. The identification of oligosaccharide ligands and proteins that recognize them (carbohydrate-protein interaction) has been achieved using various biochemical and cell biological approaches, and has often involved many years of research. There is a need for sensitive, high-throughput technologies that perform analyses of carbohydrate-protein interactions. Microarray approaches, analogous to those developed for DNA [180] and proteins [181], are ideal to address this need. In the development of these carbohydrate microarrays,

carbohydrate-lectin interactions are often employed to demonstrate and test the technology as they are a relatively simple and well-characterized class of carbohydrate-protein interactions.

Lectins are sugar-binding proteins or glycoproteins of non-immune origin; they do not have enzymatic activity towards sugars to which they bind and do not require free glycosidic hydroxyl groups on these sugars for their bindings [182]. Lectins have at least one binding site which can bind free or glycosidically linked carbohydrates. Lectins do not have immunoglobulin structure [182]. Most of the lectins recognize just a few natural monosaccharides such as mannose, glucose, galactose and fucose while these monosaccharides are typical constituents of animal glycoconjugates and are also present on surfaces of cells, including erythrocytes [183]. Hemagglutination (agglutination of erythrocytes) is routinely employed for detection of lectins. The agglutinating and precipitating activities of lectins are similar to those of antibodies. They can likewise be specifically inhibited by low molecular weight compounds such as haptens, which in the case of lectins are sugars or sugar-containing ones. Therefore, many of the methods used in lectin research are based on immunochemical techniques but lectins are not capable of an immune response.

Stillmark was the first to describe the activity of lectin in 1888 [184]. He described the agglutinating properties of a toxic protein called ricin, which can be extracted and partially purified from castor seeds (*Ricinus communis*). He tested its effect on erythrocytes, liver cells, leukocytes and epithelial cells and noted that erythrocytes from different species reacted in different ways. Three years later, Hellin described the agglutinating and serum-properties of a toxic extract of jequirity seeds (*Abrus precatorius*), abrin [185]. Lectins are found in plants, viruses, microorganisms and animals and the detailed information is discussed in a review by Kocourek [185]. Most of the lectins used in lectinology (research in lectins) in the earlier stage are plant lectins as they can be easily isolated and the sources (seeds) are easily available. After discovery of ricin and abrin, the father of modern immunology, Paul Ehrlich, recognized the value of abrin and ricin as antigenic model substances and carried out a number of experiments that established the fundamental concepts of immunology in 1891 [185]. He reported that rabbits fed with small amounts of jequirity seeds developed a certain degree of immunity against abrin. The anti-abrin found in serum of rabbit could neutralize the activity of abrin but not that of ricin and vice versa. His experiments demonstrated the antigen-antibody reaction.

On the investigation of lectins as recognition molecules, Boyd described blood group specificity of lectins in 1945 [185]. He discovered that certain seeds contain agglutinins that are specific for some human blood group antigens. The principle of agglutination is the multivalent lectin bound to cell surface carbohydrates and cross-linked the cells. Over 100 blood group-specific lectins were discovered between 1945 and 1964. For example, tufted vetch seeds (*Vicia cracca*) contain agglutinins which bind A antigen more strongly than B or O antigens; agglutinins from *Bandeiraea simplicifolia* bind B antigen and agglutinins from gorse seeds (*Ulex europaeus*) bind O antigen [185]. Moreover, lectins can be a tool for cancer research based on analysis of cell surface carbohydrates of normal and malignant cells. Aub discovered that certain types of malignant cells are more readily agglutinated by lectins (known as wheat germ agglutinin (WGA)) than the corresponding normal cells in 1963 [183]. It is because the carbohydrate expression and glycosylation patterns on cellular surfaces of cancer cells are commonly modified [186].

Since the late 1980s, research on lectins in biology and medicine has shifted from plant to those on animals and bacteria, especially on the biological significance

of their interactions with carbohydrates [187]. Animal lectins can be divided into two main families: S-type lectins and C-type lectins. S-type lectins (also known as galectins) are soluble in the absence of surfactants and usually β -galactose-specific while C-type lectins (subfamilies: selectins and collectins) are Ca^{2+} dependent (requiring Ca^{2+} for activity) and exhibit different carbohydrate specificities. The first animal lectin was identified in 1982 and they were found on all cell-surface membranes. This sparked the interest in the wider roles of carbohydrates and lectins within biological systems [188]. Lectins produced by microorganisms and bacteria are commonly called microbial lectins and bacterial lectins. These microbial and bacterial lectins play an important role in initiation of viral and microbial infections by mediating adhesion to host cells as they bind readily to saccharide sequences of cell-surface glycoproteins and glycolipids [187]. Now, it is known that the attachment of bacteria via their surface lectins to cell surface sugars is a prerequisite for the initiation of bacterial infection [189]. For example, influenza virus hemagglutinin (surface lectin of influenza virus) can initiate the infection by attachment of the virus to the target cells via binding to sialic acid-containing carbohydrates on the surface of the cells [190]. This results in fusion of the viral and cellular membranes allowing release of the viral genome into the cytoplasm and subsequent replication. Therefore, the studies of sialic acid-hemagglutinin

interactions provide a possible basis for the design of antiviral drugs that would block viral attachment to cells [190]. Lectin-based immunosensor techniques have been routinely used for identifying pathogen and viral species expressing particular carbohydrates on their surface. On the other hand, it was found that suitable monosaccharides, oligosaccharides, synthetic or natural carbohydrate derivatives can inhibit the binding of a large number of viral, bacterial and protozoan pathogens to carbohydrate structures of glycoproteins or glycolipids present on epithelial and other cells as the derivatives have a high affinity for the bacterial lectins [188, 189]. As a result, carbohydrate-lectin interactions play an important role in various biological functions, such as cell-cell recognition, adhesion, and communication and this type of interaction is attracting increasing interests in applications such as drug delivery systems [191, 192] and drug design.

1.4.2 Recent development on high-throughput carbohydrate sensors for carbohydrate-protein interaction studies

As lectins exhibit strong binding to specific carbohydrate moieties (glycans), this property has been extensively exploited as a basis for biosensor design and has been employed as a platform for the extraction and analysis of various proteins [186],

drug discovery, diagnosis and glycomics (the study of full complements of carbohydrates in cells, tissues or organisms) [193]. In most of these applications, carbohydrates are immobilized on solid support and functioned as recognition elements followed by generation of measurable signals. In the recent development of carbohydrate sensors, it was focused on fabrication of high-throughput carbohydrate sensors (microarrays) as a tool for rapid analysis of carbohydrate-protein interactions.

High-throughput carbohydrate sensors (microarrays) are newly developed tools for carbohydrate-protein interaction studies, the first carbohydrate microarray was introduced in 2002 by Wang et al. [194]. There are two methods applied in the immobilization of carbohydrates on surfaces: non-covalent and covalent attachment. In 2002, Wang et al. described a carbohydrate-based microarray for biomedical research on carbohydrate-mediated molecular recognition and anti-infection responses [195]. They immobilized carbohydrate antigens (dextrans) including most known human microbial pathogens, autoantigens, and tumor-associated antigens on a nitrocellulose-coated glass slides without chemical conjugation by a high-precision robot which was designed to produce cDNA microarrays. The glass slides were then incubated at room temperature with anti-carbohydrate antibodies

and followed by secondary fluorescent antibodies. Finally, the stained slides were scanned for fluorescent signals. The microarray developed by Wang et al. demonstrated the carbohydrate-binding specificity of antibodies and other proteins. For example, $\alpha(1,6)$ -glucose linkages (found in dextrans) could be detected by $\alpha(1,6)$ -glucose specific 4.3F1 antibody. However, the attachment of oligosaccharides with higher molecular weight was better than the lower one.

Another carbohydrate array prepared by non-covalent attachment for high-throughput detection and specificity assignments of carbohydrate-protein interactions was introduced by Feizi and co-workers [196]. They made the arrays by non-covalent immobilization of oligosaccharides, glycosaminoglycans and oligosaccharide fractions from brain on nitrocellulose membranes. Their results obtained from the arrays revealed some new findings such as a relative abundance of the Lewis^x sequence based on *N*-acetyllactosamine in human brain recognized by anti-L5, and a paucity of the Lewis^x sequence based on poly-*N*-acetyllactosamine recognized by anti-SSEA-1.

On the other hand, Chi-Huey Wong's research group constructed non-covalent arrays of oligosaccharides on polystyrene microtiter plates and used

them for high-throughput analysis of carbohydrate-protein interactions [197-199]. They have synthesized a series of hydrophobic group-linked carbohydrates for non-covalent binding to microtiter plates through hydrophobic interaction with the polystyrene surface [197]. Their results showed that monosaccharides linked to the saturated hydrocarbon between 13 to 15 carbons in length could be retained after aqueous washing. Furthermore, they applied 1,3-dipolar cycloaddition reaction (between azides and alkynes) to attach an azido group-containing carbohydrate *in-situ* to an alkyne-containing C₁₄-hydrocarbon hydrophobically adsorbed on the microtiter plates as shown in Figure 1.4 [198]. The lectin-binding assays had been performed with the functionalized plates. Several carbohydrates with various types and linkages of a terminal sialic acid were immobilized on microtiter plates and screened with fluorescein-labeled *Sambucus nigra* lectin (SNA). Moreover, studies on the inhibition of a biotransformation (biosynthesis of sialyl Lewis^x via the enzymatic fucosylation) had been carried out and the IC₅₀ value of a known inhibitor was determined by these arrays. In addition, they introduced another immobilization technique, urea bond linkage, to immobilize carbohydrates on microtiter plates [199]. The microarray was prepared by mixing tetradecyl isocyanate (isocyanate-containing C₁₄-hydrocarbon) and 2-aminoethyl-β-D-galactopyranoside (amine-containing carbohydrate) in microwell

of microtiter plate and was shown in Figure 1.5. This transformation is clean, quick and coupling reagent-free [199]. The lectin-binding assay was performed using fluorescein-labeled galactose-specific lectin and the lectin responded in a concentration dependent manner to the galactose as they expected.

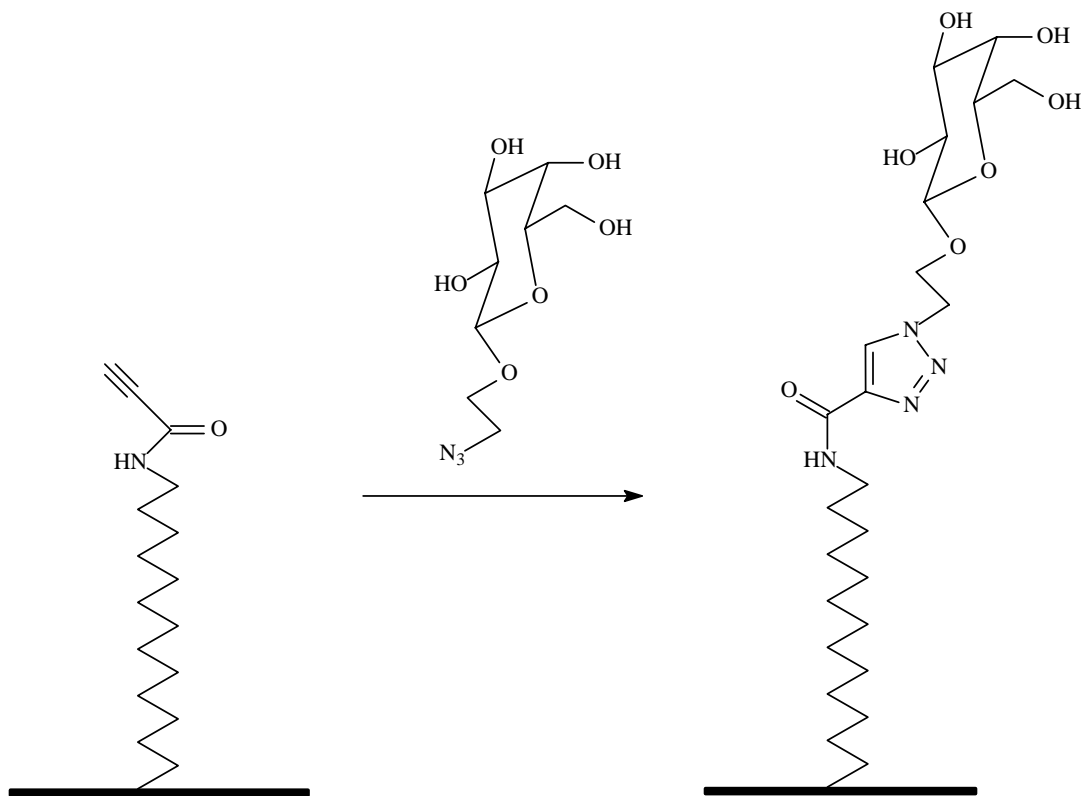


Figure 1.4 Non-covalent immobilization of carbohydrate by 1,3-dipolar cycloaddition on microtiter plate [198].

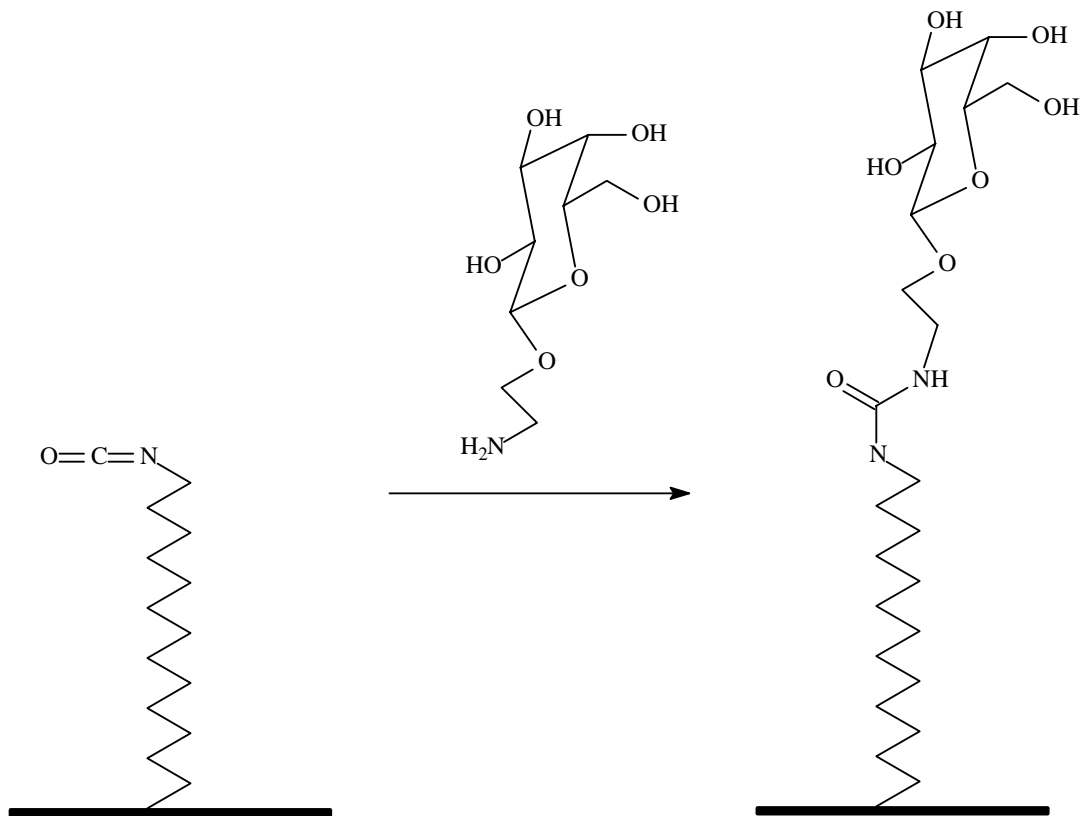


Figure 1.5 Non-covalent immobilization of carbohydrate by urea formation on microtiter plate [199].

Apart from non-covalent immobilization of carbohydrates on substrate, the most widely used method is covalent immobilization. Carbohydrates covalently linked to substrate could give a defined and uniform orientation and enhance the accessibility of the carbohydrates toward binding [200]. Mrksich and Houseman developed arrays of monosaccharides by covalent attachment to gold surface for the characterization of carbohydrate-protein interactions [201]. The monosaccharides were covalently bound to gold surface via the Diels-Alder cycloaddition between carbohydrate-cyclopenta-diene conjugates and benzoquinone-containing gold surface as shown in Figure 1.6. They performed the lectin binding tests and IC_{50} value determination by the carbohydrate arrays. Their results obtained from the arrays showed that the mannose- and glucose-specific lectin concanavalin A (ConA) bound only to mannose, glucose and N-acetylglucosamine on the arrays and did not bind to other carbohydrates.

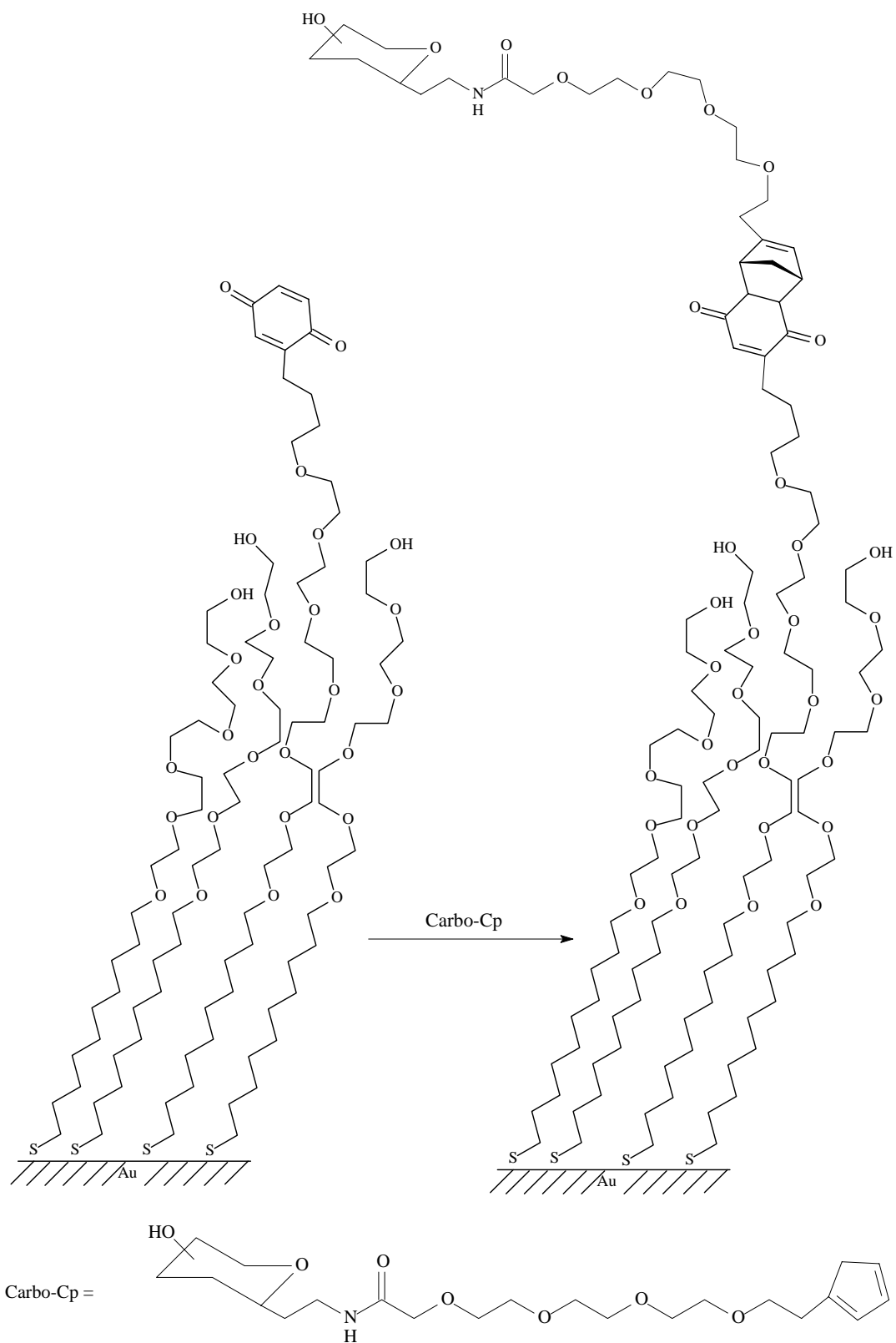


Figure 1.6 Carbohydrate immobilized on a benzoquinone-containing gold surface via the Diels-Alder cycloaddition [201].

Another approach had been employed by Mrksich's group and Seeberger's group. They immobilized thiol-functionalized carbohydrates on maleimide-functionalized self-assembled monolayers (on gold surface deposited in glass slide) [202] or maleimide-functionalized glass slides [203-206]. Mrksich and co-workers reported a carbohydrate array by immobilizing carbohydrate-thiol conjugates to self-assembled monolayers of alkanethiolates presenting maleimide groups on gold (SAMs) and the lectin binding properties of the substrates were examined [202]. The fabrication was based on the reaction between the maleimide group present in the monolayers and thiol-terminated carbohydrate as shown in Figure 1.7. The arrays had been examined for lectin binding and tyrosine kinase activity assays. In the lectin binding study, the results showed that each of the lectins associated specifically with its corresponding carbohydrate on the array.

Seeberger's research group reported carbohydrate arrays on maleimide-functionalization glass slides and their applications in HIV study [203, 204], pathogen detection [205] and antibiotic study [204]. One of the carbohydrate arrays was fabricated by immobilizing thiol-functionalized carbohydrates on maleimide-functionalized glass slide [203, 206]. Another one was prepared by spotting amino-functionalized carbohydrates onto glass slides that had been

functionalized with the amine-reactive homobifunctional disuccinimidyl carbonate linker [204, 205].

Furthermore, Shin and co-workers prepared carbohydrate microarrays by covalent attachment of maleimide-linked carbohydrates on thiolated glass slides for studying carbohydrate-lectin interactions as shown in Figure 1.8 [207, 208]. The results of lectin binding experiments showed that the lectins were specifically bound to corresponding carbohydrates with different binding affinities. The IC_{50} values of soluble carbohydrates determined with the carbohydrate microarrays were used to quantitatively analyze the binding affinities of lectins. They found that lectin bindings were dependent on the length of the linker between the carbohydrate and the maleimide group as well as on the concentration of immobilized carbohydrates.

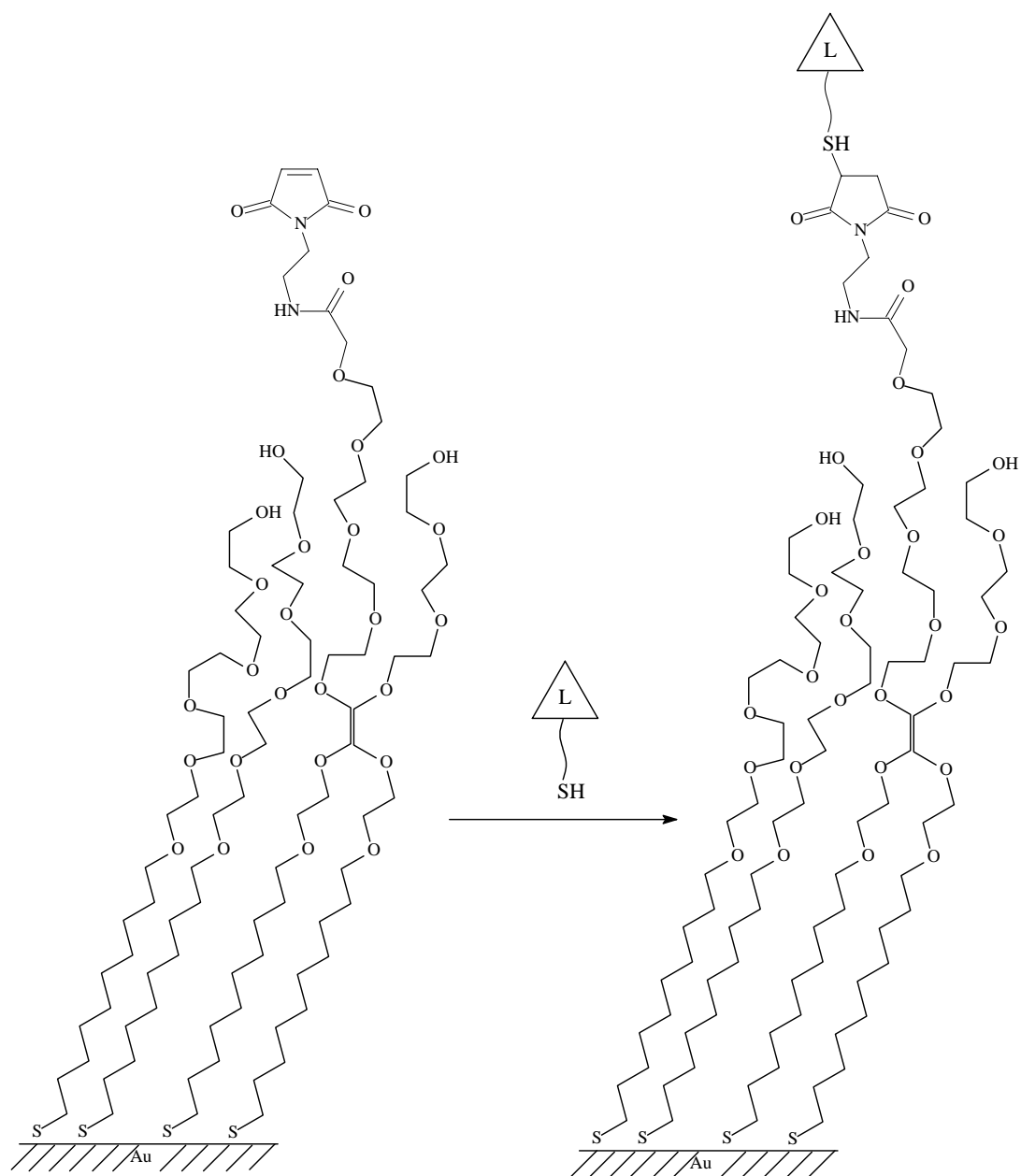


Figure 1.7 Structure of a self-assembled monolayer used to immobilize thiol-terminated carbohydrates (L) [202].

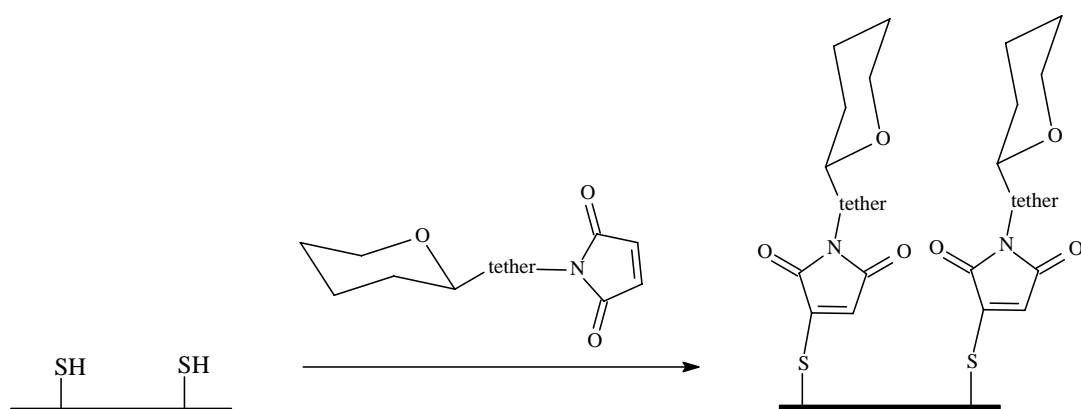


Figure 1.8 Immobilization of maleimide-linked carbohydrates on thiolated glass slides [207].

Recently, Wong's research group also developed another microplate-based carbohydrate array by covalent immobilization of azido-containing carbohydrate via 1,3-dipolar cycloaddition [209]. Before the immobilization of carbohydrates, they employed two different ways to functionalize the microtiter plate with alkyne groups and the scheme is shown in Figure 1.9. The first method of alkyne functionalization was carried out by the attachment of propynoic acid [2-(2-amino-ethyl)disulfanyl]-ethyl]-amide (linker 1) to the N-hydroxysuccinimide-coated microtiter plate. Another one was prepared by attachment of propynoic acid (2-{2-[3-(4-isothiocyanato-phenyl)-thioureido]-ethyl)disulfanyl}-ethyl)-amide (linker 2) to the amine-coated microtiter plate. After that, the alkyne functionalized microtiter plates were treated with azido-containing carbohydrates which underwent 1,3-dipolar cycloaddition. This reaction covalently attached the carbohydrates on the microtiter plates which were then used for lectin binding studies.

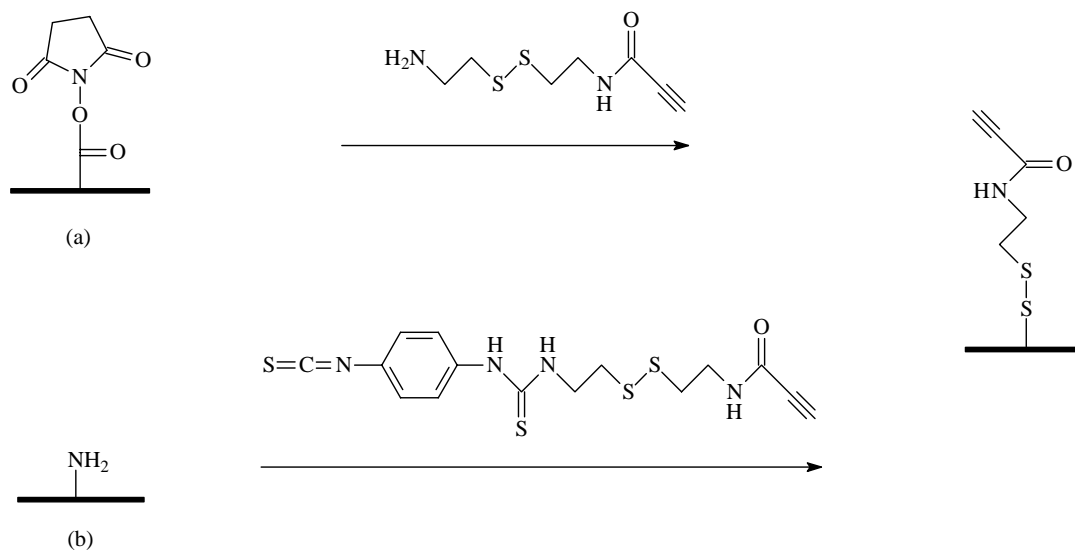


Figure 1.9 Alkyne functionalization by (a) linker 1 with NHS-coated microtiter plate and (b) linker 2 with amine-coated microtiter plate [209].

1.5 Aims and Objectives of this Project

As microtiter plates can provide a useful platform for the development of high-throughput multi-parameter sensors, modification of microtiter plates for attachment of various types of sensing elements have become an important research topic. This project is aimed at developing high-throughput microplate-based biosensors for multi-sample analysis of dissolved oxygen, toxicity, biochemical oxygen demand (BOD) and carbohydrate-protein interactions. Although the oxygen sensing microtiter plates are now commercially available, oxygen sensing films are made of polymers such as silicone rubber. The Stern-Volmer plots of these oxygen sensors are nonlinear which presents difficulty in sensor calibration. Moreover, the silicone rubber surface does not allow the easy adhesion of microbial or enzymatic films which makes the conversion of these sensors into other biosensors difficult. Recently, investigations on organically modified silicates (ORMOSILs) as supporting materials for $[\text{Ru}(\text{dpp})_3]^{2+}$ indicated that certain ORMOSILs can yield linear Stern-Volmer calibration plots for the oxygen sensors [22, 24, 88]. ORMOSIL oxygen sensors have attempted to be fabricated on polystyrene microtiter plates for the measurement of oxygen concentration. The performance of the sensing film have been compared with other oxygen sensing

films with $[\text{Ru}(\text{dpp})_3]^{2+}$ and the results will be discussed in chapter 2 of this thesis.

The development of high-throughput biosensors based on optical detection of oxygen concentration is also interested. In combination with suitable biological components, it is expected that biosensors that can measure different parameters can be constructed. In this project, the ORMOSIL oxygen sensors on microtiter plate were used as high-throughput biosensors for testing the toxicity of some antimalarial drugs on a heterologous yeast model. The IC_{50} values (drug concentration which produced 50% inhibition of growth rate) of antimalarial drugs have been determined and compared to the conventional optical density method by measuring the absorbance of yeast cells at 595 nm (OD_{595}). In addition, high-throughput BOD biosensors have been fabricated by immobilizing a bacterium, *Stenotrophomonas maltophilia*, onto the ORMOSIL oxygen sensing film. Results obtained from BOD biosensor have been compared with those obtained from the conventional 5-day method (BOD_5). Results on IC_{50} and BOD determinations will be discussed in chapters 3 and 4 of this thesis respectively.

As the ORMOSIL can be easily modified with different functional groups such as isocyanate, various sensors can be constructed by attaching target ligands to

the ORMOSIL films. A microplate-based carbohydrate sensor array by covalent immobilization of aminated carbohydrates onto the isocyanate functionalized ORMOSIL film has been developed. This is a simple and convenient method to fabricate carbohydrate sensors compared with those previously reported in literature [203-209]. The microplate-based carbohydrate sensors have been evaluated by the well-established carbohydrate-lectin interactions. Results will be discussed in chapter 5 of this thesis.

Chapter 2

Fabrication and Evaluation of $[\text{Ru}(\text{dpp})_3]^{2+}$ -Entrapped Organically Modified Silicate (ORMOSIL) Oxygen Sensing Films on Polystyrene Microtiter Plate

2.1 Introduction

The rapid development of optical oxygen sensing by luminescence quenching of oxygen-sensitive dyes in the past decade [9, 210] allows the monitoring of dissolved oxygen concentration in microtiter plates in a high throughput manner [90, 171, 174, 175, 211, 212]. Now microtiter plates specially designed for dissolved oxygen measurement are commercially available [155, 172]. These microtiter plates were prepared by immobilization of oxygen-sensitive particles in a gas permeable polymer matrix on the bottom of the wells. The oxygen-sensitive particles consist of an oxygen-sensitive luminescent dye, either tris(4,7-diphenyl-1,10-phenanthroline)ruthenium (II) ($[\text{Ru}(\text{dpp})_3]^{2+}$) or a platinum porphyrin, adsorbed on silica or polystyrene particles for better dispersion in the polymer matrix. Previous studies have shown that the performance of the oxygen sensors depends strongly on the properties of the immobilization matrix, and various polymeric materials including silicone rubber [11, 17], polystyrene [66], poly(vinyl chloride) [45], polymethylmethacrylate [105], ion-exchange polymers [21], fluoropolymers [109], cellulose acetate butyrate [213] and sol-gel derived materials [116] have been investigated. The Stern-Volmer plots for the dyes in the polymer matrix, however, are usually nonlinear [36, 55, 65] in these commercial available

oxygen sensing plates [175], and this is a major drawback for sensor calibration. Moreover, microtiter plates are commonly made of polystyrene, the surface of which can be damaged by most organic solvents in which those polymers are soluble [17, 45, 66, 105, 109]. For this reason, water-based [156] or alcohol soluble polymers [211] are often used to coat the oxygen sensor films on microtiter plate, and this limits the choice of polymers in sensor fabrication. Recently, investigations on organically modified silicates (ORMOSILs) as supporting materials for $[\text{Ru}(\text{dpp})_3]^{2+}$ indicated that certain ORMOSILs can yield linear Stern-Volmer calibration plots for the oxygen sensors [22-24, 88]. This was attributed to the homogeneous environment provided by the ORMOSIL matrix to the embedded dye molecules. Besides homogeneity, ORMOSILs are transparent, hydrophobic, thermally and photochemically stable and sufficiently porous to allow fast diffusion of oxygen. Moreover, condensation of ORMOSIL takes place in aqueous medium, which will not damage the surface of polystyrene microtiter plates. However, the poor adhesion of ORMOSILs on most polystyrene surfaces prevented the fabrication of ORMOSIL-based oxygen sensors on microtiter plates. The adhesion problem have been overcome by placing dimethoxy dimethylsilane (DiMe-DMOS) based ORMOSILs containing $[\text{Ru}(\text{dpp})_3]^{2+}$ onto surface-treated polystyrene microtiter plates. The fabrication method and the performance of the resulting oxygen sensors

are reported herein.

2.2 Experimental Section

2.2.1 Materials

[Ru(dpp)₃]Cl₂ (dpp = 4,7-diphenyl-1,10-phenanthroline) was synthesized and purified in our laboratory according to a literature method [214]. Tetramethyl orthosilicate (or tetramethoxysilane, TMOS, 98%), and dimethoxy dimethylsilane (DiMe-DMOS, 95%) were purchased from Aldrich. Oxygen and nitrogen gases (99 % purity) were purchased from Hong Kong Oxygen Company. Microtiter plates (no. 3603, 96 wells, flat clear bottom black polystyrene, TC-treated) were obtained from Corning. Aluminum microplate sealing foils were obtained from USA Scientific. All aqueous solutions were prepared in double deionized water (Milli-Q). All other chemicals and solvents were analytical-reagent grade and were used without further purification.

2.2.2 Physical measurements

All luminescence measurements were conducted on a POLARstar OPTIMA microplate reader (BMG Labtech Inc., Germany) with a microcomputer. The

wavelength of bandpass filters used for excitation and emission were centered at 460 nm and 610 nm respectively. The luminescence intensity was measured in the bottom plate reading configuration and at room temperature. The concentration of oxygen (percentage of oxygen, v/v) was varied by changing the flow rate of oxygen and nitrogen flowing into the microwell containing the oxygen sensing film. The flow rates of nitrogen and oxygen were controlled by two flow meters, respectively.

2.2.3 Preparation and properties of oxygen sensing films on microtiter plate

A solution of $[\text{Ru}(\text{dpp})_3]\text{Cl}_2$ in ethanol (2.85 mg ml^{-1}) were prepared. The silica sol was prepared by mixing TMOS, 0.1M HCl and deionized water in the volume ratio of 1.0:1.7:1.1 and various volumes of DiMe-DMOS. The sol mixture was stirred at 500 rpm for 3.5 h at 25 °C in a water bath. The sol was then centrifuged at 7500 rpm (Beckman Coulter, centrifuge model: Allegra 64R, rotor: C0650) for 4 minutes. The thickened sol at the bottom of the centrifuge tube (1 ml) was pipetted out and thoroughly mixed with 250 μl of the ruthenium complex solution. Portions (32 μl) of the sol-ruthenium mixture was then transferred to each well of the microtiter plate and allowed to stand for six days at room temperature in dark for gelation and drying. After gelation, the microtiter plate was kept away from direct light before use.

A schematic diagram showing the oxygen sensing films coated on 96-well microtiter plate is shown in Figure 2.1.

The optimum composition of sol-gel sensing film was determined by measuring the quenching response, Q_{DO} , where

$$Q_{DO} = [(I_{deoxy} - I_{oxy}) / I_{deoxy}] \times 100 ; \quad (2.1)$$

I_{deoxy} = luminescence intensity under a fully deaerated environment; and

I_{oxy} = luminescence intensity under a fully oxygenated environment.

A series of films with the same concentration of ruthenium complex but different volume ratio of DiMe-DMOS to TMOS were fabricated according to the procedures mentioned before. The quenching response, Q_{DO} , was determined by measuring the luminescence intensity of films under a sodium sulfite solution for chemical removal of dissolved oxygen (I_{deoxy}) [215, 216] and a fully oxygenated deionized water (I_{oxy}) solution respectively. The plot of quenching response versus volume ratio of DiMe-DMOS to TMOS was then obtained.

The Stern-Volmer plots were obtained by measuring the luminescence intensity under various gaseous oxygen or dissolved oxygen concentrations. The gaseous oxygen concentration was varied by changing the relative flow rates of oxygen and nitrogen before feeding into the well. The dissolved oxygen concentration was varied by dissolving different concentrations of gaseous oxygen in water and calibrated by Winkler titration [217] or by a YSI 5000 dissolved oxygen meter (YSI Incorporated, Yellow Springs, Ohio, USA).

The leaching of ruthenium complex from the sol-gel sensing film was also tested. The film was soaked in phosphate buffer solutions of different pH values (pH 1.5, 7.0 and 8.9), deionized water and organic solvents of different concentrations (e.g. dimethyl sulfoxide, acetonitrile and ethanol). The luminescence intensity of the solution at 610 nm, which indicated the leaching of ruthenium compound, was monitored at seven-day intervals over three weeks for deionized water and aqueous buffer solutions and at one-day intervals for organic solvent containing solutions.

The photostability of the sol-gel sensing film was measured by illuminating at its excitation wavelength (460 nm) and monitoring the change of its luminescence intensity (610 nm) for 16 h under air in the microplate reader. The long-term

stability was monitored by measuring the quenching response (Q_{DO}) of the sensing films over 110 days.

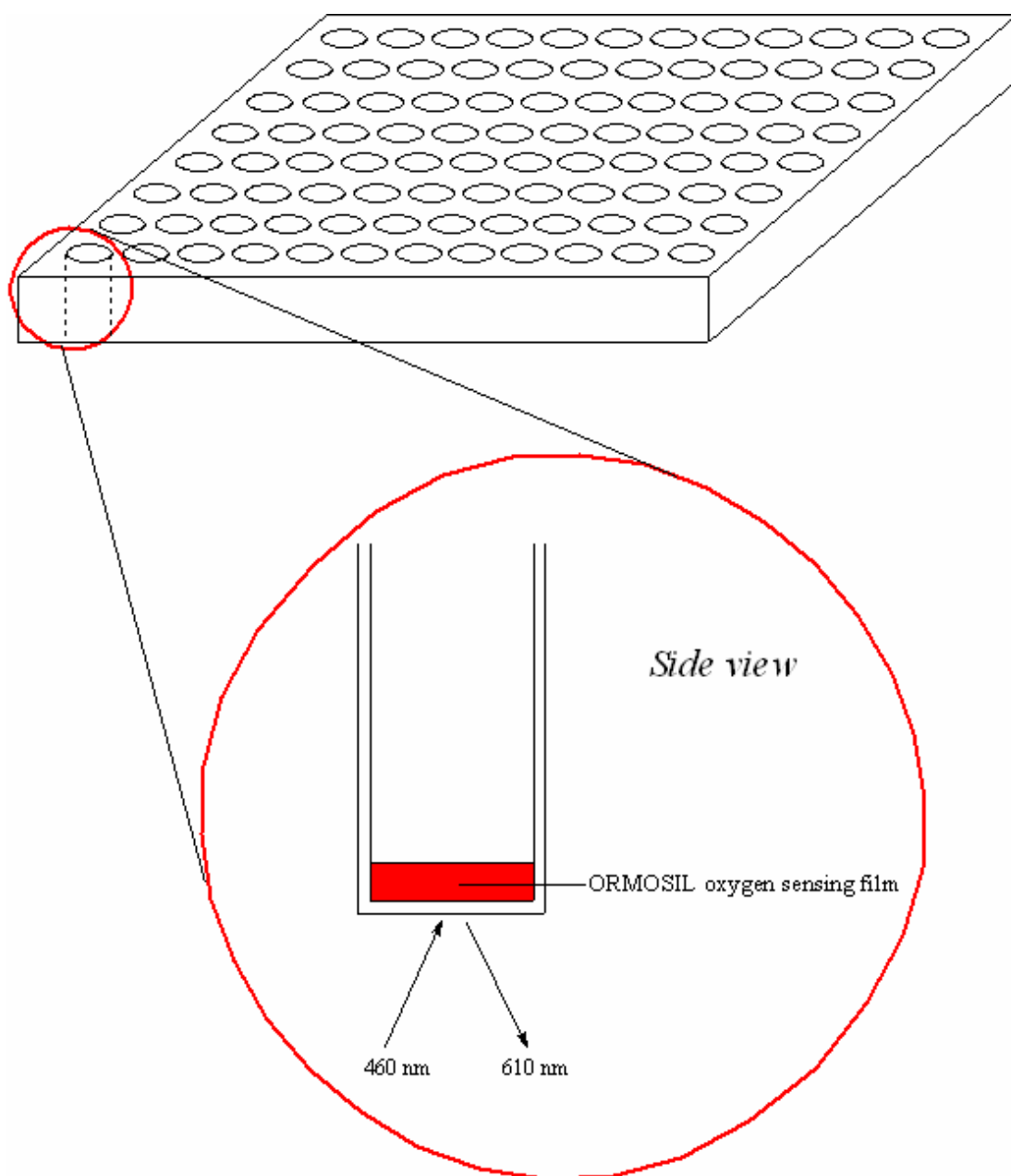


Figure 2.1 A schematic diagram showing the oxygen sensing films coated on 96-well microtiter plate.

2.3 Results and Discussion

2.3.1 Optimization of the oxygen sensing film

2.3.1.1 Organic methyl group in ORMOSIL oxygen sensing film

Oxygen sensing films with different content of organic methyl groups were prepared by mixing different volume ratios of DiMe-DMOS to TMOS in the presence of 0.01 M HCl and $[\text{Ru}(\text{dpp})_3]\text{Cl}_2$ solution whereas the volume ratio of TMOS : 0.01 M HCl : $[\text{Ru}(\text{dpp})_3]\text{Cl}_2$ (2.85 mg ml^{-1}) was fixed at 1.0:1.7:1.1. The ORMOSIL oxygen sensing films took one week to solidify and this is more time saving than other sol-gel processes that take two weeks[75, 218].

The findings indicated that the possible range of volume ratio of DiMe-DMOS : TMOS to be used for successful fabrication of the ORMOSIL films should be below 2.30:1 (v/v). The DiMe-DMOS:TMOS volume ratios used in the fabrication of sol-gel films in this study are summarized in Table 1. If the volume ratio is higher than 2.30:1, the film cannot solidify completely and stays as a viscous liquid. This is because the presence of excess methyl groups from DiMe-DMOS terminates the condensation process and prevent the formation of a crosslinked

three-dimensional network.

Table 2.1 A summary of the DiMe-DMOS : TMOS volume ratios used in the fabrication of oxygen sensing films.

Sample no.	TMOS (ml)	DiMe-DMOS (ml)	0.01M HCl (ml)	Deionized water (ml)	Volume ratio of DiMe-DMOS : TMOS
1	1.00	1.50	1.70	1.10	1.50 :1
3	1.00	1.55	1.70	1.10	1.55 :1
3	1.00	1.60	1.70	1.10	1.60 :1
4	1.00	1.65	1.70	1.10	1.65 :1
5	1.00	1.70	1.70	1.10	1.70 :1
6	1.00	1.75	1.70	1.10	1.75 :1
7	1.00	1.80	1.70	1.10	1.80 :1
8	1.00	1.85	1.70	1.10	1.85 :1
9	1.00	1.90	1.70	1.10	1.90 :1
10	1.00	1.95	1.70	1.10	1.95 :1
11	1.00	2.00	1.70	1.10	2.00 :1
12	1.00	2.05	1.70	1.10	2.05 :1
13	1.00	2.10	1.70	1.10	2.10 :1
14	1.00	2.15	1.70	1.10	2.15 :1
15	1.00	2.20	1.70	1.10	2.20 :1

It was also found that sol-gel films derived from TMOS alone or with DiMe-DMOS : TMOS volume ratio less than 1.5:1.0 v/v shrinks significantly and peel off easily from the treated polystyrene surface after condensation. Therefore, only ORMOSIL with DiMe-DMOS:TMOS ratios in the range of 1.5:1.0 to 2.2:1.0 give films that adhere strongly on the polystyrene surface. It is known that the surface of the tissue-culture-treated polystyrene microtiter plates from Corning has been modified by corona discharge or gas-plasma to give oxygen-containing (e.g. hydroxyl) functional groups [219]. Although most sol-gel derived materials do not adhere on polystyrene surface, Dislich reported that certain sol-gel films can be formed on treated polystyrene surface through covalent bond formation between the hydroxyl groups on treated polystyrene and the alkoxy silane during condensation [220]. It was found that the ORMOSIL films derived from DiMe-DMOS/TMOS adhere firmly on treated polystyrene surface, which is probably a result of both covalent bond formation between the hydroxyl groups on polystyrene and the alkoxy silane as well as hydrophobic interaction between the organic groups in ORMOSIL and the polystyrene surface. As a control experiment, the adhesion of the ORMOSIL films on untreated polystyrene microtiter plates has also tested and confirmed that the DiMe-DMOS/TMOS derived films do not adhere on untreated polystyrene surface.

The optimal composition of the ORMOSIL film is a compromise between adhesion, curing time and sensitivity of the resulting film. The response of the film towards oxygen quenching increases with the organic content of the ORMOSIL film due to the improvement in hydrophobicity and oxygen diffusivity [88]. However, addition of excess DiMe-DMOS in the fabrication of the sensing films will lead to exceedingly long curing time. As a result, an optimal DiMe-DMOS : TMOS volume ratio of 2.15:1.0 was used to fabricate the oxygen sensing films in this study. The photograph of a 96-well microtiter plate partly coated with ORMOSIL oxygen sensing films is shown in Figure 2.2.



Figure 2.2 A 96-well microtiter plate with some of the microwells coated with ORMOSIL oxygen sensing films.

2.3.1.2 Effect of hydrochloric acid concentration

Hydrochloric acid (HCl) was used as a catalyst in the hydrolysis of sol-gel. This is an important step in controlling the rate of film formation. When the concentration of HCl is over 0.01M, the rate of polycondensation is very rapid which makes the liquid sol mixed poorly (emulsion formation) with the $[\text{Ru}(\text{dpp})_3]\text{Cl}_2$ solution. When the rate of hydrolysis and condensation are too fast, shrinkage of the film becomes very serious and it detaches from the bottom surface of the well. Therefore, 0.01M HCl was chosen for fabrication of crack-free ORMOSIL oxygen sensing films with good adhesion in a relatively short period of time.

2.3.1.3 Optimum volume of sol-gel solution for fabrication of ORMOSIL oxygen sensing films in the microwells of microtiter plate

As the film thickness affects the response time of the sensing film, it should be as thin as possible. The optimum volume of sol-gel solution for fabrication of films in the microwells can be judged from the phosphorescence of the film measured at the bottom of the wells. When the volume of the sol is not sufficient to completely cover the bottom of wells, phosphorescence will only be detected at the

periphery of the well. The oxygen sensing films are thicker at the periphery of the well than at the center due to capillary action between the sol and the wall of the microtiter plate, as evidenced by the higher luminescence intensity at the periphery. Figure 2.3 shows how different volumes of sol added affect the phosphorescence of the film. The minimum volume of sol-gel solution which can cover the whole well bottom was found to be 32 μl . The film thickness at the centre was estimated to be less than 10 μm based on the volume of sol used. This volume of sol was selected for subsequent fabrication of oxygen sensing films.

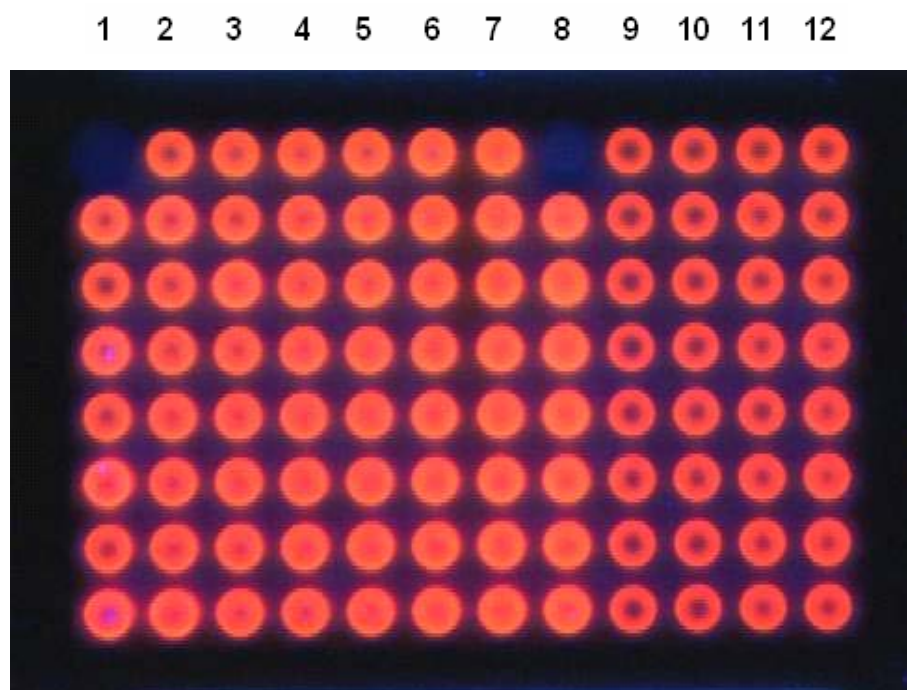


Figure 2.3 The effect of addition of different volumes of sol on the phosphorescence of the sensing films (volume of sol added from column 1 to 8: 30, 31, 32, 33, 34, 35, 36, 37 μl ; column 9 to 12: 26, 27, 28, 29 μl ; the first well (top) in column 1 and 8 are empty). The ORMOSIL sensing films were illuminated under long wavelength UV light (366 nm).

2.3.1.4 Effect of methyl group content on the sensitivity of the oxygen sensing film

The optimal composition of sol-gel for the fabrication of oxygen sensing films should provide the highest sensitivity. The sensitivity of the sensing film can be expressed by the quenching response (Q_{DO}) and quenching ratio (I_0/I_{100} , where I_0 is the luminescence intensity at 100% N_2 and I_{100} is the luminescence intensity at 100% O_2); the higher the quenching response (or quenching ratio), the higher is the sensitivity. The effect of volume ratio of DiMe-DMOS to TMOS on the quenching response is shown in Figure 2.4. An increase in quenching response was observed with increased volume of DiMe-DMOS. A summary of the DiMe-DMOS:TMOS ratios effect on the Q_{DO} values is summarized in Table 2.2.

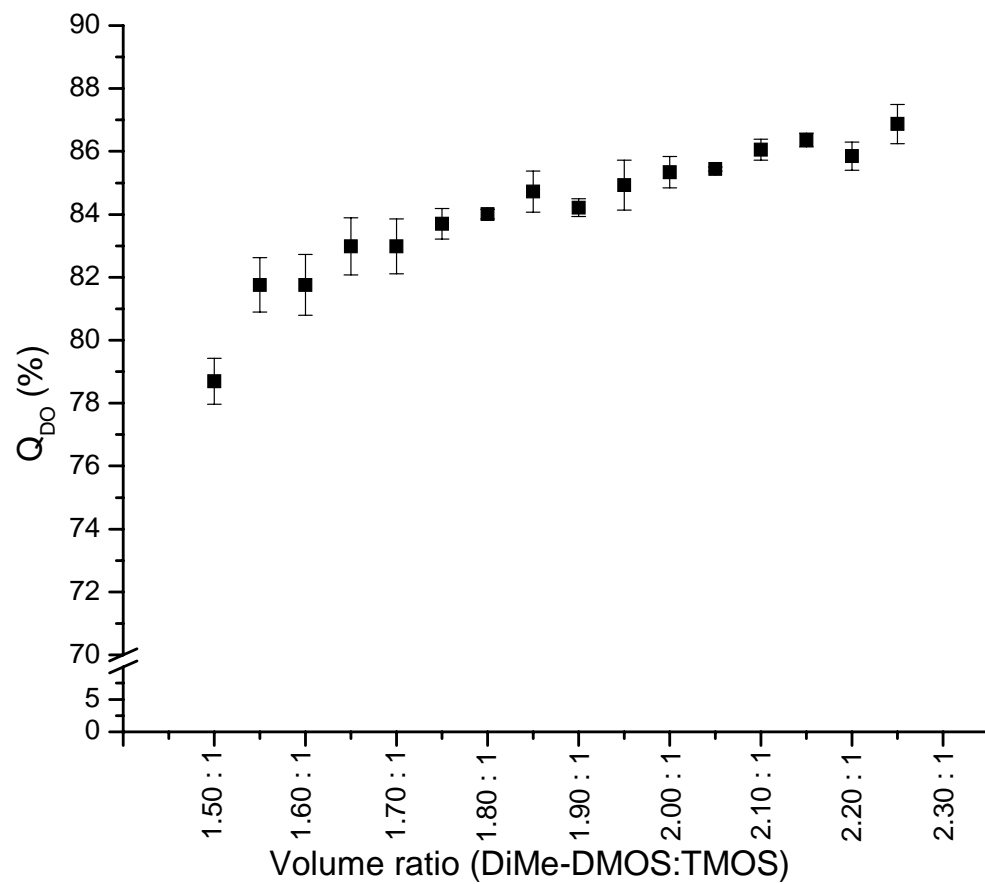


Figure 2.4 The effect of volume ratio of DiMe-DMOS to TMOS on the quenching response (Q_{DO}).

Table 2.2 A summary of the DiMe-DMOS : TMOS ratio vs. the quenching response in the ORMOSIL oxygen sensing film.

Composition DiMe-DMOS:TMOS (v/v)	Quenching response (%)
1.50 : 1	78.7 ± 0.7
1.55 : 1	81.8 ± 0.9
1.60 : 1	81.8 ± 1.0
1.65 : 1	83.0 ± 1.0
1.70 : 1	84.0 ± 0.9
1.75 : 1	83.7 ± 0.5
1.80 : 1	84.0 ± 0.2
1.85 : 1	84.7 ± 0.7
1.90 : 1	84.2 ± 0.3
1.95 : 1	84.9 ± 0.8
2.00 : 1	85.3 ± 0.5
2.05 : 1	85.4 ± 0.1
2.10 : 1	86.1 ± 0.3
2.15 : 1	86.4 ± 0.2
2.20 : 1	85.8 ± 0.4
2.25 : 1	86.9 ± 0.6

The increase in quenching response upon increasing the volume of DiMe-DMOS could be attributed to the improvement of porosity and hydrophobicity of the film. Since the alkyl groups of DiMe-DMOS can terminate the condensation reaction in sol-gel process, any unreacted alkyl groups (hydrophobic) will form pores inside the sol-gel film after gelation. As the volume of DiMe-DMOS increases, the porosity of the film also increases. Thus the ruthenium complex can easily get access to oxygen in the quenching process, and the quenching response will be improved. The ORMOSIL precursor improves the sensitivity (quenching response) of the sol-gel film due to the increased oxygen diffusivity and solubility in these more hydrophobic films. According to the quenching response, transparency, adhesion, etc., the optimum composition of the sol-gel film was found to be 2.15:1 (DiMe-DMOS:TMOS, v/v). Films fabricated under these conditions were used in subsequent studies to evaluate the performance of the optical oxygen sensor.

A comparison of the Q_{DO} and I_0/I_{100} values for $[\text{Ru}(\text{dpp})_3]^{2+}$ on different supports is given in Table 2.3. As shown in the table, the sensitivity of ORMOSIL film fabricated by DiMe-DMOS with TMOS is better than those fabricated by pure TEOS, TMOS, MTMS, MTEOS and ETEOS due to the higher porosity in the DiMe-DMOS/TMOS films. On the other hand, the hydrophobicity of

DiMe-DMOS films is higher than those of MTMS and MTES as there are two methyl groups in DiMe-DMOS whereas only one methyl group is present in MTMS and MTEOS. As the porosity and hydrophobicity increase, the oxygen gas can diffuse from aqueous solution into the sol-gel film more easily. Therefore, the sensitivity of ORMOSIL oxygen sensing film fabricated by DiMe-DMOS/TMOS composite is higher than those fabricated by MTMS/TEOS, MTEOS/TEOS and ETEOS/TEOS composite ORMOSIL. Besides, its sensitivity is comparably higher than other oxygen sensing films prepared by polystyrene, ethylcellulose, PVC and silicone polymer [65]. It can be concluded that DiMe-DMOS/TMOS composite is a good material for ORMOSIL oxygen sensors.

Table 2.3 A comparison of the Q_{DO} and I_0/I_{100} values for $[Ru(dpp)_3]^{2+}$ on different supports.

Matrix	Quenching ratio, I_0/I_{100}	Quenching response, Q_{DO} (%)	Reference
DiMe-DMOS : TMOS 2.15 :1 (v/v)	13.4 ± 0.6	86.4 ± 0.2	This work
100% TEOS	3.11		[117]
100% TEOS	8.4		[75]
50% TEOS / 50% MTMS	6.07		[117]
100% MTMS	10.17		[117]
polystyrene	2.0		[65]
ethylcellulose	3.0		[65]
PVC	3.6		[65]
silicone polymer	4.3		[65]
zeolite	3.5		[68]
silica	4.3		[68]
sol-gel	8		[116]
silicone rubber with silica (LM-130)	13.7		[76]
silicone rubber	6.31		[76]
100% TEOS		30	[129]
100% TMOS		71	[129]
100% MTMS		65	[129]
100% MTEOS		69	[129]
MTEOS : TEOS (1:1)		56	[152]

MTEOS : TEOS (2:1)	62	[152]
MTEOS : TEOS (3:1)	70	[152]
100% MTEOS	73	[152]
ETEOS : TEOS (1:1)	72	[152]
100% ETEOS	80	[152]

DiMe-DMOS = dimethoxy dimethylsilane

TMOS = tetramethoxysilane

TEOS = tetraethoxysilane

MTMS = methyltrimethoxysilane

MTEOS = methyltriethoxysilane

ETEOS = ethyltriethoxysilane

2.3.2 Stern-Volmer plots

The relationship between luminescence intensity and oxygen concentration is described by the Stern-Volmer equation 2.2 [25, 221]:

$$I_0 / I = 1 + K_{sv} [O_2] \quad (2.2)$$

where I_0 is the luminescence intensity in the absence of oxygen, I the luminescence intensity at the oxygen concentration $[O_2]$, and K_{sv} the Stern-Volmer constant. The Stern-Volmer plots of the ORMOSIL oxygen sensing film for dissolved and gaseous oxygen are shown in Figures 2.5 and 2.6 respectively. The solid line represents the best linear fit generated by the least-squares method. The plots show excellent linearity, which indicate negligible matrix heterogeneity effects and allow a simple two-point calibration for both of the dissolved and gaseous oxygen sensors. It is interesting to note that two-point calibration is often adopted as an approximation to generate the calibration curve for polymer-based oxygen sensors on microplates [90, 163, 171, 172, 174], even though the Stern-Volmer plots in these systems are not strictly linear. In this aspect, the ORMOSIL oxygen sensor platform offers a distinct advantage over the commercial product. The linearity of the Stern-Volmer

plot may result from the homogeneous microenvironment when ORMOSIL films of appropriate composition are used [131]. It can be explained by the hydrophobic nature of the ORMOSIL which allows the $[\text{Ru}(\text{dpp})_3]^{2+}$ with its hydrophobic dpp ligands to distribute more uniformly in the sol-gel matrix. As a result, all $[\text{Ru}(\text{dpp})_3]^{2+}$ molecules are dispersed in a very similar microenvironment within the sol-gel. Furthermore, DiMe-DMOS has two methyl groups, which do not undergo hydrolysis throughout the sol-gel process. These two methyl groups inside the structure provide higher porosity and hydrophobicity. As the pores serve as oxygen channels to the ruthenium dyes entrapped in the matrix, and oxygen has a higher affinity for hydrophobic surface, this may also contribute to the linear response of the oxygen sensor.

The standard deviation of luminescence intensity for films in different wells as determined by the I_0 value and the I_0/I_{100} quenching ratio (I_0 is the luminescence intensity at 100% N_2 and I_{100} is the luminescence intensity at 100% O_2) are $\pm 8\%$ and $\pm 3\%$ respectively. As the contribution due to drift in light source intensity is evened out in the I_0/I_{100} [11], the deviation in luminescence intensity due to non-uniform thickness is about $\pm 3\%$. The detection limit of this sensor, taken as the concentration of dissolved oxygen to produce an analytical signal equal to $I_0/(I_0-3S)$

(S/N ratio = 3, I_0 = mean luminescence intensity in N_2 -saturated water and S is the standard deviation) is about 0.05 mg l^{-1} , which is close to that of the silicone rubber based oxygen sensors [99].

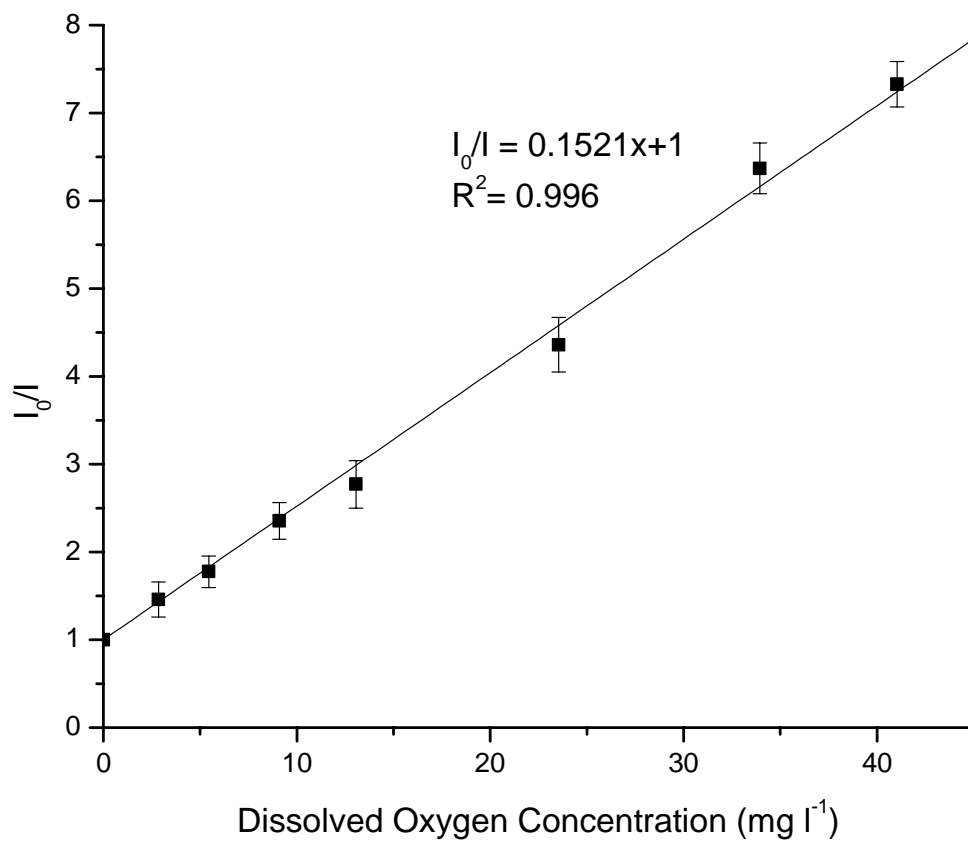


Figure 2.5 Stern-Volmer plot of the [Ru(dpp)₃]Cl₂ immobilized in ORMOSIL sensing films for dissolved oxygen.

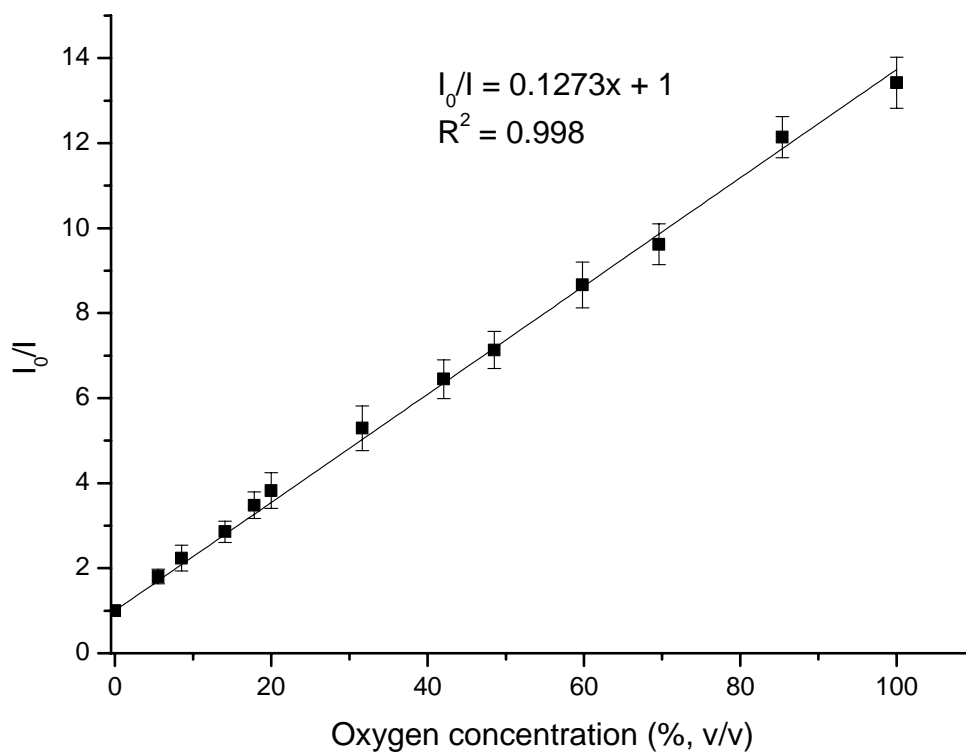


Figure 2.6 Stern-Volmer plot of the $[\text{Ru}(\text{dpp})_3]\text{Cl}_2$ immobilized in ORMOSIL sensing films (DiMe-DMOS : TMOS = 2.15 : 1.0) for gaseous oxygen.

2.3.3 Leaching of ruthenium complex from ORMOSIL films

Dye leaching is a common shortcoming of sensors based on entrapped dyes. As the optical oxygen sensor is used for measuring dissolved oxygen concentration in liquid samples, it should be able to resist the leaching of sensing material to the aqueous and organic environment. The leaching of ruthenium complex in different aqueous solutions of different pH and organic solvents was studied.

There was no observation of ruthenium complex leaching out from ORMOSIL films in pH buffers (0.1M pH 1.5, pH 7 and pH 8.9 phosphate buffers) or deionized water over three weeks. This may be due to the fact that sol-gel is a highly cross-linked three-dimensional polymer and the pores can trap the complex molecules effectively without leaching. Furthermore, the hydrophobicity of the film protects the complex from leaching into the aqueous solution.

The ORMOSIL films can also tolerate organic solvents such dimethyl sulfoxide, acetonitrile and ethanol at concentrations up to about 10 %, 5% and 2% (v/v) respectively without damage of film surface or leaching of the ruthenium dye (Figure 2.7). However, there is leaching of ruthenium dye when the concentration

of the organic solvent is greater than the concentrations mentioned above, at which swelling of the ORMOSIL films by the organic solvent can be observed.

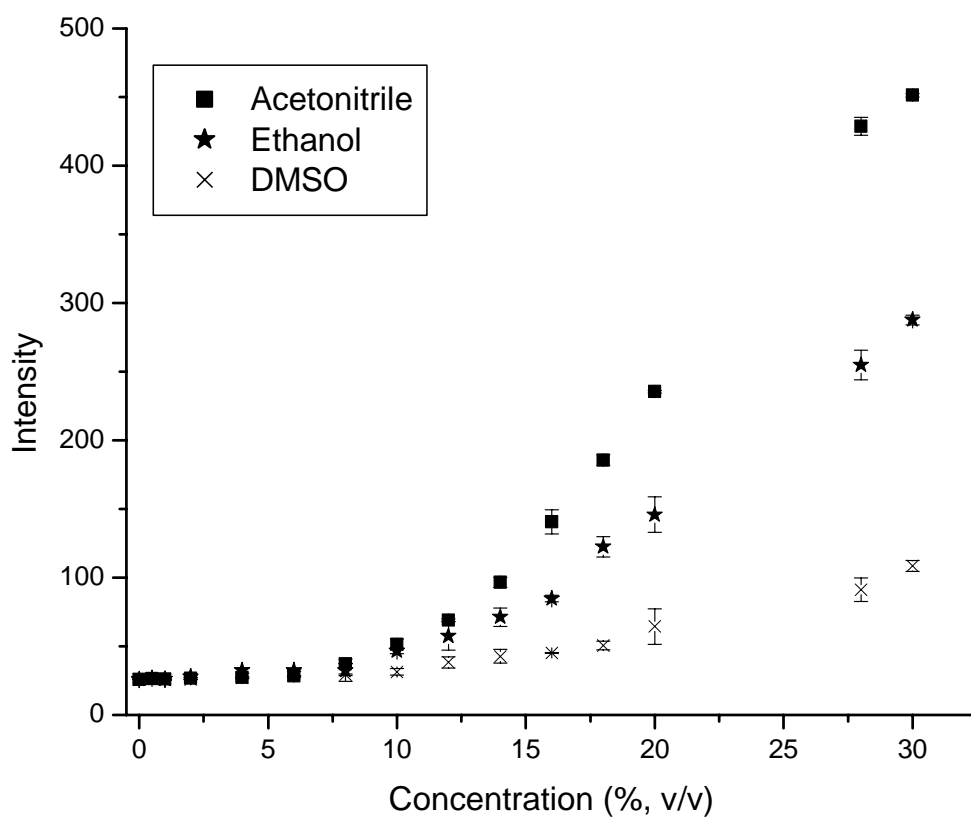


Figure 2.7 Leaching of [Ru(dpp)₃]Cl₂ from ORMOSIL films (DiMe-DMOS : TMOS

= 2.15 : 1.0) in aqueous solution of organic solvents of different concentrations.

2.3.4 Stability of the ORMOSIL films

2.3.4.1 Photostability of the ORMOSIL films

$[\text{Ru}(\text{dpp})_3]\text{Cl}_2$ is known to be a relatively stable dye towards photochemical degradation [11]. Under the experimental conditions, the immobilized $[\text{Ru}(\text{dpp})_3]^{2+}$ was irradiated at its excitation wavelength (460 nm) for 16 h and the change in luminescence intensity with time is shown in Figure 2.8. There was no significant photo-bleaching of $[\text{Ru}(\text{dpp})_3]^{2+}$ over the whole period of illumination. It implies that the complex has high photostability and is a good choice for oxygen sensing material.

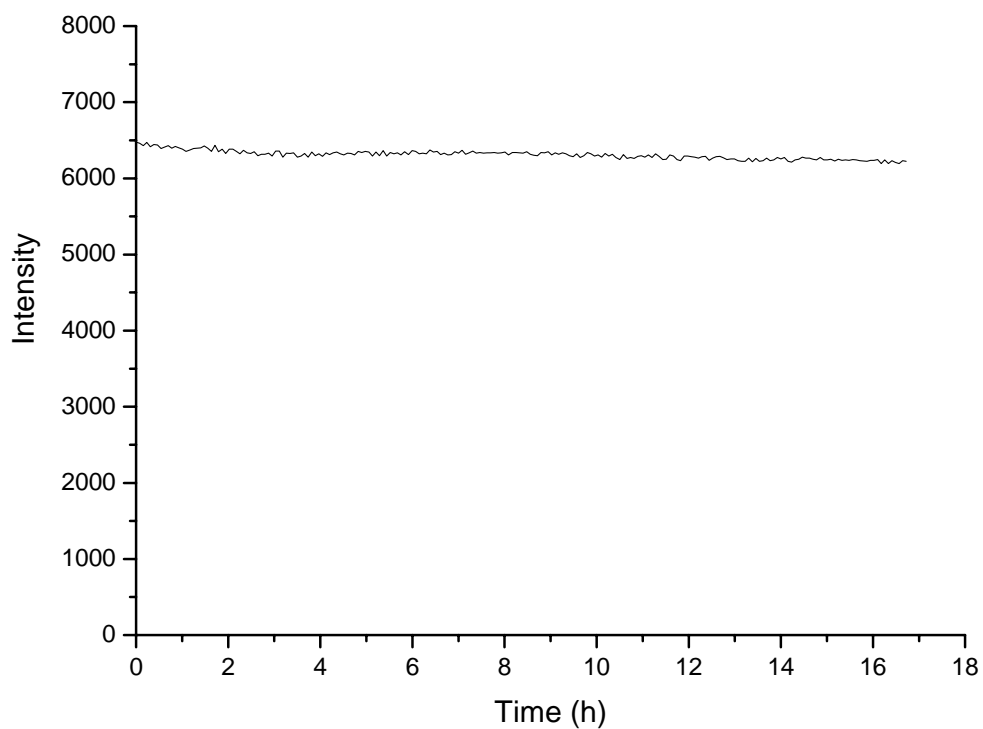


Figure 2.8 The photostability of the ORMOSIL film (DiMe-DMOS : TMOS = 2.15 :

1.0) immobilized with $[\text{Ru}(\text{dpp})_3]\text{Cl}_2$ (excitation wavelength, 460 nm; emission

wavelength, 610 nm).

2.3.4.2 Long-term stability of the ORMOSIL films

A good oxygen sensor must provide a stable response with high reproducibility. The quenching response of the ORMOSIL films was monitored over a period of 110 days. In between measurements the film was stored in darkness. As shown in Figure 2.9, there is no significant change in the quenching response over the whole period. The ORMOSIL film exhibits good long-term storage stability which can be attributed to the chemical inertness and stability of sol-gel (no interaction with other substances / contaminants) during measurement and storage.

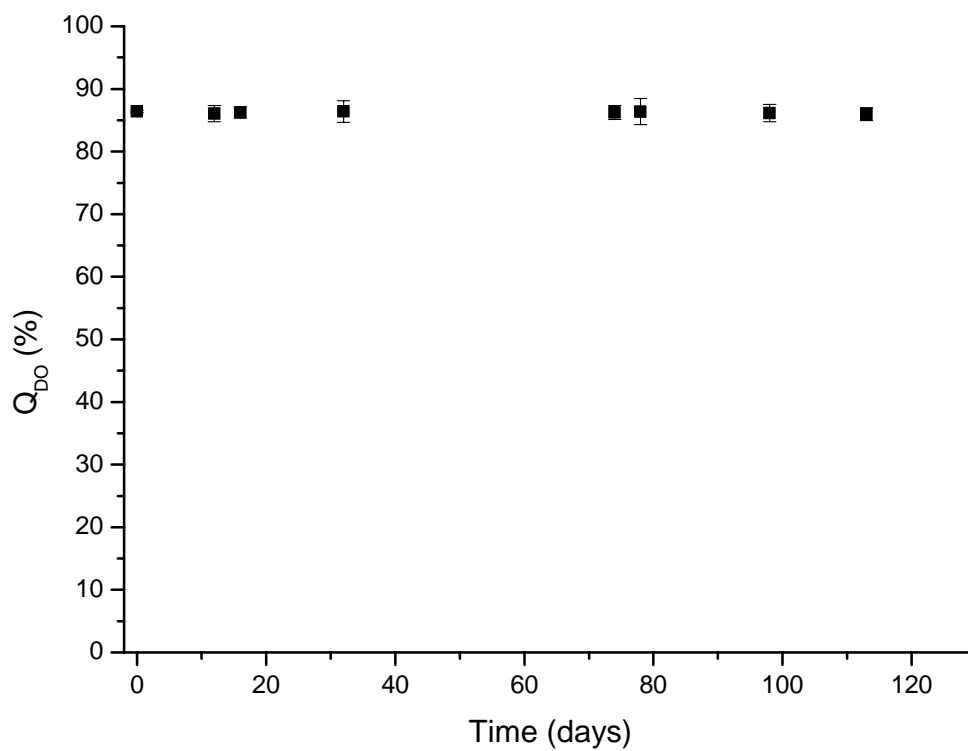


Figure 2.9 The long-term stability of the ORMOSIL film immobilized with [Ru(dpp)₃]Cl₂ (excitation wavelength, 460 nm; emission wavelength, 610 nm).

2.4 Concluding Remarks

Sol-gel is a suitable matrix for fabrication of oxygen sensors due to its high oxygen permeability, thermal stability, photostability and chemical inertness. A simple and convenient method for the fabrication of ORMOSIL optical oxygen sensors on polystyrene microtiter plates has been presented and which can be done in most laboratories. The quenching ratio I_0/I_{100} (13.4 ± 0.6) and quenching response (86.4 ± 0.2 %) of this ORMOSIL oxygen sensing film are superior over other oxygen sensing films. The oxygen sensors yielded linear Stern-Volmer plots which allow simple two-point calibration. This sensing film was subsequently utilized for a cell-based screening assay and BOD determination the results of which will be discussed in chapters 3 and 4 respectively.

Chapter 3

Application of the $[\text{Ru}(\text{dpp})_3]^{2+}$ -Entrapped Organically Modified Silicate (ORMOSIL) Oxygen Sensing Films on Microtiter Plate for IC_{50} Determination of Drugs on a Heterologous Yeast Model

3.1 Introduction

Oxygen consumption by microorganisms and aerobic cells is an important indicator of their metabolic activity and state of growth. Monitoring and measurement of dissolved oxygen concentration in cell cultures is thus of interest for drug screening, cell cultivation, toxicity tests and environmental analysis. With the ever increasing number of samples and the limited availability of microbial cells and expensive biochemicals, there is a need to develop high throughput systems for multi-sample analyses with small sample volumes. Rapid determination of IC_{50} (Inhibitory Concentration at 50%) of drugs on various microorganisms is important in drug screening. The conventional optical density method for IC_{50} determination is an end point method and cannot give information on the process of cell deactivation [176]. Besides, it can be easily interfered by color or turbidity in the cell culture.

In Chapter 2, a simple and convenient method for the fabrication of ORMOSIL optical oxygen sensors on polystyrene microtiter plates has been described. This sensor exhibits a linear Stern-Volmer relationship which allows simple two-point calibration. The determination of oxygen concentration by this

biosensor has certain distinct advantages over other oxygen sensing films. The application of this oxygen sensing microplate in the determination of IC_{50} values of some antimalarial drugs on a heterologous yeast model will be discussed in this chapter.

3.2 Experiment Section

3.2.1 Materials

[Ru(dpp)₃]Cl₂ (dpp = 4,7-diphenyl-1,10-phenanthroline) was synthesized and purified in our laboratory according to a literature method[214]. Tetramethyl orthosilicate (TMOS, 98%), and dimethoxy dimethylsilane (DiMe-DMOS, 95%) were purchased from Aldrich. Fine graphite powder (extra pure) was purchased from Merck. Yeast-peptone-dextrose (YPD) broth was purchased from USB Corp. Yeast nitrogen base and amino acid supplement mixture were purchased from Qbiogene. The antimalarial drugs, chloroquine (CQ) and quinacrine (QNC), were obtained from Sigma. Oxygen and nitrogen gases (99.7 % purity) were purchased from Hong Kong Oxygen Company. Microtiter plates (no. 3603, 96 wells, flat clear bottom black polystyrene, TC-treated) were obtained from Corning. Aluminum microplate sealing foils were obtained from USA Scientific. All aqueous solutions were prepared in double deionized water (Milli-Q). All other chemicals and solvents were of analytical-reagent grade and were used without further purification.

3.2.2 Preparation of oxygen sensing films on microtiter plate

A solution of $[\text{Ru}(\text{dpp})_3]\text{Cl}_2$ in ethanol (2.85 mg ml^{-1}) was prepared. The silica sol was prepared by mixing TMOS, DiMe-DMOS, 0.1M HCl and deionized water in the volume ratio of 1.0:2.15:1.7:1.1. The sol mixture was stirred at 500 rpm for 3.5 hours at $25 \text{ }^\circ\text{C}$ in a water bath. The sol was then centrifuged at 7500 rpm (Beckman Coulter, centrifuge model: Allegra 64R, rotor: C0650) for 4 minutes. The thickened sol at the bottom of the centrifuge tube (1 ml) was pipetted out and thoroughly mixed with 250 μl of the ruthenium complex solution. Portions (32 μl) of the sol-ruthenium mixture was then transferred to each well of the microtiter plate and allowed to stand for six days at room temperature in dark for gelation and drying. A light-insulating layer of graphite-containing sol-gel coating was placed on the top of the oxygen sensing film to eliminate scattered light and background luminescence from sample solution. This light-insulating coating was prepared by pipetting 15 μl of a mixture of thickened sol (1 ml), graphite (0.1 g) and 0.1 M phosphate buffer (pH 7.0, 50 μl) onto the surface of each of the gelatinized oxygen sensing film and allowed to stand for another 6 days. After gelation, the microtiter plate was stored from direct light prior to use. A schematic diagram of the biosensor is shown in Figure 3.1.

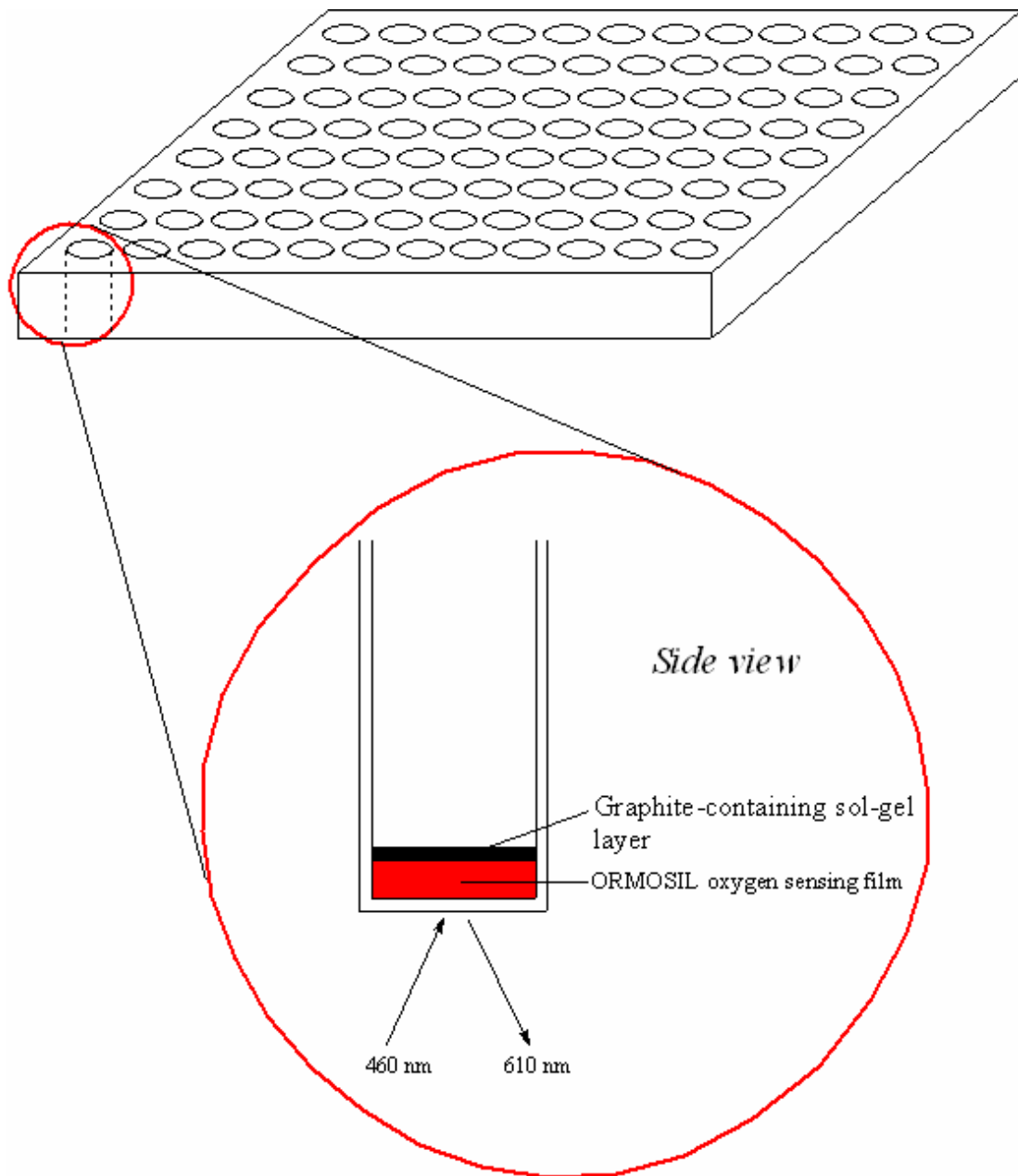


Figure 3.1 A schematic diagram showing the oxygen sensing part of the biosensor.

3.2.3 Instrumentation

Luminescence measurements were conducted on a BMG Labtech POLARstar microplate reader connected to a microcomputer. The center wavelengths of bandpass filters used for excitation and emission were 460 nm and 610 nm respectively. The luminescence intensity was measured in the bottom plate reading configuration and at room temperature. Absorbance monitoring of yeast cell growth was performed on a Bio-Rad model 550 microplate reader.

3.2.4 Yeast strains

The yeast (*Saccharomyces cerevisiae*) strains YPH 499(pYX113), YHW 1052(pYX113) and YRP 3 used in this study were obtained from Dr. Larry M.C. Chow. This is a well-defined heterologous yeast model used to address the problem of drug resistance [222]. The yeast strains YHW 1052 (*Dpdr5::TRP1*, *Dsnq2::hisG*, *Dpdr10::hisG*) and YRP 3 (*Dpdr5::TRP1*, *Dsnq2::hisG*, *Dste6::hisG*, *Derg6::LEU2*) were utilized for this study along with its isogenic parental strain YPH 499 (*MATa ade2-101oc*, *his3D200*, *leu2-D1*, *lys2-801am*, *trp1-D1*, *ura3-52*).

Strain YPH 499 is a wild type and is refractory to drug substrates. Strain YHW 1052 is a mutant with deletions in the *PDR5*, *PDR10*, and *SNQ2* multidrug resistance genes and is thus more susceptible to drug substrates. Strain YRP 3 is another mutant with the *PDR5*, *SNQ2*, *STE6* and *ERG6* genes deleted. *ERG6* is a special gene responsible for synthesizing the plasma membrane lipid ergosterol on the yeast plasma membrane. Deleting this gene would result in a 'leakage' on the plasma membrane and therefore allowing drug substrates to enter the yeast cell. YRP 3 is therefore very sensitive to all kinds of drugs.

3.2.5 Preparation of culture media and antimalarial drug solutions

The yeast-peptone-dextrose (YPD) medium was prepared by dissolving YPD broth powder in deionized water followed by autoclaving at 121 °C for 20 minutes. The YPD medium used in all experiments was made up to a final concentration of peptone (20 g l⁻¹), yeast extract (10 g l⁻¹) and D-glucose (20 g l⁻¹). This YPD medium was used for all experiments with chloroquine (CQ).

As quinacrine (QNC) is insoluble in the presence of uracil, the synthetic complete medium minus uracil (SC-Ura) [223] was prepared for all experiments with

QNC. The SC-Ura medium was made up to a final concentration of yeast nitrogen base (1.7 g l^{-1}), ammonium sulfate (5 g l^{-1}), D-glucose (20 g l^{-1}) and amino acid supplement mixture (0.8 g l^{-1}). It was sterilized by autoclaving at 121°C for 20 minutes before use.

Stock solutions of chloroquine (200 mg ml^{-1}) and quinacrine (20 mg ml^{-1}) in deionized water were prepared. The solutions were then sterilized by filtration through a cellulose or nylon syringe filter of $0.2 \text{ }\mu\text{m}$ pore diameter. Various concentrations of CQ and QNC solutions were prepared by dilution of the stock solutions with sterilized deionized water.

3.2.6 Incubation of yeast cell

Single colony of yeast was inoculated into 5 ml of sterilized YPD or SC-Ura medium. The above operation was performed with aseptic technique with the assistance of a Bunsen flame. The culture was then incubated for 24 h at 30°C and 250 rpm.

3.2.7 Calibration of biosensor

Each well of microtiter plate with the oxygen sensing film was calibrated by two-point calibration (air saturated water [224] and deoxygenated water by chemical removal [215, 216]) with the Stern-Volmer equation 3.1.

$$I_0/I = 1 + K_{sv} [O_2] \quad (3.1)$$

3.2.8 Determination of IC₅₀ values by measurement of dissolved oxygen concentration

After incubation of yeast cell, the concentration of yeast cells in culture medium was checked by measuring the absorbance at 595 nm (OD₅₉₅) with a 1 cm path length cuvette. The cell culture was then diluted to an absorbance of 0.01 with YPD or SC-Ura medium. The diluted cell culture (125 µl) and antimalarial drug solution of various concentrations (125 µl) were added to each well of the microtiter plate to make up a final volume of 250 µl. The control consisted of 125 µl diluted cell culture further diluted to 250 µl with sterilized deionized water. The microtiter

plate was then sealed with an aluminum microplate sealing foil to minimize the interference from atmospheric oxygen.

The dissolved oxygen concentration recorded as luminescence intensity was plotted against incubation time. The growth rate (R) of yeast was taken as the slope between the beginning of the plateau baseline in the oxygen depletion curve to the point at which 2 mg l⁻¹ of dissolved oxygen had been consumed. The percentage inhibition, I (%), of the drug solution on the growth rate of the yeast cells was calculated from equation (3.1):

$$I (\%) = [(R_c - R_t) / R_c] \times 100\% \quad (3.2)$$

where R_c and R_t represent the growth rate of the control and the testing sample respectively. The IC₅₀ value (drug concentration which produced 50% inhibition of growth rate) was obtained from the plot of I (%) versus drug concentration.

3.2.9 Determination of IC₅₀ values by the optical density (OD₅₉₅) method

The sample was prepared in the same as in 3.2.8, except that there was a blank needed for background absorbance measurement. The covered microplate was incubated in an oven at 30 °C for 48 h. After the incubation, the absorbance at 595nm under various drug concentrations was measured by a Bio-Rad model 550 microplate reader and subtracted from the blank.

The IC₅₀ value can also be obtained from the plot of percentage of relative growth versus the drug concentration. The IC₅₀ value was found by determining the 50% relative growth. The percentage of relative growth can be calculated by equation 3.2:

$$\text{Relative growth (\%)} = [(\text{OD}_{595} \text{ with drug} / \text{OD}_{595} \text{ of control})] \times 100\% \quad (3.3)$$

3.3 Results and Discussion

3.3.1 Determination of IC₅₀ values of antimalarial drugs by measurement of dissolved oxygen concentration

The performance of the oxygen sensors in the determination of IC₅₀ values of drugs was tested on a well-defined heterologous yeast model. The yeast strains YPH 499(pYX113), YHW 1052(pYX113) and YRP 3 in this model have different levels of resistance towards antimalarial drugs [222]. The change in dissolved oxygen concentration during the incubation of yeast cells in the presence of chloroquine (CQ) or quinacrine (QNC) was monitored. The luminescence intensity was converted to dissolved oxygen concentration by equation (3.1) and plotted against the incubation time to give the oxygen depletion curves.

3.3.1.1 Determination of IC₅₀ values of chloroquine (CQ)

The chloroquine (CQ) resistance level of different yeast strains, YPH 499(pYX113), YHW 1052(pYX113) and YRP 3, was studied. During the incubation of the yeasts in different concentrations of CQ, the luminescence intensity

was measured and recorded simultaneously. Then the luminescence intensity was converted to dissolved oxygen concentration by equation (3.1) and plotted against the incubation time to give the oxygen depletion curves in Figures 3.2 to 3.4.

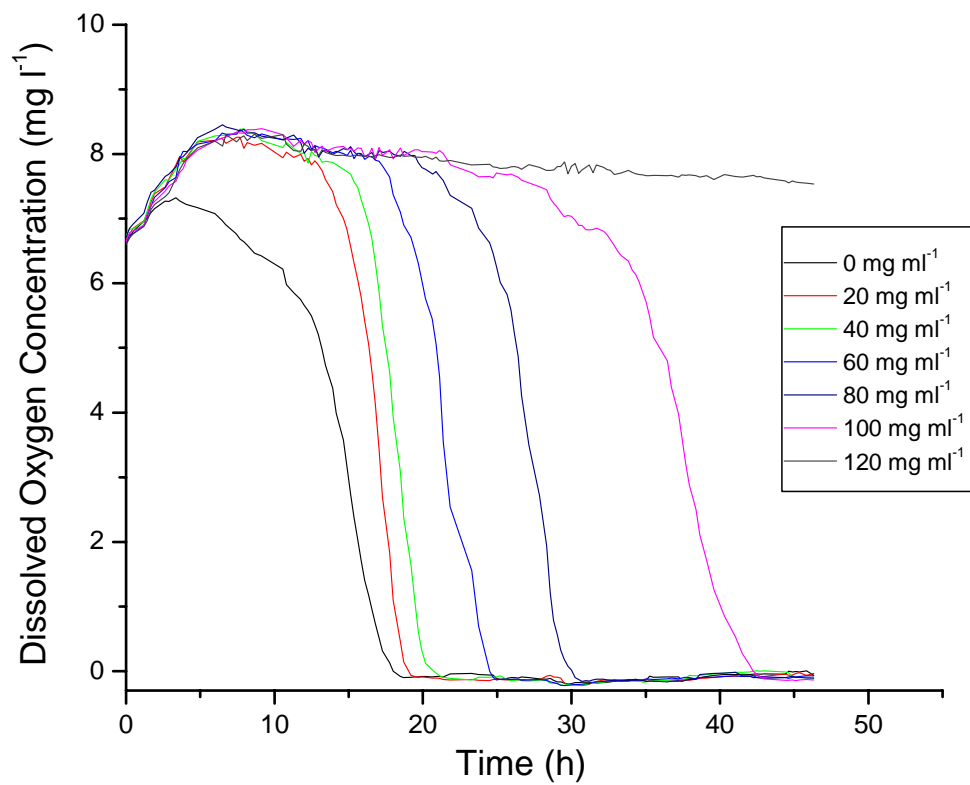


Figure 3.2 Incubation of the yeast strain YPH 499(pYX113) in different concentrations of chloroquine (CQ).

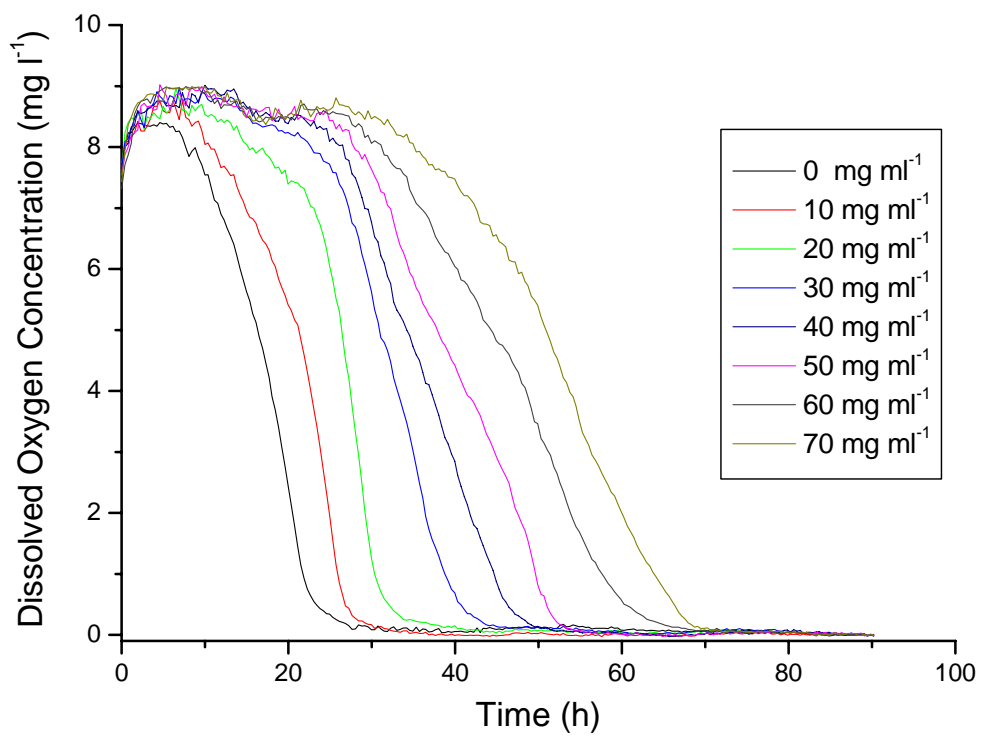


Figure 3.3 Incubation of the yeast strain YHW 1052(pYX113) in different concentrations of chloroquine (CQ).

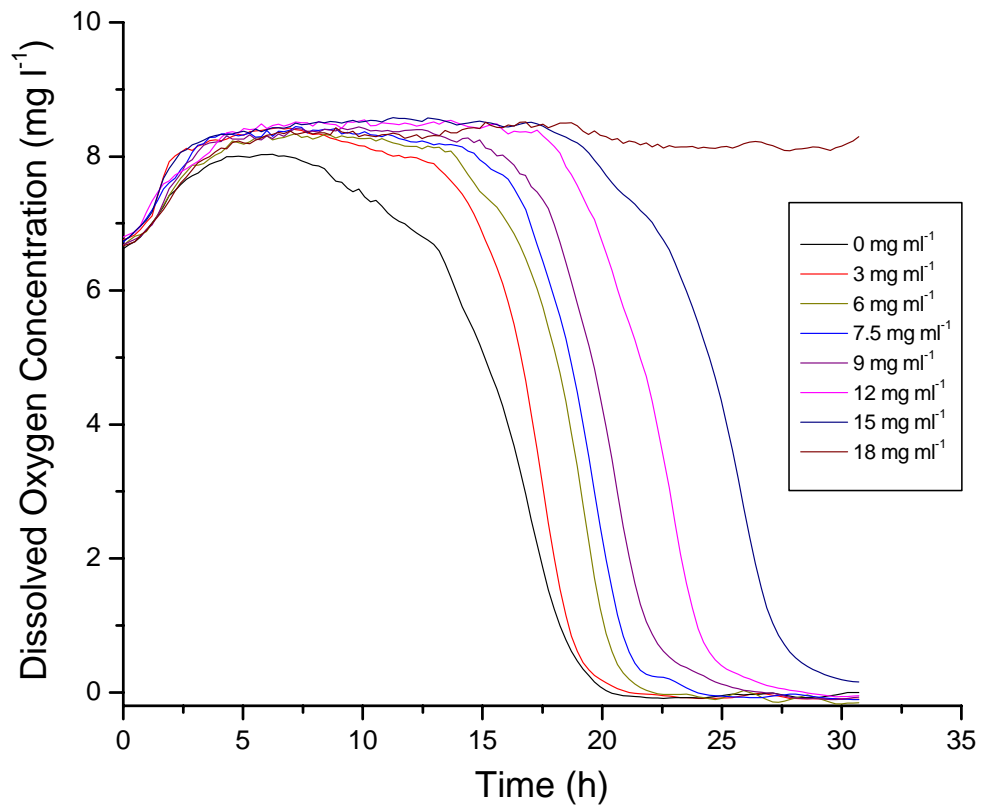


Figure 3.4 Incubation of the yeast strain YRP 3 in different concentrations of chloroquine (CQ).

At the beginning of experiment, there was an increase in dissolved oxygen concentration. This phenomenon is also observed in other commercially available polymer-based oxygen sensors on microtiter plates [172]. This increase in oxygen concentration is not due to hydration of the oxygen sensing films, as it cannot be eliminated by pre-soaking the oxygen sensors with water, phosphate buffer or the culture medium before measurement. On the other hand, pre-warming the oxygen sensing microtiter plate in an oven at 25 °C for 15 minutes can eliminate these humps in the oxygen depletion curves (Figure 3.5). Thus the initial increase in oxygen concentration can be attributed to the warming up of the microtiter plate in the microplate reader, which gave an increase in oxygen concentration due to increase in oxygen diffusion rate. The oxygen concentration then leveled off to a plateau before consumption by yeast cells took place. Due to the inhibition of growth of the yeast by the antimalarial drug, CQ, the yeast showed a delay in oxygen consumption that depended on CQ concentration. The oxygen levels in each well then declined gradually to 0% and stayed at this level. With increasing CQ concentration, the yeast cells grew more slowly, as indicated by the increasing delay time and decreasing oxygen consumption rate.

The growth rate was taken as the slope from the beginning of the plateau to

the data point where 2 mg l^{-1} of dissolved oxygen had been consumed. The concentration of CQ that produced 50% growth inhibition, IC_{50} , was obtained from the plots of percentage inhibition versus CQ concentration (Figures 3.6 to 3.8). The IC_{50} values of CQ for yeast strains YPH 499(pYX113), YHW 1052(pYX113) and YRP 3 are $68.0 \pm 7.5 \text{ mg ml}^{-1}$, $17.0 \pm 2.0 \text{ mg ml}^{-1}$ and $7.5 \pm 2.0 \text{ mg ml}^{-1}$, respectively.

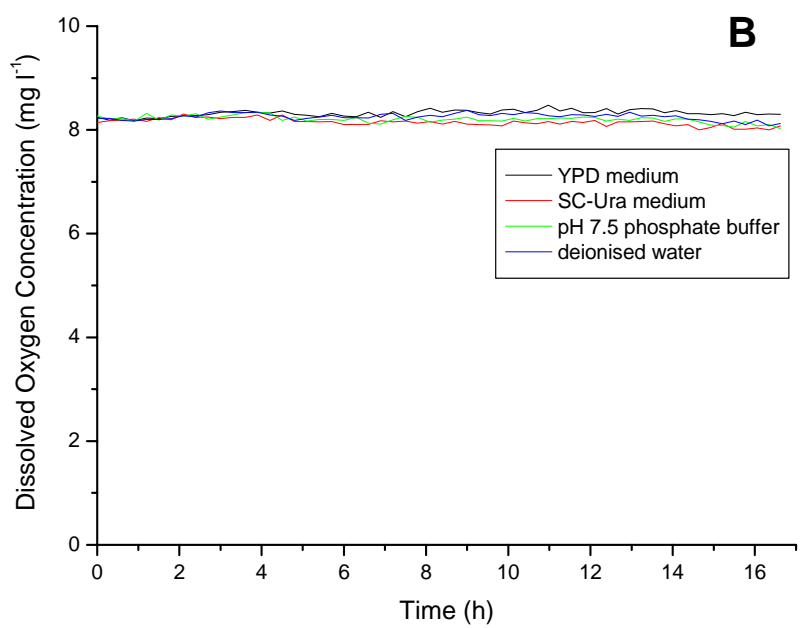
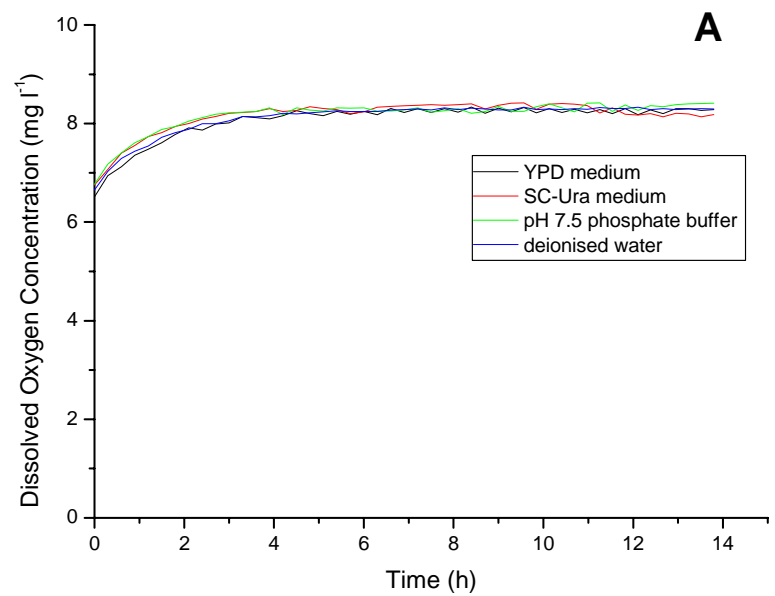


Figure 3.5 Effect of pre-warming the microtiter plate sensing platform before measurement. (A) Control without pre-warming and (B) with pre-warming at 25°C for 15 minutes.

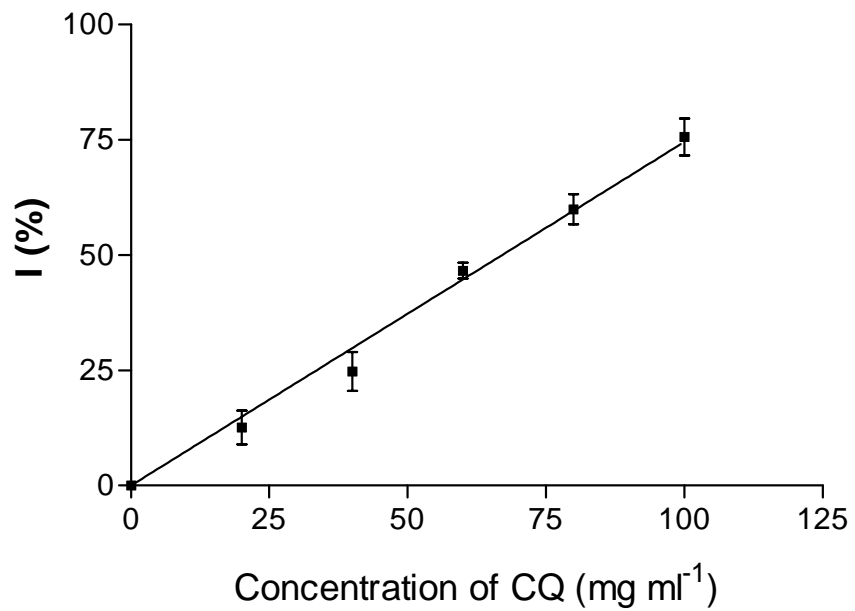


Figure 3.6 Plot of percentage inhibition in growth rate (I %) versus the concentration of chloroquine (CQ) for the yeast strain YPH 499(pYX113).

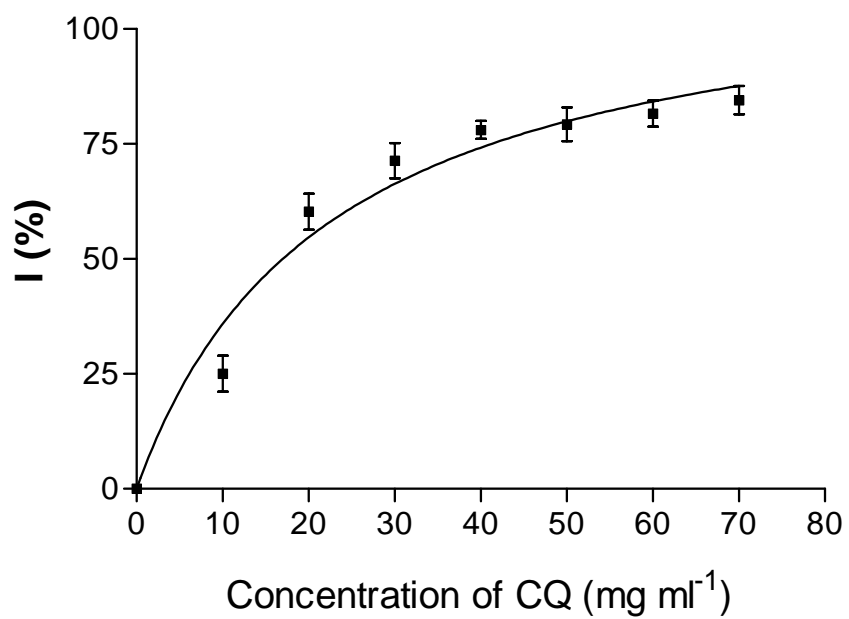


Figure 3.7 Plot of percentage inhibition in growth rate (I %) versus the concentration of chloroquine (CQ) for the yeast strain YHW 1052(pYX113).

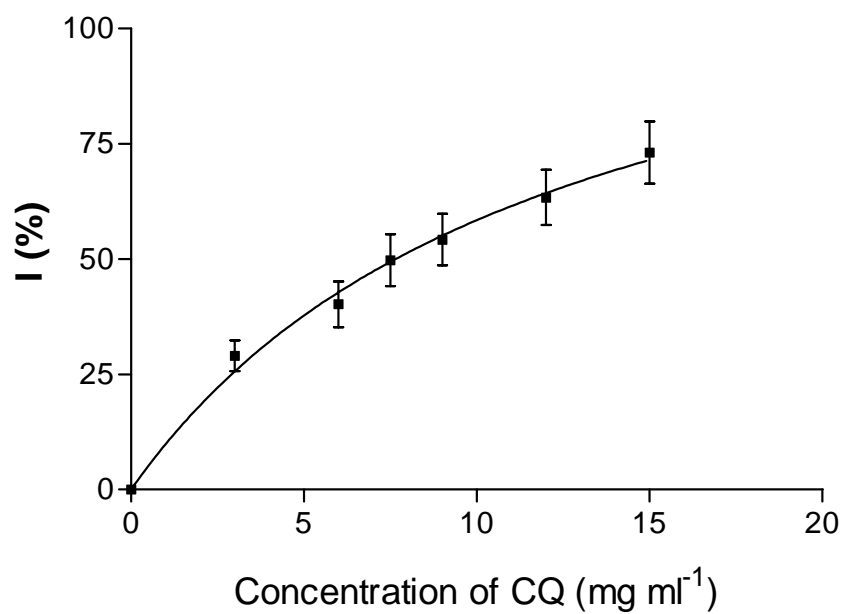


Figure 3.8 Plot of percentage inhibition in growth rate (I %) versus the concentration of chloroquine (CQ) for the yeast strain YRP 3.

3.3.1.2 Determination of IC₅₀ values of quinacrine (QNC)

As the yeast YRP 3 cannot grow in the SC-Ura medium, the IC₅₀ for quinacrine (QNC) was therefore not determined. The QNC resistance level of yeast strains, YPH 499(pYX113) and YHW 1052(pYX113), have been studied. The dissolved oxygen concentration measurement procedure was the same as in section 3.3.1.1 but the yeasts were incubated in different concentrations of QNC. The plots of dissolved oxygen concentration against incubation time are shown in Figures 3.9 to 3.10.

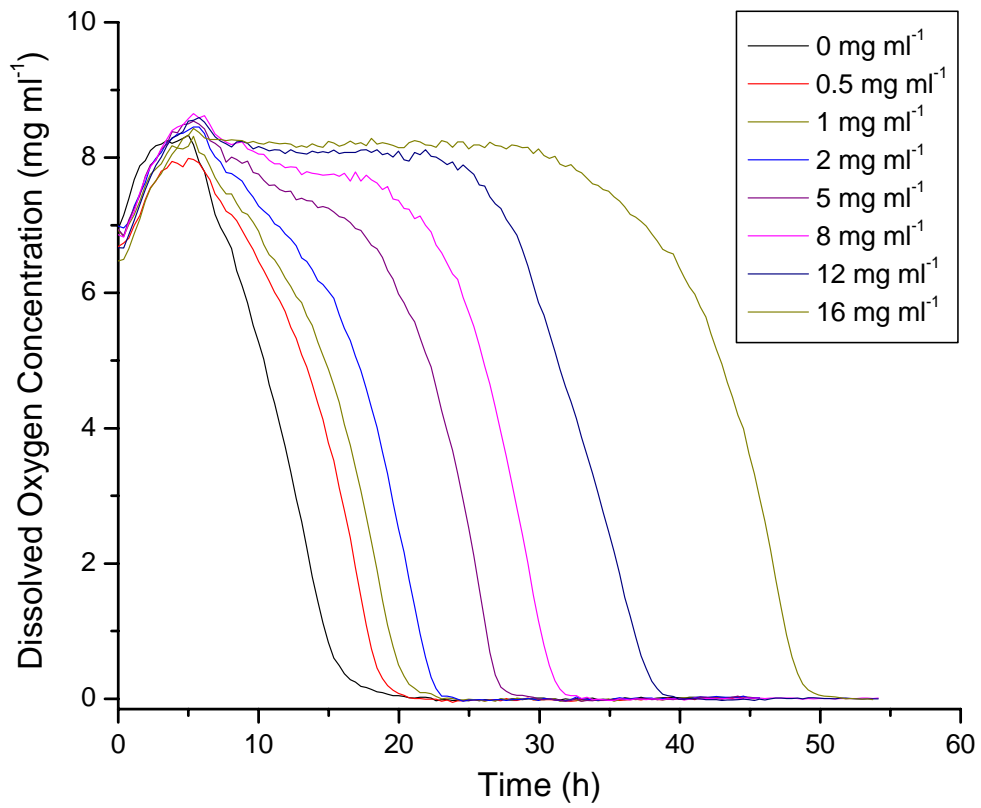


Figure 3.9 Incubation of the yeast strain YPH 499(pYX113) in different concentrations of quinacrine (QNC).

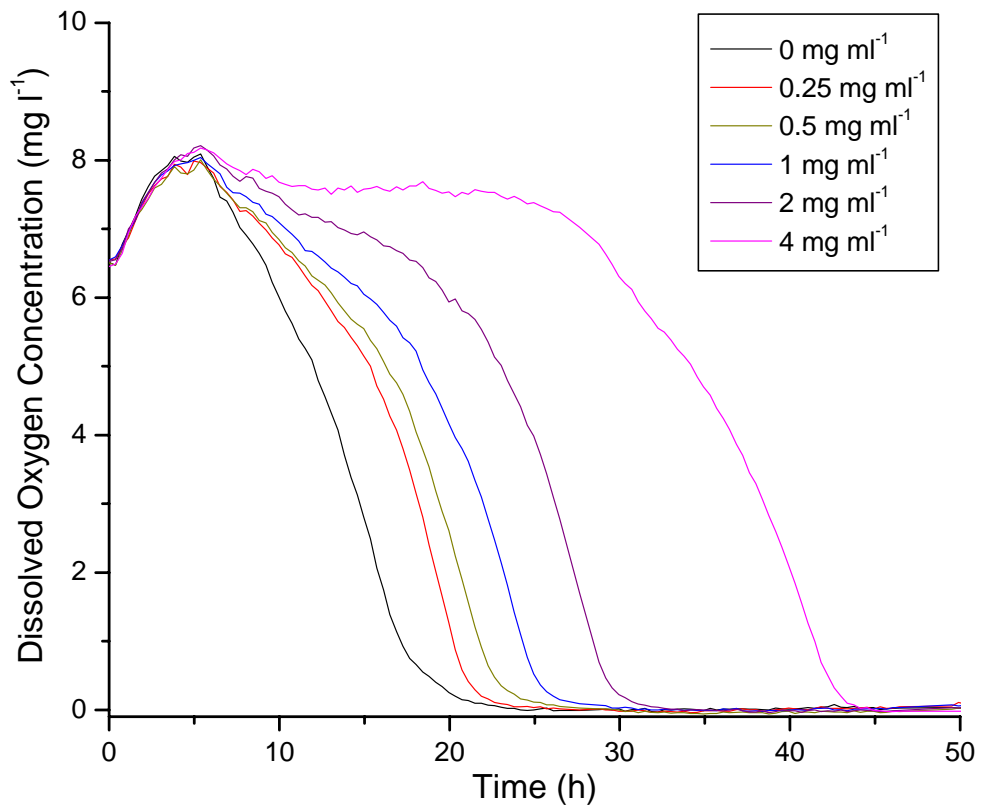


Figure 3.10 Incubation of the yeast strain YHW 1052(pYX113) in different concentrations of quinacrine (QNC).

The oxygen depletion curves were similar to those obtained from incubation of the yeast strains in the presence of chloroquine (CQ). The growth rate was taken as the slope from the beginning of the plateau to the data point where 2 mg l⁻¹ of dissolved oxygen had been consumed. The concentration of QNC that produced 50% growth inhibition, IC₅₀, was obtained from the plots of percentage inhibition versus QNC concentration (Figures 3.11 to 3.12). The IC₅₀ values of QNC for yeast strains YPH 499(pYX113) and 1052(pYX113) are 1.3 ± 0.2 mg ml⁻¹ and 0.6 ± 0.2 mg ml⁻¹, respectively.

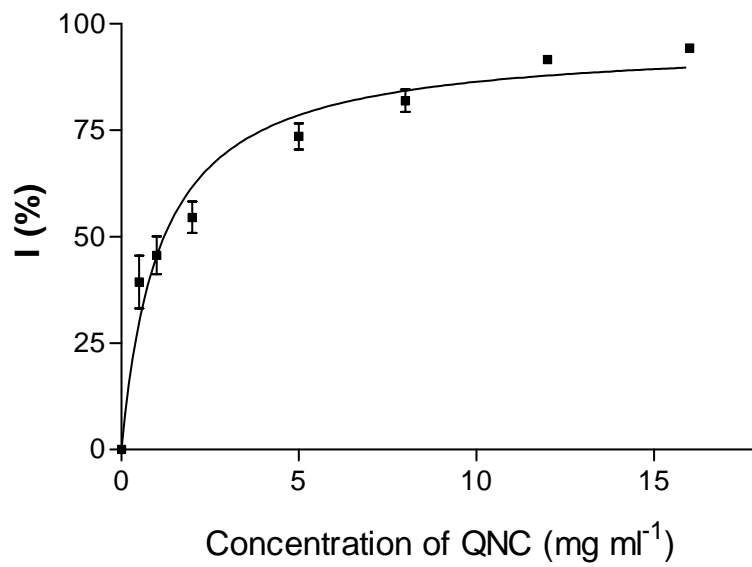


Figure 3.11 Plot of percentage inhibition in growth rate (I%) versus the concentration of quinacrine (QNC) for the yeast strain YPH 499(pYX113).

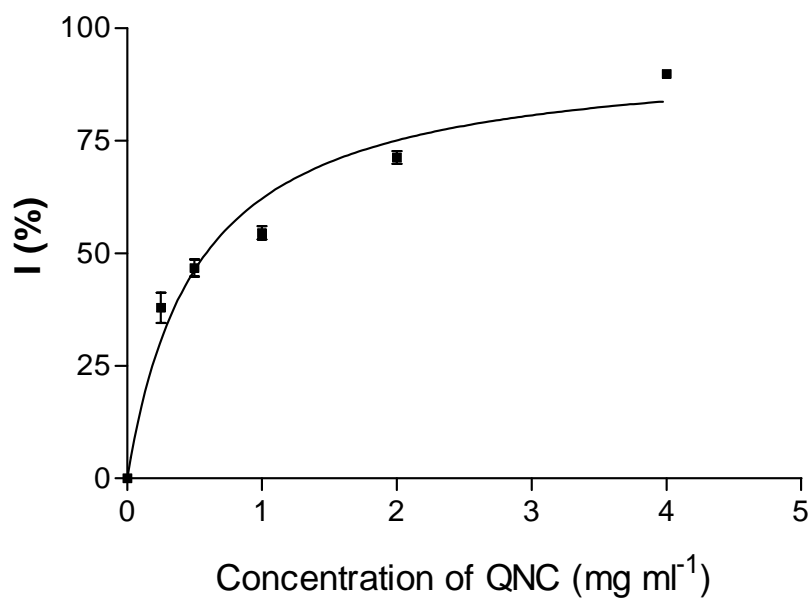


Figure 3.12 Plot of percentage inhibition in growth rate (I%) versus the concentration of quinacrine (QNC) for the yeast strain YHW 1052(pYX113).

3.3.2 Comparison of IC₅₀ values determined by optical oxygen sensors and conventional optical density (OD₅₉₅) method

The yeast strains YPH 499(pYX113), YHW 1052(pYX113) and YRP 3 were chosen because they have different tolerance to drug treatments. Yeast strain YRP 3 has the lowest drug resistance level because it has a gene (*ERG6*), which is responsible for synthesizing the plasma membrane lipid ergosterol on the yeast plasma membrane, deleted. Hence, in the absence of this ergosterol in YRP 3, drug substrates can enter the cell more easily. On the other hand, due to the deletion of three multidrug resistance genes (*PDR5*, *PDR10*, and *SNQ2*) in YHW 1052(pYX113), it is less resistant to drugs when compared to the wild-type parental strain YPH 499(pYX113). Therefore, the value of IC₅₀ for YHW 1052(pYX113) is lower than that for YPH 499(pYX113).

The IC₅₀ values obtained by the conventional optical density (OD₅₉₅) method are listed in Table 3.1 together with those obtained by the optical oxygen sensors. Table 3.1 shows clearly that the IC₅₀ values determined by the oxygen sensors are in agreement with those of the conventional optical density (OD₅₉₅) method. This is true for all three strains with different level of drug resistance. It is also true for

both drugs, CQ and QNC.

Table 3.1 A comparison of the IC₅₀ values obtained from the oxygen sensors and the conventional optical density (OD₅₉₅) method.

Method	YPH 499(pYX113)		YHW 1052(pYX113)		YRP 3
	IC ₅₀ of CQ	IC ₅₀ of QNC	IC ₅₀ of CQ	IC ₅₀ of QNC	IC ₅₀ of CQ
	(mg ml ⁻¹)	(mg ml ⁻¹)	(mg ml ⁻¹)	(mg ml ⁻¹)	(mg ml ⁻¹)
Oxygen sensors	68.0 ± 7.5	1.3 ± 0.2	17.0 ± 2.0	0.6 ± 0.2	7.5 ± 2.0
OD ₅₉₅	69.0 ± 7.5	1.4 ± 0.5	12.2 ± 3.0	0.4 ± 0.4	8.0 ± 2.0

Nowadays, screening for potent drugs from a large pool of drug candidates in high-throughput manner is a basic requirement. However, the conventional optical density method, which measures the change in absorbance of the cell culture at the end point, is interfered by light scattering during the measurement and the sinking of cells to the bottom of the microwell during incubation. Besides, it cannot give information on the cell growth (or death) profile and adaptation of cells to drugs. In addition, certain drugs absorb at 595 nm therefore interfere with the optical density method. In contrast, the oxygen sensor method is based on the measurement of oxygen consumption rate from cells, is relatively simple to perform and is not subject to interference from cell turbidity, color or precipitation.

3.4 Concluding Remarks

The oxygen sensors on microtiter plate produced reliable and reproducible results in the determination of IC_{50} values of some antimalarial drugs on a yeast model. The IC_{50} values determined by the oxygen sensors are in agreement with those measured by the conventional optical density (OD_{595}) method. Besides, it can monitor the cell growth process in the presence of various concentration of drug. The evaluation of IC_{50} values by the oxygen sensors is relatively simple to perform and is not subject to interference from cell turbidity, color or precipitation. This high-throughput biosensor is expected to find its application in the pharmaceutical industry for screening of potent drugs.

Chapter 4

A High-Throughput Biosensor Based on $[\text{Ru}(\text{dpp})_3]^{2+}$ -Entrapped Organically Modified Silicate (ORMOSIL) Oxygen Sensing Films on Microtiter Plate for Multi-Sample Determination of Biochemical Oxygen Demand (BOD)

4.1 Introduction

Although biochemical oxygen demand (BOD) can be determined by the conventional five day (BOD_5) method, a high-throughput biosensor system is highly desirable for measurement of a large number of samples in environmental and process monitoring. Since the development of the first optical BOD biosensor [167], effort has been made on the improvement of the biosensor from remote sensing to high-throughput sensing [60, 166-169]. Wong's group has previously reported a scanning sensor system for the analysis of dissolved oxygen and BOD_5 based on optical oxygen sensing [60] but the sensor takes five days for the measurement and the procedure is tedious, cumbersome and not suitable for on-line monitoring. Recently, they have introduced a scanning BOD biosensor for rapid (20 min) and multi-sample analysis of dissolved oxygen and BOD by scanning the excitation light source and the detector fiber optic cable underneath the glass sample vials [166]. However, the number of samples for determination is limited to six samples at a time. Moreover, most of the optical oxygen sensors were prepared by immobilization of ruthenium dye in silicone rubber, the Stern-Volmer calibration curves of these sensors always exhibited non-linear downward curvature which is a major drawback in the calibration of sensor.

The work reported in this chapter aims to develop a microplate-based high-throughput BOD biosensor with ORMOSIL oxygen sensing films for fast and reliable BOD measurement. The high-throughput BOD biosensor was fabricated by combining an ORMOSIL oxygen sensing film with a microbial film containing *Stenotrophomonas maltophilia* on a 96-well polystyrene microtiter plate. This high-throughput biosensor platform is easy to calibrate (i.e. linear calibration plot) and can be placed in a conventional microplate reader for the BOD determination of numerous samples simultaneously.

4.2 Experimental Section

4.2.1 Materials

[Ru(dpp)₃]Cl₂ (dpp = 4,7-diphenyl-1,10-phenanthroline) was synthesized and purified in our laboratory according to a literature method[214]. Tetramethoxysilane (TMOS) (98%), methyltrimethoxysilane (MTMS) (95%), dimethoxy dimethylsilane (DiMe-DMOS) (95%) and polyvinyl alcohol (PVA, molecular weight 124,000-186,000) were obtained from Aldrich. Graphite fine powder (extra pure) was purchased from Merck. Nutrient agar, nutrient broth, marine broth, D-glucose, tryptone, yeast extract, peptone, beef extract and urea were obtained from Sigma. All other chemicals and reagents were of analytical grade. All aqueous solutions were prepared in deionized water (Milli-Q). Oxygen and nitrogen gases (99.7 %) were obtained from Hong Kong Oxygen Company. Wastewater samples were collected from the Shatin Sewage Treatment Works of Drainage Services Department, Hong Kong. The bacterium *Stenotrophomonas maltophilia* used in this BOD study was isolated from activated sludge sample from the Shatin Wastewater Treatment Plant by Dr. N. Y. Kwok. This particular strain of *S. maltophilia* was identified by the MIDI Sherlock Microbial Identification System

at Microbial ID Inc. (Newark, DE, U.S.A.) and shows a high assimilation activity towards simple organics such as glucose and glutamic acid [225].

4.2.2 Incubation of *Stenotrophomonas maltophilia*

Single colony of *Stenotrophomonas maltophilia* was inoculated and spread into 100 ml of sterilized medium in a 1-L conical flask by a sterilized platinum wire. The above operation was performed with aseptic technique with the assistance of a Bunsen flame. The culture was incubated for about 24 h at 30 °C with shaking at 250 rpm in a medium containing 1.5 % (w/v) peptone, 1.2 % (w/v) sodium chloride, 0.5 % (w/v) glucose, 1 % (w/v) tryptone, 0.3 % (w/v) beef extract and 1.9 % (w/v) yeast extract. The culture was centrifuged at 6000 rpm (Beckman Coulter, centrifuge model: Allegra 64R, rotor: C0650) for 5 min and washed twice with pH 7.5 phosphate buffer (0.1 M) before used. The resulting cell pellet was suspended in the phosphate buffer solution before used.

4.2.3 Construction of the BOD biosensor

4.2.3.1 Preparation of ORMOSIL oxygen sensing film

The oxygen sensing film and light insulating coating were prepared as described in chapter 3 (section 3.2.2). A solution of $[\text{Ru}(\text{dpp})_3]\text{Cl}_2$ in ethanol (2.85 mg ml^{-1}) was prepared. The silica sol was prepared by mixing TMOS, DiMe-DMOS, 0.1M HCl and deionized water in the volume ratio of 1.0:2.15:1.7:1.1. The sol mixture was stirred at 500 rpm for 3.5 hours at 25 °C in a water bath. The sol was then centrifuged at 7500 rpm (Beckman Coulter, centrifuge model: Allegra 64R, rotor: C0650) for 4 minutes. The thickened sol at the bottom of the centrifuge tube (1 ml) was pipetted out and thoroughly mixed with 250 μl of the ruthenium complex solution. Portions (32 μl) of the sol-ruthenium mixture was then transferred to each well of the microtiter plate and allowed to stand for six days at room temperature in dark for gelation and drying. A layer of graphite-containing sol-gel coating was placed on the top of the oxygen sensing film to eliminate scattered light and background luminescence from sample solution. This light-insulating coating was prepared by pipetting 15 μl of a mixture of thickened sol (1 ml), graphite (0.1 g) and 0.1 M phosphate buffer (pH 7.0, 50 μl) onto the surface of each of the gelatinized oxygen sensing film and allowed to stand for another 6 days. After gelation, the microtiter plate was stored from direct light before use.

4.2.3.2 Construction of microbial film

A sol-gel stock solution was prepared by mixing 0.74 ml TMOS, 0.36 ml MTMS and 0.5 ml of 0.01 M HCl. This silica sol stock solution was allowed to stand at room temperature for half an hour. A silica sol/PVA mixture solution was prepared by mixing a PVA aqueous solution (8 % w/w) with the silica sol stock solution in the ratio of 2:1 (v/v). A suitable amount of *Stenotrophomonas maltophilia* was added into the solution mixture. A minimum amount of the resulting mixture, 20 µl, just enough to cover the oxygen sensing film was pipetted to the surface of the black graphite layer and allowed to cure at 4 °C for 24 h. The microtiter plate was subsequently stored at 4 °C before use. A schematic diagram of the BOD biosensor is shown in Figure 4.1.

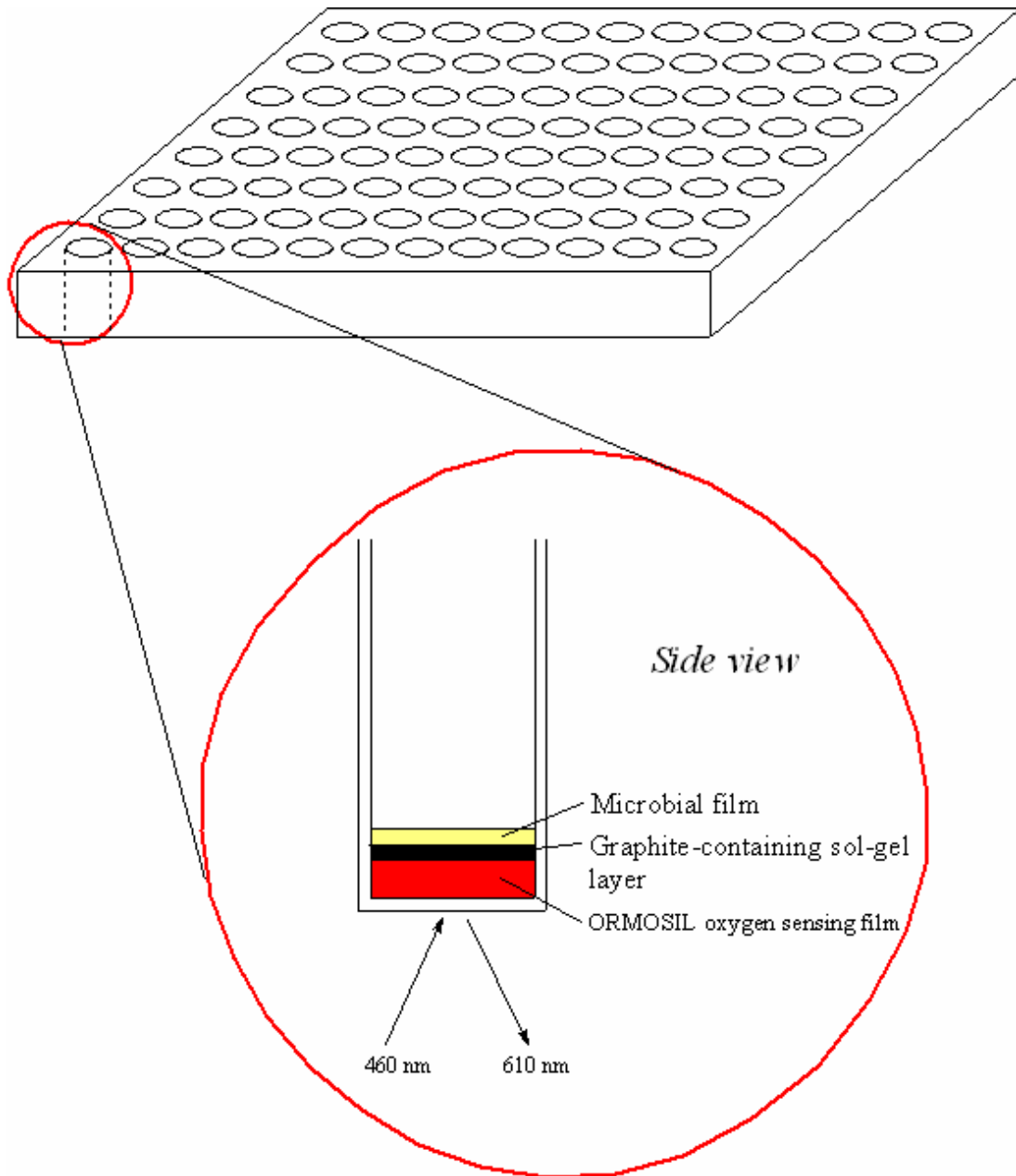


Figure 4.1 A schematic diagram of the BOD biosensor.

4.2.4 Preparation of standard glucose-glutamic acid (GGA) solution

The standard glucose-glutamic acid (GGA) solution has been commonly used as BOD standard in calibration [226-229]. The standard solution was prepared according to the Japanese Industrial Standard [230], in which a mixture of 150 mg l⁻¹ glucose and 150 mg l⁻¹ glutamic acid is equivalent to a BOD₅ value of 220 ± 10 mg l⁻¹. The glucose and glutamic acid were dried in an oven at 103 °C for 1 h prior to preparation of the standard solution.

4.2.5 Preparation of synthetic wastewater

The synthetic wastewater was prepared according to the Organization for Economic Cooperation and Development (OECD) standard [231]. The OECD synthetic wastewater contains peptone (1.6 % w/w), meat extract (1.1 % w/w), urea (0.3 % w/w), sodium chloride (0.07 % w/w), calcium chloride dihydrate (CaCl₂·2H₂O, 0.04 % w/w), magnesium sulfate heptahydrate (MgSO₄·7H₂O, 0.02 % w/w) and dipotassium hydrogen phosphate (K₂HPO₄, 0.28 % w/w) in 1 liter of water.

4.2.6 Measurement of dissolved oxygen concentration

250 μl diluted standard or wastewater sample (GGA, OECD or domestic) was added into the each microwell of BOD biosensor (with immobilized *Stenotrophomonas maltophilia*). The microtiter plate was then sealed with an aluminum microplate sealing foil to minimize the interference from atmospheric oxygen. During assimilation of organic matters in the presence of microorganisms, the dissolved oxygen concentration (mg l^{-1}) recorded as luminescence intensity was plotted against incubation time (min). The experiment was completed as the oxygen in microwell had been totally consumed by the bacteria at which the luminescence intensity would level off. The conventional 5-day BOD (BOD_5) was determined by the standard method [165]. All experiments were performed at room temperature unless otherwise stated.

4.3 Results and Discussion

4.3.1 Optimization of microbial film

The microbial film was prepared by incorporation of the microorganisms into a silica/PVA composite material which is biocompatible and shows good adhesion on sol-gel surface. The relationship between the dissolved oxygen (DO) initial consumption rate and the amount of microorganisms immobilized in the silica/PVA composite material is shown in Figure 4.2. The optimum loading of immobilized *Stenotrophomonas maltophilia* is about 1.6 mg ml^{-1} as shown in the figure, which is used thereafter. Further increase in cell loading of the membrane did not improve the BOD sensor response, probably because under such circumstances the performance of the biosensor is limited by diffusion of organic substrates and dissolved oxygen in the microbial layer [166, 168, 232].

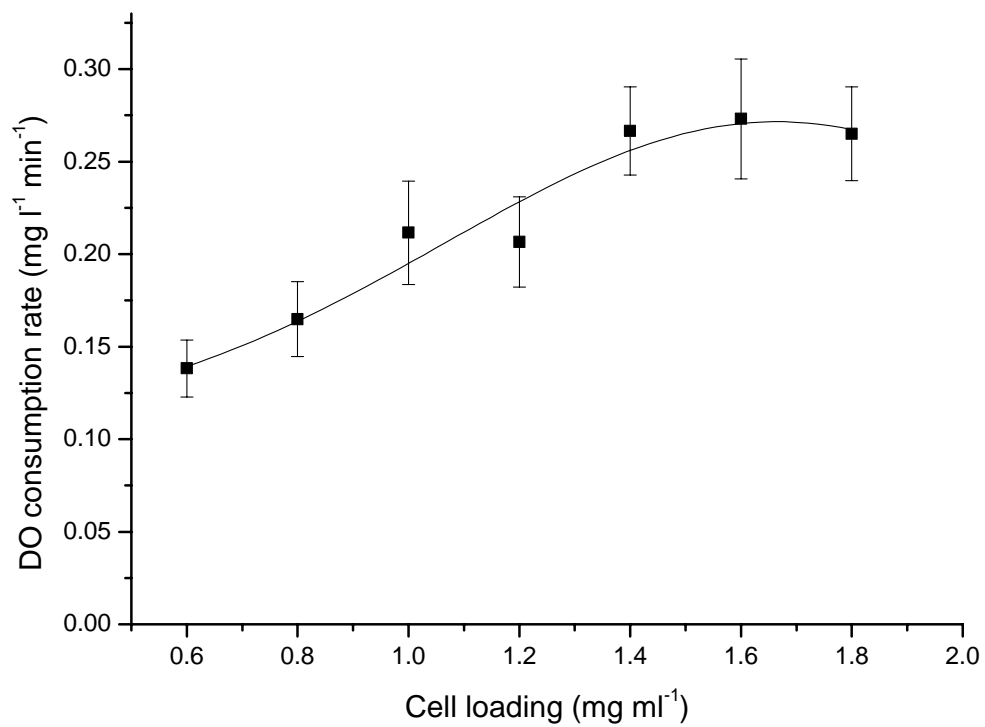


Figure 4.2 Effect of cell loading of immobilized *Stenotrophomonas maltophilia* on the initial DO consumption rate as determined by the BOD biosensor at 20 °C and pH 7.0 in a GGA standard solution of 20 mg l⁻¹.

4.3.2 Calibration of BOD biosensor

Dissolved oxygen (DO) is consumed by microorganisms in the assimilation of organic compounds. For BOD measurement, the initial rate of oxygen consumption is correlated with the organic content of the water sample. Typical responses of the biosensor with immobilized *Stenotrophomonas maltophilia* to GGA standard solutions and wastewater samples are shown in Figures 4.3 and 4.4. From the plot of DO concentration versus time, the initial rate of oxygen consumption was determined from the change in DO concentration in the first 20 min. The calibration curve obtained by plotting the initial oxygen consumption rate against the BOD value of the GGA solutions in the presence of immobilized *Stenotrophomonas maltophilia* is shown in Figure 4.5. A linear relationship between DO consumption rate and BOD was observed for BOD values up to about 70 mg l⁻¹. This BOD biosensor shows a comparable good linear measuring range when compare to other microbial BOD sensors. The linear BOD measuring range of the biosensor with immobilized *Stenotrophomonas maltophilia* is compared with other microbes and summarized in Table 4.1.

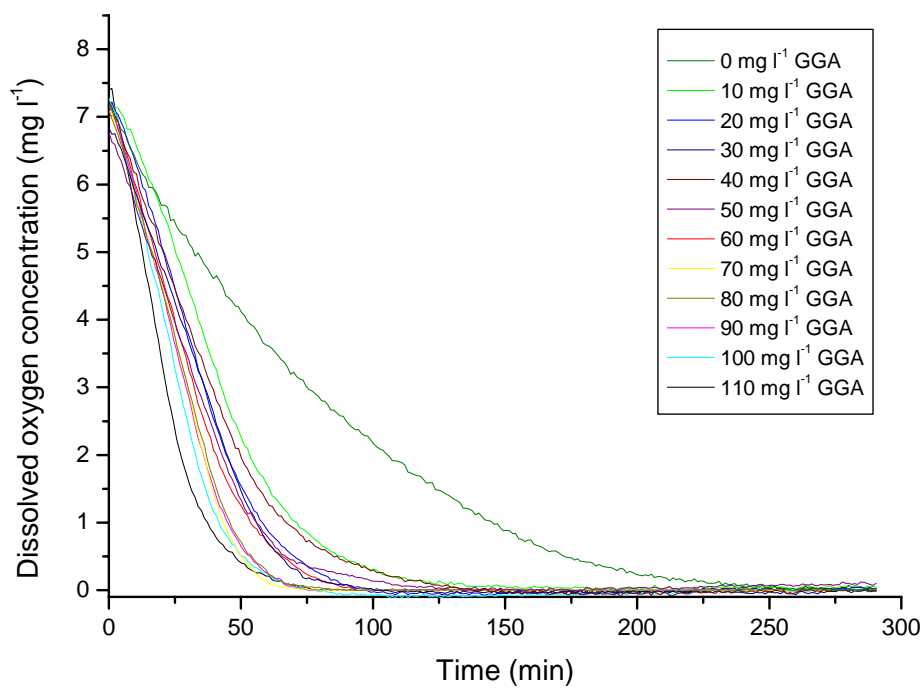


Figure 4.3 Typical DO concentration vs. time curves of the biosensor in various concentrations of GGA solution.

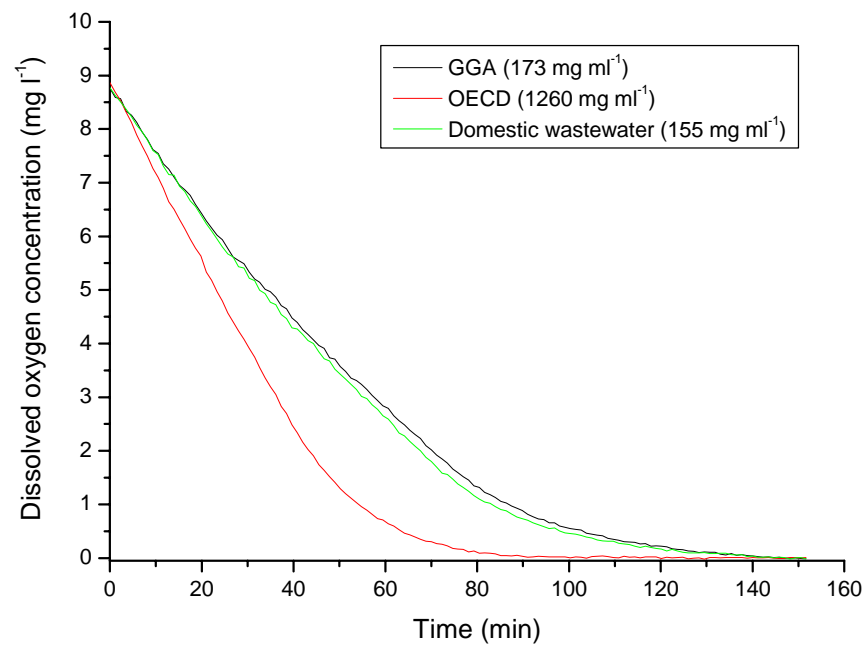


Figure 4.4 Typical DO concentration vs. time curves of the biosensor (with immobilized *Stenotrophomonas maltophilia*) in various sample solutions.

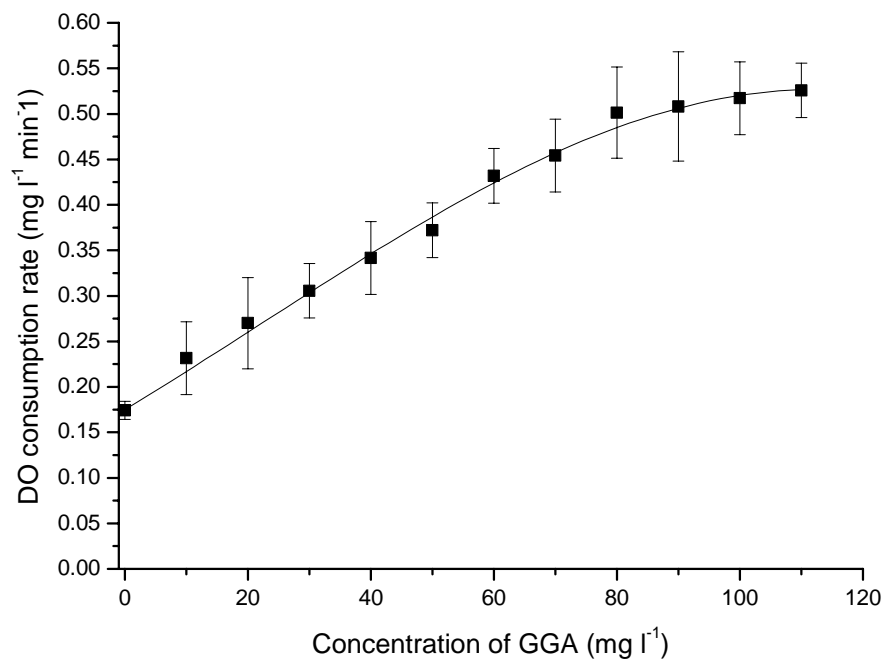


Figure 4.5 Calibration plot for the BOD biosensor with immobilized *Stenotrophomonas maltophilia* using GGA standard solutions.

Table 4.1 A comparison on BOD measuring range with different microbes.

Immobilized microbes	Measuring range (mg l ⁻¹ BOD) ^a	References
<i>Stenotrophomonas maltophilia</i>	0-70	This work
<i>Trichosporon cutaneum</i>	<60	[228]
<i>Hansenula anomala</i>	1-45	[233]
<i>Klebsiella oxytoca</i> AS1	<44	[234]
<i>Bacillus subtilis</i>	2-22	[235]
	0-25	[166]
Thermophilic bacteria	<10	[236]
<i>Citrobacter sp.</i> + <i>Enterobacter sp.</i>	6-18	[237]
Multi-species culture (BODSEED)	0-45	[238]
Activated sludge	0-60	[166]

^a Glucose and glutamic acid (GGA) standard solution.

4.3.3 Effects of pH and temperature

The physiological state of microorganisms, especially the respiratory activity, depends on pH and temperature [166], the effects of which on the performance of the biosensor were investigated for BOD of 20 mg l⁻¹. The effect of pH on the performance of the biosensor was investigated over the pH range 6.0 – 9.0. As shown in Figure 4.6, the optimal pH for *Stenotrophomonas maltophilia* is 7.5 at which the highest dissolved oxygen consumption rate was observed. The pH 7.5 phosphate buffer was chosen and all sample solutions were adjusted to pH 7.5 in subsequent experiments.

On the other hand, the response of the BOD sensor upon exposure to a GGA solution of BOD 20 mg l⁻¹ was studied over the temperature range 25-45 °C. The results for *Stenotrophomonas maltophilia* are shown in Figure 4.7. The respiratory rate of *Stenotrophomonas maltophilia* as indicated by the BOD sensor increases with temperature from 25 °C to 35 °C. The oxygen consumption rate dropped when the working temperature was above 35 °C. Apparently, *Stenotrophomonas maltophilia* is inactivated above this temperature. Similar inactivation by high temperature was also observed for *Bacillus subtilis* [166] and *Pseudomonas putida* [168].

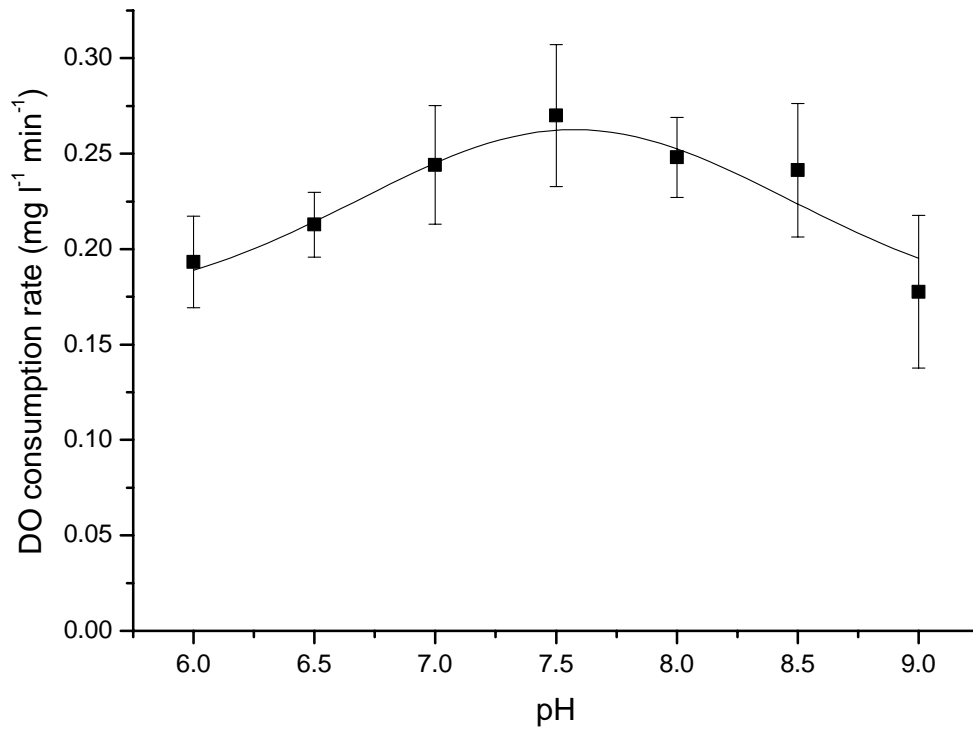


Figure 4.6 Effect of pH (temperature kept at 25 °C) on the initial DO consumption rate of immobilized *Stenotrophomonas maltophilia* in a GGA standard solution of BOD 20 mg l⁻¹.

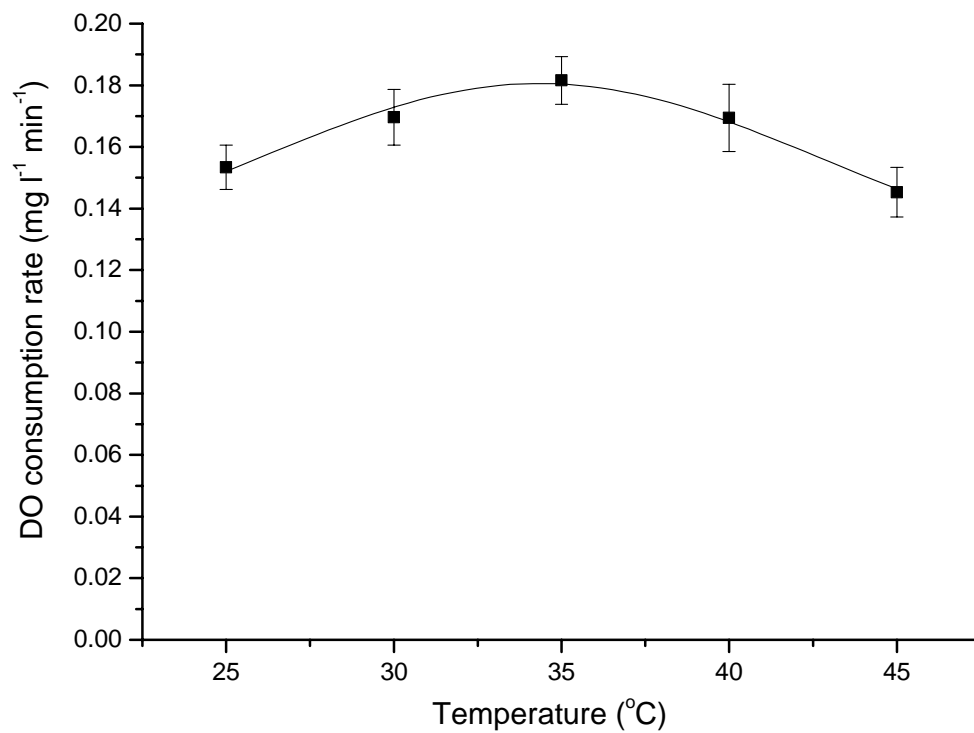


Figure 4.7 Effect of temperature (pH 7.5) on the initial DO consumption rate of immobilized *Stenotrophomonas maltophilia* in a GGA standard solution of BOD 20 mg l⁻¹.

4.3.4 Influence of heavy metal ions on BOD

Heavy metals are most often found in municipal wastewater and the presence of heavy metal ions such as Zn^{2+} , Pb^{2+} , Cu^{2+} , Ni^{2+} , Cd^{2+} and Cr^{3+} may interfere with the activity of microorganisms [166, 239-241]. Therefore, the influence of heavy metal ions on BOD measurement was studied. The influence of heavy metal ions on the biosensor response was investigated at a concentration of 3.0 ppm, as most heavy metal concentration commonly found in wastewater samples in Hong Kong would not exceed this concentration [166]. In this study, *Stenotrophomonas maltophilia* was incubated in a phosphate buffered GGA solution (equivalent to BOD_5 of 20 mg l^{-1}) in the presence of different heavy metal ions at 3.0 ppm. The influence of various heavy metal ions on BOD measurement by the biosensor are tabulated in Table 4.2. All the heavy metal ions studied show inhibitory effect on the microbial activity. The least inhibition was observed for Ni^{2+} , whereas Zn^{2+} , Pb^{2+} , Cu^{2+} , Cd^{2+} and Cr^{3+} were strong inhibitors. The inhibitory effect of various heavy metal ions can be ranked in following order:

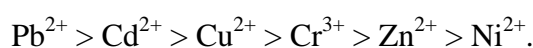


Table 4.2 Influence of 3.0 ppm heavy metal ion on BOD measurement.

Metal ion	Inhibition (%) [*]
Zn ²⁺	11.9 ± 3.6
Pb ²⁺	19.2 ± 3.3
Cu ²⁺	17.5 ± 7.9
Ni ²⁺	6.3 ± 2.5
Cd ²⁺	17.6 ± 2.2
Cr ³⁺	16.3 ± 2.8

* Inhibition (%) = $[(R_c - R_t) / R_c] \times 100\%$

where R_c and R_t represent the DO consumption rate of *Stenotrophomonas maltophilia* in the absence of heavy metal ions and in the presence of heavy metal ions, respectively.

4.3.5 Comparison of BOD values obtained by BOD biosensor and BOD₅ method

The BOD values of GGA, OECD synthetic wastewater and domestic wastewater obtained by the biosensor were correlated with those obtained by the conventional BOD₅ method. The results are summarized in Table 4.3. It illustrates clearly that the BOD biosensor with *Stenotrophomonas maltophilia* as the biological component is well suited for wastewater with simple organic molecules and low BOD levels. The BOD values for both methods are almost identical for GGA standards. On the other hand, domestic wastewater and OECD standard are composed of complex organic substrates, and *Stenotrophomonas maltophilia* cannot assimilate the complex molecules in a short time. Therefore, the BOD values of OECD standard and domestic wastewater obtained by the biosensor deviate from those obtained by the 5-day test (BOD₅ method). Under such circumstances, the BOD biosensor gives consistently lower readings than the conventional BOD₅ method. This is due to the fact that in such a short measurement time large organic molecules are not easily assimilated by the immobilized microbes. Even though the BOD data obtained by the biosensor is not identical to the BOD₅, a fairly good correlation with the conventional BOD₅ could be obtained (Figure 4.8).

Table 4.3 Correlation of BOD values obtained by BOD biosensor and BOD₅

Sample	BOD biosensor (mg l ⁻¹)	BOD ₅ (mg l ⁻¹)	Ratio (BOD biosensor / BOD ₅)
GGA ^a	169.0 ± 21.9	157.4 ± 30.8	1.07
OECD ^b	1246.5 ± 21.8	1423.3 ± 108.8	0.88
GGA + OECD	658.2 ± 76.7	727.1 ± 77.5	0.91
Domestic wastewater sample	154.7 ± 25.5	182.5 ± 46.9	0.85

^a GGA: glucose and glutamic acid (150 mg l⁻¹ each).

^b OECD synthetic wastewater contains peptone 0.16 % (w/v), meat extract 0.11 % (w/v), urea 0.03 % (w/v), NaCl 0.007 % (w/v), CaCl₂·2H₂O 0.004 % (w/v), MgSO₄·7H₂O 0.002 % (w/v), K₂HPO₄ 0.028 % (w/v).

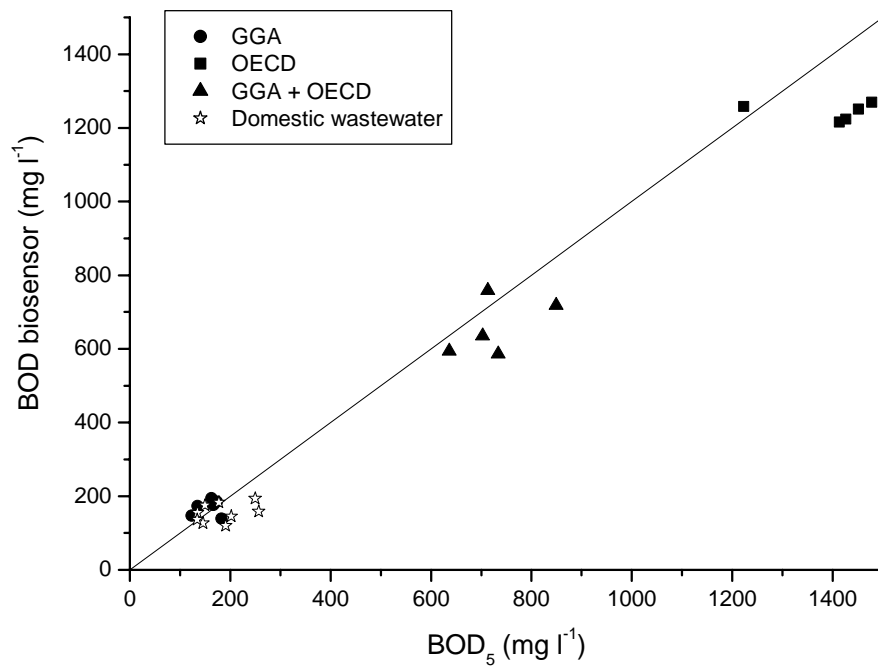


Figure 4.8 Correlation of BOD values evaluated by the BOD biosensor with those obtained by the BOD₅ method. The solid lines in the figures represent the lines of unit gradient (slope of 1).

4.3.6 Stability and service life

The activity of microbial film in this biosensor had been studied for one month and it was stored in the presence of phosphate buffered GGA solution (100 mg l⁻¹, pH 7.5) at 4 °C. The stability of the biosensor over 30 days was determined in the presence of GGA solution (20 mg l⁻¹) at 25 °C and pH 7.5. The results are summarized in Figure 4.9. As shown in the figure, the activity of the microbial film slowly deteriorates upon long-term storage, which is probably due to the gradual lysing of the microbial cells. The BOD biosensor was found to retain about 89% of its initial activity for *Stenotrophomonas maltophilia* after 8 days and the activity decreased to 46 % of its initial activity after 30 days. When compared with the stability and service life among microbes, *Stenotrophomonas maltophilia* (46 % after 30 days) has a slightly longer service life than that of *Pseudomonas fluorescens* bv.V (34 % after 30 days) [232] and bacterial mixed culture (*Citrobacter sp.* + *Enterobacter sp.*) (33 % after 20 days) [237]. However, its service life is shorter than that of activated sludge (77 % after 30 days) and *Bacillus subtilis* (88 % after 30 days) [166]. Therefore, this BOD biosensor should be used within one week after preparation.

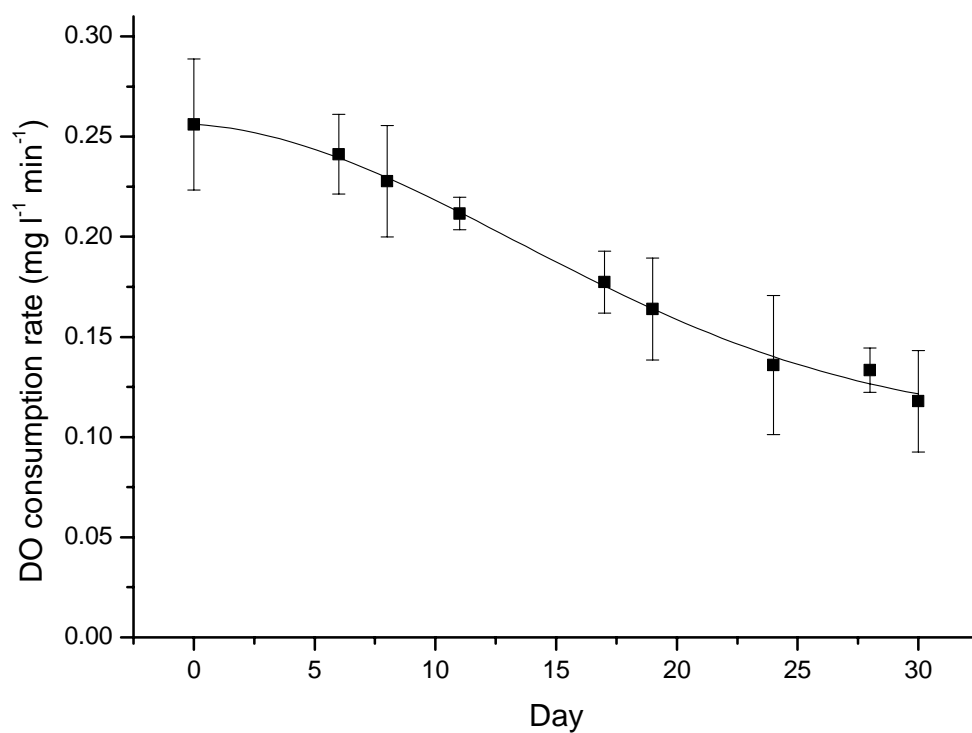


Figure 4.9 The DO consumption rates of the microbial films for immobilized *Stenotrophomonas maltophilia* over a period of 30 days at 20 °C and pH 7.5 in a GGA standard solution of 20 mg l⁻¹.

4.4 Concluding Remarks

A high-throughput BOD biosensor was constructed by immobilizing *Stenotrophomonas maltophilia* in ORMOSIL-PVA composite material. The dissolved oxygen consumption rate as recorded by the biosensor increases linearly with the BOD concentration up to about 70 mg l⁻¹. The BOD values determined by this biosensor correlate well with those obtained by the conventional BOD₅ method. This BOD biosensor can determine a large number of wastewater samples in environmental and on-line process monitoring within a relatively short period of time with better precision than the BOD₅ method.

Chapter 5

Organically Modified Silicate (ORMOSIL) Films on Microtiter Plate for the Construction of Carbohydrate Microarrays

5.1 Introduction

Carbohydrate-protein interaction plays an important role in biological processes such as cell-cell communication, cell adhesion, inflammation and tumor cell metastasis [208]. As a result, the investigation of biological processes and drug design can be assisted by understanding the molecular basis of carbohydrate-protein interactions [208]. However, current methods for carbohydrate-protein interaction studies such as X-ray crystallography, NMR spectroscopy, surface plasmon resonance (SPR) and isothermal titration calorimetry (ITC) do not allow rapid screening of libraries of biological compounds to assess the carbohydrate-binding properties of their constituent [242]. Therefore, a high-throughput analytical tool for carbohydrate-protein interaction screening in the microarrays format is highly desirable. Up to date, most of the carbohydrate arrays were fabricated on glass slides which need sophisticated instruments for signal detection and carbohydrate spots pinning [195, 202, 204, 206-208]. So far, the development of carbohydrate arrays is mainly focused on attachment (or immobilization) of carbohydrates on glass or other substrates. The immobilization techniques included the non-covalent immobilization (early carbohydrate arrays) and covalent immobilization in the more recent carbohydrate arrays.

This chapter is aimed at the development of a high-throughput microplate-based carbohydrate sensor for carbohydrate-protein interaction study. Although microtiter plates provide a convenient means for high-throughput screening, the polystyrene surface is difficult to modify for the immobilization of carbohydrates. In this study, microtiter plate was firstly modified by sol-gel and the carbohydrates were then immobilized covalently on the sol-gel layer through a simple chemical reaction. Therefore, the construction of a high-throughput carbohydrate array sensor by a simple, convenient and low-cost method was achieved and it can be made in most laboratories.

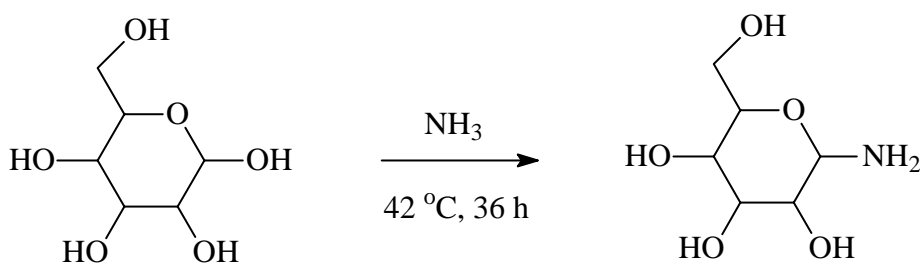
5.2 Experimental Section

5.2.1 Materials

Tetramethyl orthosilicate (TMOS, 98%), dimethoxy dimethylsilane (DiMe-DMOS, 95%), 3-(triethoxysilyl)propyl isocyanate (TESPI, 95%) and D-lactose Monohydrate (ACS reagent) were purchased from Aldrich. D-mannose (99%), D-glucose (ACS reagent), D-galactose monohydrate (99%), albumin from bovine serum (BSA, lyophilized powder, 96%) and polyethylene glycol sorbitan monolaurate (Tween 20) were obtained from Sigma. Fluorescein-labeled lectins (fluorescein isothiocyanate conjugate-lectin, FITC-lectins) were used in this study. Fluorescein-labeled *Concanavalin A* (FITC-ConA) and *Erythrina cristagalli* (FITC-EC) were purchased from Vector Laboratories Inc.. The lectin inhibitors, anti-ConA and methyl α -D-mannopyranoside, were obtained from Sigma. Microtiter plates (no. 3603, 96 wells, flat clear bottom black polystyrene, TC-treated) were obtained from Corning. All aqueous solutions were prepared in double deionized water (Milli-Q). All other chemicals and solvents were analytical-reagent grade and were used without further purification.

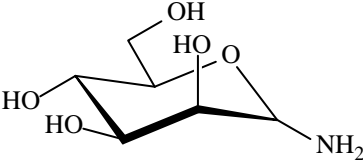
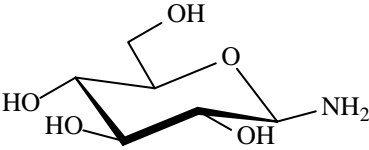
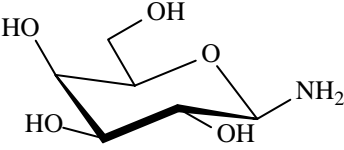
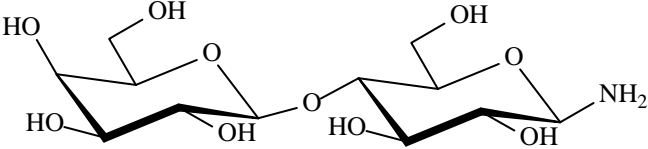
5.2.2 Synthesis of glycosylamines

A total of 4 glycosylamines were synthesized from mono- and di-saccharides according to a literature procedure [243] as shown in Scheme 5.1. 0.2 M of the corresponding reducing sugar (D-mannose, D-glucose, D-galactose and D-lactose) was mixed with 0.2 M ammonium hydrogen carbonate and dissolved in aqueous 16 M ammonia. The mixture was heated at 42 °C for 36 h. This solution was then concentrated to half volume and freeze-dried. The D-mannosylamine, D-glucosylamine, D-galactosylamine and D-lactosylamine were stored in a desiccator. The structures of the glycosylamines are given in Table 5.1.



Scheme 5.1

Table 5.1 A summary of the structure of glycosylamines in this study.

Glycosylamine	Structure
D-mannosylamine	
D-glucosylamine	
D-galactosylamine	
D-lactosylamine	

5.2.3 Fabrication of carbohydrate microarrays on microtiter plate

The carbohydrate microarrays were fabricated by coating an ORMOSIL film on the microtiter plate with a 3-(triethoxysilyl)propyl isocyanate linker followed by covalent bonding to the carbohydrate as shown in Figure 5.1. Details of the sensor fabrication are given in the sections below.

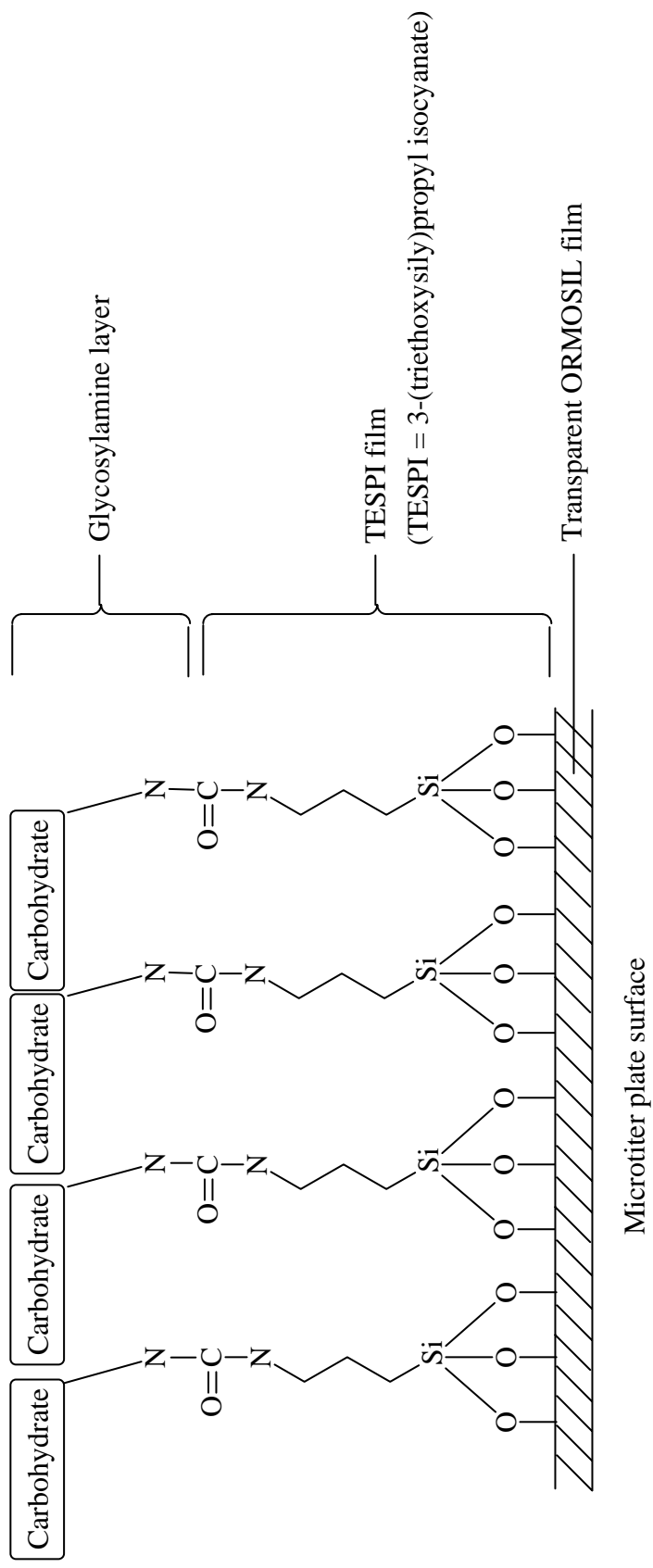


Figure 5.1 A schematic diagram showing the construction of carbohydrate microarrays on polystyrene microtiter plate.

5.2.3.1 Preparation of transparent ORMOSIL films with the 3-(triethoxysilyl)propyl isocyanate (TESPI) linkers

Firstly, a transparent ORMOSIL film was coated on the microtiter plate. The ORMOSIL film was prepared by a sol mixture of TMOS, DiMe-DMOS, 0.1M HCl and deionized water in the volume ratio of 1.0:2.0:1.7:1.1. The sol mixture was stirred at 500 rpm for 3.5 h at 25 °C in a water bath. The sol was then centrifuged at 7500 rpm (Beckman Coulter, centrifuge model: Allegra 64R, rotor: C0650) for 4 minutes. The thickened sol at the bottom of the centrifuge tube (1 ml) was pipetted out and thoroughly mixed with 250 µl of absolute ethanol. Portions (32 µl) of the clear sol mixture were then transferred to each well of the microtiter plate and allowed to stand for six days at room temperature for gelation and drying.

After the ORMOSIL film has dried, the linker 3-(triethoxysilyl)propyl isocyanate (TESPI) was immobilized onto the transparent ORMOSIL film. The TESPI was pre-hydrolyzed by mixing water and 0.01M HCl in the volume ratio of 1.0:2.0:0.2. The TESPI mixture was stirred at 500 rpm for 2 h at 25 °C in a water bath. The TESPI mixture was then centrifuged at 10000 rpm (Beckman Coulter, centrifuge model: Allegra 64R, rotor: F2402) for 10 minutes. The thickened sol at

the bottom of the centrifuge tube (1 ml) was pipetted out and portions (5 μ l) transferred to each well of the microtiter plate. This TESPI layer condensed with the surface hydroxyl groups on the ORMOSIL film, forming a silane polymer at the surface of the ORMOSIL layer [220, 244]. The TESPI layer was allowed to stand for 24 h at room temperature for complete polymerization of the silane. Subsequently, each well of the microtiter plate was washed by ethanol (5 times) to remove any excess free monomer.

5.2.3.2 Immobilization of carbohydrate on microtiter plate

The corresponding glycosylamine (D-mannosylamine, D-glucosylamine, D-galactosylamine and D-lactosylamine) was covalently immobilized on the microtiter plate via urea formation between the isocyanate group of 3-(triethoxysilyl)propyl isocyanate (TESPI) and the amino group of the glycosylamine [199, 245-247] as shown in Figure 5.1. Glycosylamine solutions were pipetted into the well of the TESPI-coated microtiter plate and stored for 24 h to allow complete reaction of glycosylamine with TESPI. The microtiter plate was then washed 5 times with deionized water (Milli-Q).

5.2.4 Instrumentation

All luminescence measurements were conducted on a BMG Labtech POLARstar microplate reader connected to a microcomputer. The wavelength of bandpass filters used for excitation and emission were centered at 490 nm and 520 nm respectively. The luminescence intensity was measured in the bottom plate reading configuration and at room temperature.

5.2.5 Investigations of carbohydrate-lectin interactions with carbohydrate sensor

5.2.5.1 Screening of lectin-binding patterns

To study the carbohydrate-lectin interactions and to screen lectin-binding patterns, a microtiter plate with various glycosylamines has been prepared as in section 5.2.3.2. Each well of microtiter plate containing different carbohydrates was then treated with 3% bovine serum albumin (BSA) in phosphate buffered saline (PBS, pH 6.8) containing 0.2% Tween 20 to minimize nonspecific binding of proteins on the surface [207, 208]. Next, the BSA-treated wells were probed with

solutions of the fluorescein-labeled lectins (40 μl of 10 $\mu\text{g ml}^{-1}$) such as FITC-ConA and FITC-EC in PBS containing 0.1% Tween 20 for 1 h. After extensive washing (five times with PBS containing 0.1% Tween 20 for 10 minutes) of the lectin-probed microtiter plate, 40 μl of PBS was added to each well and lectin binding was detected by measuring the fluorescence on a microplate reader.

5.2.5.2 Optimization of carbohydrate concentration for lectin-binding

To study the effects of the concentration of immobilized carbohydrates on the subsequent protein binding, various concentrations (40 μl of 0 to 558 mM) of glycosylamines were pipetted into the wells of the TESPI-treated microtiter plate. The microtiter plate was allowed to stand for 24 h and each well was then washed 5 times by deionized water (Milli-Q). After that, each well of microtiter plate containing different concentrations of carbohydrate was treated with 3% bovine serum albumin (BSA) in phosphate buffered saline (PBS, pH 6.8) containing 0.2% Tween 20. The BSA-treated wells were then probed with solutions of the FITC-labeled lectins (40 μl of 10 $\mu\text{g ml}^{-1}$) such as FITC-ConA and FITC-EC in PBS containing 0.1% Tween 20 for 1 h. After extensive washing (five times with PBS containing 0.1% Tween 20 for 10 minutes) of the lectin-probed microtiter plate, 40

μl of PBS was added in each well and lectin-binding was detected and quantitated by the microplate reader.

5.2.5.3 Study of the effect of ConA inhibitors on ConA-mannosylamine binding

To study the effect of inhibitions on lectin binding with the carbohydrate sensor, each well of the microtiter plate was immobilized with 112 mM mannosylamine and then treated with 3% bovine serum albumin (BSA) in phosphate buffered saline (PBS, pH 6.8) containing 0.2% Tween 20. The BSA-treated wells were then probed with solutions of FITC-ConA ($20\ \mu\text{l}$ of $20\ \mu\text{g ml}^{-1}$) in PBS containing 0.1% Tween 20 with various concentrations of ConA inhibitor (anti-ConA or methyl α -D-mannopyranoside) ($20\ \mu\text{l}$) for 1 hour. After extensive washing (five times with PBS containing 0.1% Tween 20 for 10 minutes) of the microtiter plate, $40\ \mu\text{l}$ of PBS was added to each well and detected by the microplate reader.

5.3 Results and Discussion

5.3.1 Carbohydrate-lectin interactions

We have immobilized four amino-carbohydrates on the microtiter plate with ORMOSIL modification. The lectin-binding patterns have been investigated with the microplate-based carbohydrate sensor with immobilized mannose, glucose, galactose and lactose. The effect of the concentration of immobilized carbohydrates on lectin-binding has been studied.

5.3.1.1 Lectin-binding patterns

Four different carbohydrates were immobilized on microtiter plate and probed with the fluorescein-labeled lectins, *Concanavalin A* (FITC-ConA) and *Erythrina cristagalli* (FITC-EC), for the investigation of lectin-binding patterns.

As expected, only the microwells that contained mannose and glucose showed fluorescent signals after probing with FITC-ConA, whereas fluorescence of FITC-EC was observed only in the lactose-containing microwells. The results are

summarized in Figure 5.2 and 5.3. Besides, Figure 5.2 shows that ConA lectin binds mannose more effectively than glucose. The results obtained by the carbohydrate sensors revealed that ConA is a mannose and glucose binding lectin and EC is a lactose binding lectin. These results are consistent with those previously reported [183, 248, 249]. On the other hand, our results illustrated that the carbohydrates were immobilized successfully on the microwell through the urea-formation reaction. Therefore, this carbohydrate sensor can be used for screening of different carbohydrate binding proteins. However, it is known that the binding affinity of lectins for carbohydrates on the sensors depends on the length of linker [207, 208]. Figure 5.3 shows the lactose connected in this length of linker (TESPI) only bound to FITC-EC weakly, thus TESPI may not be the best linker for FITC-EC binding though it is good for FITC-ConA binding. As a result, further investigations on lectin binding were only performed on FITC-ConA and mannose.

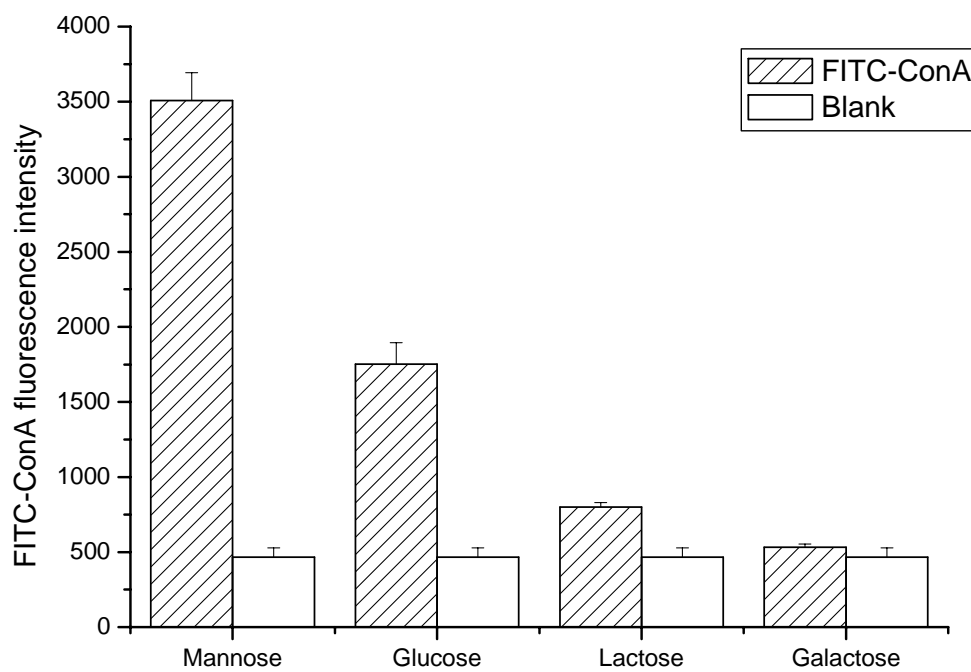


Figure 5.2 Carbohydrate sensors probed with FITC-ConA.

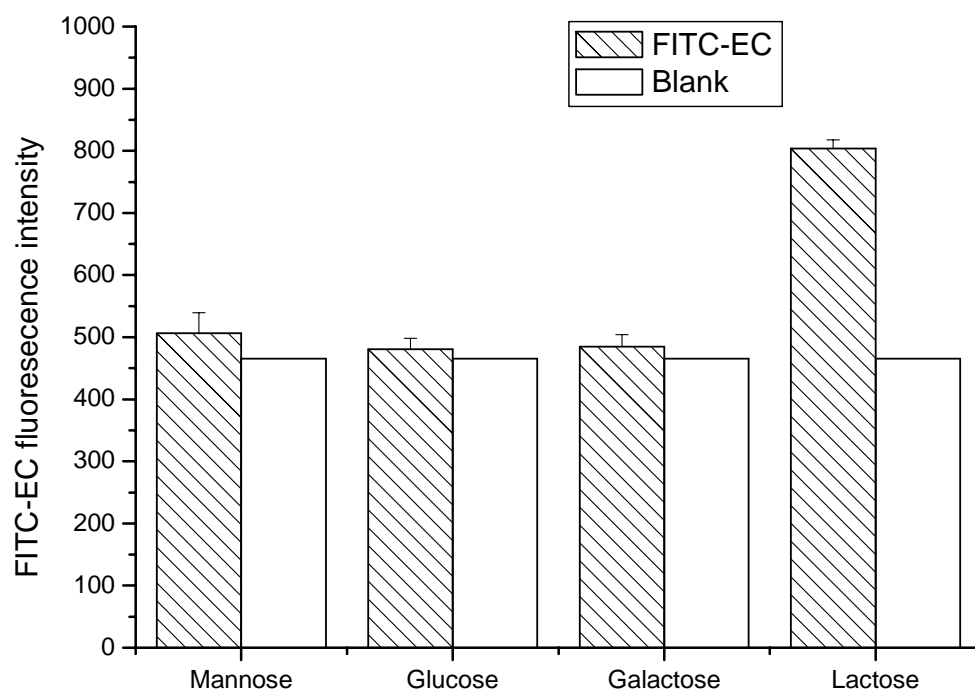


Figure 5.3 Carbohydrate sensors probed with FITC-EC.

5.3.1.2 The effect of carbohydrate concentration used in immobilization on lectin-binding

The carbohydrate sensor was also used to study the effect of concentration of carbohydrate used in the immobilization process on lectin-binding. As shown in Figure 5.4, the binding affinity of ConA for mannose increases with the concentration of the immobilized carbohydrate. The higher the immobilized carbohydrate concentration, the more is the bound lectin and as a result, the higher is the fluorescent signal.

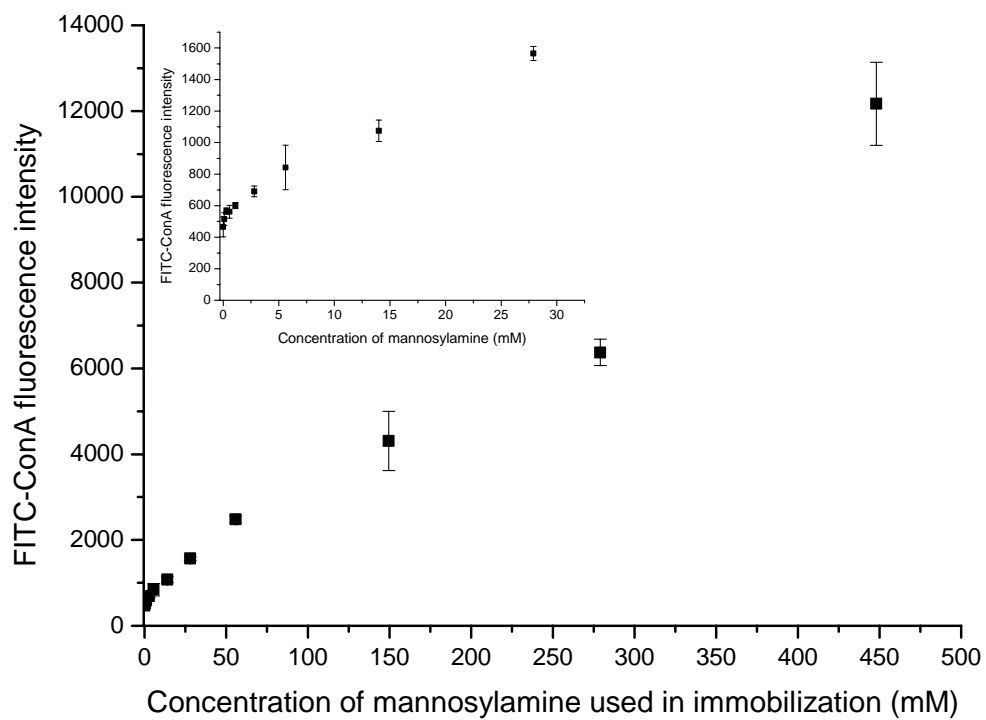


Figure 5.4 Sensors immobilized with different concentrations of mannosylamine and probed with FITC-ConA. The inset shows the increase in FITC-ConA fluorescence intensity from mannosylamine concentration of 0 to 28 mM.

5.3.2 Inhibition on carbohydrate-lectin binding

The inhibition on carbohydrate-lectin interaction by anti-ConA and methyl α -D-mannopyranoside have also been carried out on this carbohydrate sensor. The IC_{50} values of anti-ConA and methyl α -D-mannopyranoside to inhibit 50 % of lectin binding to carbohydrate were determined. A microtiter plate with mannosylamine was incubated with a series of solution mixtures of FITC-ConA ($10 \mu\text{g ml}^{-1}$) and anti-ConA (or methyl α -D-mannopyranoside) for 1 h. After extensive washing of the microtiter plate, the fluorescence intensity was measured to quantify the amount of bound lectin. The dose-dependent inhibition curves for anti-ConA and methyl α -D-mannopyranoside are plotted in Figures 5.5 and 5.6 respectively. As shown in the figures, the IC_{50} values (concentration which inhibits 50% binding) of anti-ConA and methyl α -D-mannopyranoside were determined to be 0.47 mg ml^{-1} and 0.27 mg ml^{-1} , respectively.

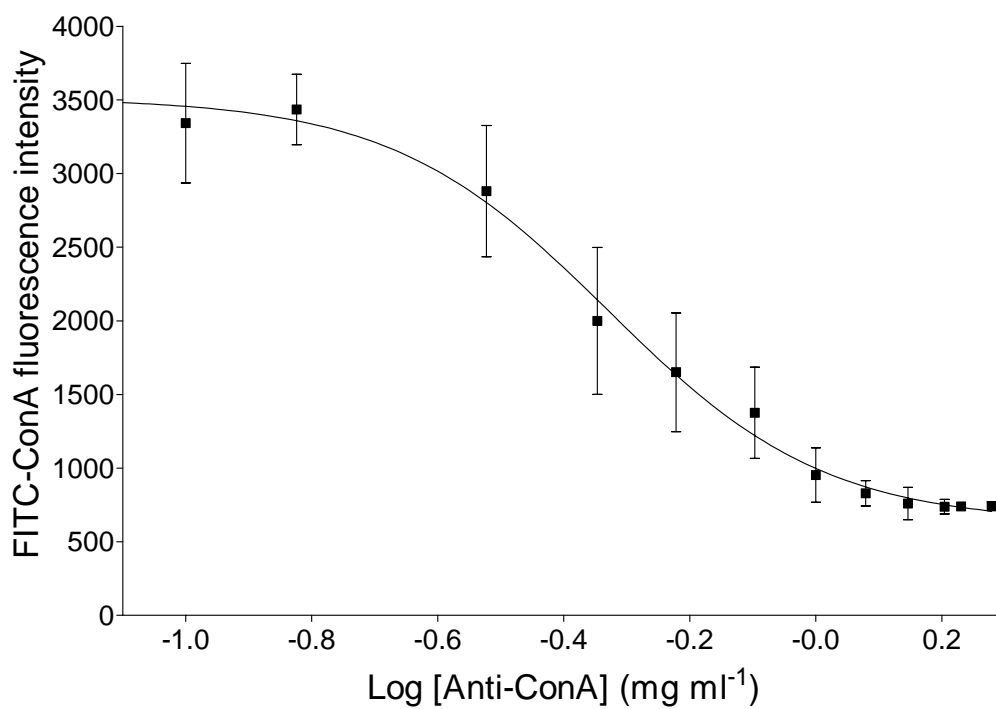


Figure 5.5 Determination of IC₅₀ of anti-ConA to inhibit 50 % of ConA binding to mannose.

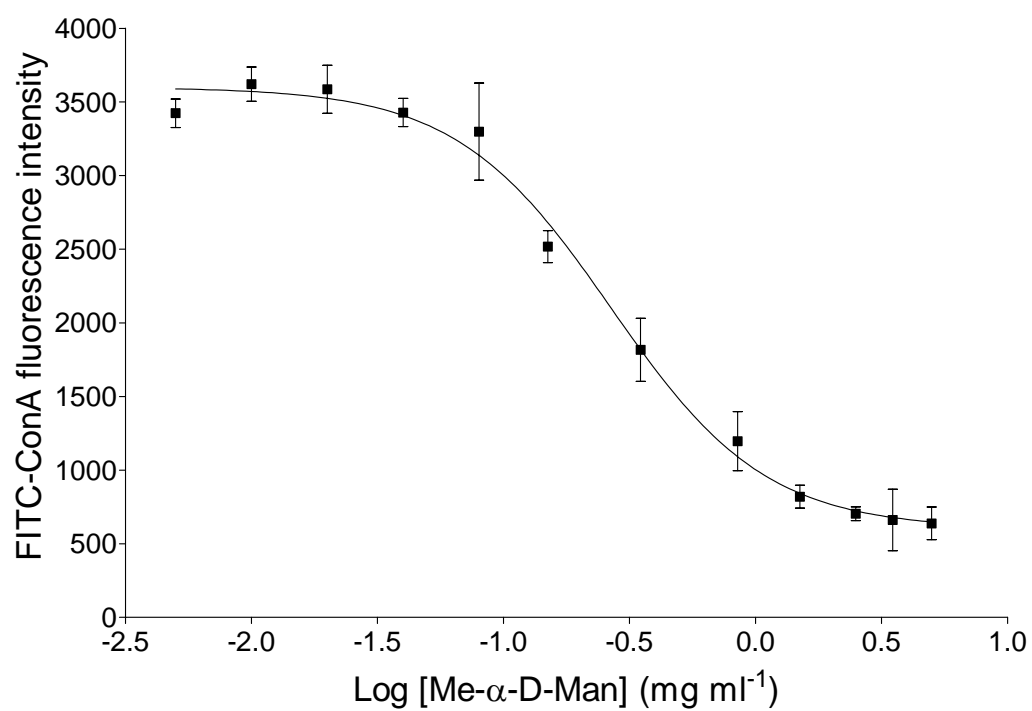


Figure 5.6 Determination of IC_{50} of methyl α -D-mannopyranoside to inhibit 50 % of

ConA binding to mannose.

5.4 Concluding Remarks

A simple, convenient and new method for the fabrication of high-throughput carbohydrate sensors on polystyrene microtiter plates has been presented. Both mono- and di-saccharides were successfully immobilized on microtiter plate via covalent linkage. The lectin-carbohydrate bindings depend on the concentration of carbohydrate and the length of the linker. In the carbohydrate screening for ConA and EC, the binding of EC with lactose is weak and this is probably due to the length of the linker. In the future, it will be interesting to synthesize different linkers for glycosylamines with different lengths. The IC_{50} values of inhibition for the carbohydrate-binding proteins can also be determined using this sensor microarray.

Chapter 6

Conclusions

With the ever increasing number of samples in environmental, medical and biochemical studies, a high-throughput system is highly desirable for multi-sample and multiparameter analysis with small sample volumes. Microtiter plate offers an excellent platform for high-throughput systems. In this study, polystyrene microtiter plates have been successfully modified into high-throughput (bio)sensors for various purposes.

A simple and convenient method for the fabrication of ORMOSIL oxygen sensors on polystyrene microtiter plates has been described. The ORMOSIL oxygen sensors were prepared by entrapping $[\text{Ru}(\text{dpp})_3]^{2+}$ into a porous sol-gel matrix of tetramethoxysilane (TMOS) with the organosilicate precursor, dimethoxy dimethylsilane (DiMe-DMOS). The oxygen sensors show good adhesion on the polystyrene microtiter plate, high sensitivity (quenching ratio or quenching response) and yield linear Stern-Volmer plots for simple two-point calibration. The surface of the ORMOSIL oxygen sensor allows the easy adhesion of enzymatic or microbial hydrogel films, which is a distinct advantage over the conventional silicone rubber or polystyrene based oxygen sensors.

The application of this high-throughput oxygen sensing microplate in

cell-based screening assays for IC₅₀ determination has been demonstrated. The effect of two antimalarial drugs chloroquine and quinacrine on a heterologous yeast model with yeast strains of different drug resistance levels have been investigated. The IC₅₀ values obtained by the high-throughput oxygen sensors were in good agreement with the conventional cell densitometry assay (OD₅₉₅ method).

In addition, the ORMOSIL oxygen sensors have been modified into high-throughput BOD biosensors for multi-sample determination of BOD. The BOD biosensors were prepared by immobilizing a particular strain of *Stenotrophomonas maltophilia* onto the ORMOSIL oxygen sensors. This particular strain shows a relatively high assimilation ability (linear measuring range) towards GGA standard (70 mg l⁻¹) compared with other microorganisms. The performance of the microbial films was found to be dependent on cell loading, temperature and pH and heavy metals. The BOD biosensors with immobilized *Stenotrophomonas maltophilia* showed a good correlation of BOD values (especially for GGA solutions) with the conventional 5-day test.

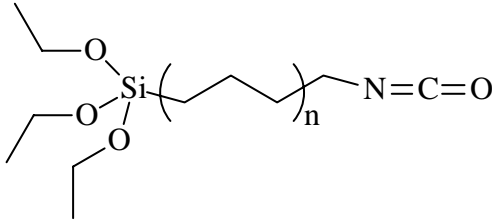
The ORMOSIL surface is easy to modify which allows easy conversion of the microtiter plate into various high-throughput sensor arrays. A high-throughput

microplate-based carbohydrate sensor on ORMOSIL modified microtiter plate has been constructed with a simple, convenient and low-cost method for carbohydrate-protein interaction study. A layer of TESPI-ORMOSIL film was prepared by coating a layer of 3-(triethoxysilyl)propyl isocyanate (TESPI) onto a transparent ORMOSIL film. Aminated carbohydrates were covalently immobilized onto the TESPI-ORMOSIL film on microtiter plates, in which high-throughput carbohydrate-lectin interactions were studied. The microplate-based carbohydrate sensors are useful for high-throughput analysis of carbohydrate-protein binding patterns and inhibitor screening (IC₅₀ determination).

Since oxidase enzymes are useful for assays of various clinically and environmentally important substrates, it is believed that various high-throughput enzyme-based biosensors can be developed in combination with suitable enzymes such as glucose oxidase and amino acid oxidase on the ORMOSIL oxygen sensors in the future. These high-throughput oxidase-based biosensors can be fabricated by immobilizing the oxidase enzyme in polyvinyl alcohol/sol-gel composite over the ORMOSIL oxygen sensing film, in which specific analytes can be quantified by measuring the dissolved oxygen consumption rate.

As the effectiveness of carbohydrate-protein interaction in carbohydrate microarrays is expected to depend on the length of linkers connecting the carbohydrate and the substrate surface, linkers (e.g. TESPI) of different length for aminated carbohydrates can be used to improve the developed high-throughput microplate-based ORMOSIL carbohydrate sensor. Besides, the aminated carbohydrates can also be synthesized with different carbon chain lengths. Some interesting linkers and aminated carbohydrates are listed in Table 6.1. These ORMOSIL carbohydrate sensors with expected improved sensitivity can probably be applied in larger lectins such as *Erythrina cristagalli* (EC) and other larger carbohydrate binding proteins.

Table 6.1 Structures of proposed linkers and aminated carbohydrate.

Linkers	Aminated carbohydrate
 <chem>CCOC(Si)(OCC)OCC(CCCO)nCCN=C=O</chem>	 <chem>OC[C@H]1O[C@@H](CCCO)nCCN[C@@H]1O</chem>
 <chem>CCOC(Si)(OCC)OCC(CCCO)nCC1OC1</chem>	

References

1. Sever, J. L. Application of a microtechnique to viral serological investigations. *Journal of Immunology*, 1962, **88**, 320-329.
2. Clark, L. C. Monitor and control of blood and tissue oxygen tensions. *Transactions of American Society for Artificial Internal Organs*, 1956, **2**, 41-57.
3. Skoog, D. A., West, D. M. and Holler, F. J., *Fundamentals of analytical chemistry, 7th ed.*, Fort Worth: Saunders College Pub., 1996.
4. Bates, M. L., Feingold, A. and Gold, M. I. Effects of anesthetics on an in vivo oxygen electrode. *American Journal of Clinical Pathology*, 1975, **64**(4), 448-451.
5. Albery, W. J., Hahn, C. E. W. and Brooks, W. N. The polarographic measurement of halothane. *British Journal of Anaesthesia*, 1981, **53**(5), 447-454.
6. Pletcher, D. and Walsh, F., *Industrial electrochemistry, 2nd ed.*, New York: Chapman and Hall, 1990.
7. Li, F. and Tan, T. C. Monitoring BOD in the presence of heavy-metal ions using a poly(4-vinylpyridine)-coated microbial sensor. *Biosensors & Bioelectronics*, 1994, **9**(6), 445-455.
8. Mills, A. and Williams, F. C. Chemical influences on the luminescence of

- ruthenium diimine complexes and its response to oxygen. *Thin Solid Films*, 1997, **306**(1), 163-170.
9. Mills, A. Optical oxygen sensors: Utilising the luminescence of platinum metals complexes. *Platinum Metals Review*, 1997, **41**(3), 115-127.
 10. Choi, M. M. F. and Xiao, D. Single standard calibration for an optical oxygen sensor based on luminescence quenching of a ruthenium complex. *Analytica Chimica Acta*, 2000, **403**(1-2), 57-65.
 11. Bacon, J. R. and Demas, J. N. Determination of oxygen concentrations by luminescence quenching of a polymer-immobilized transition-metal complex. *Analytical Chemistry*, 1987, **59**(23), 2780-2785.
 12. Bergman, I. Rapid-response atmosphere oxygen monitor based on fluorescence quenching. *Nature*, 1968, **218**, 396.
 13. Stevens, B., Instrument for determining oxygen quantities by measuring oxygen quenching of fluorescence radiation, *U.S. Patent* 3612866, 1971.
 14. Peterson, J. I., Fitzgerald, R. V. and Buckhold, D. K. Fiber-optic probe for in vivo measurement of oxygen partial pressure. *Analytical Chemistry*, 1984, **56**(1), 62-67.
 15. Wolfbeis, O. S., Offenbacher, H., Kroneis, H. and Marsoner, H. Fluorimetric analysis. 9. A fast responding fluorescence sensor for oxygen. *Mikrochimica*

- Acta*, 1984, **1**(1-2), 153-158.
16. Wolfbeis, O. S., Weis, L. J., Leiner, M. J. P. and Ziegler, W. E. Fiber-optic fluorosensor for oxygen and carbon-dioxide. *Analytical Chemistry*, 1988, **60**(19), 2028-2030.
 17. Li, X. M., Ruan, F. C. and Wong, K. Y. Optical characteristics of a ruthenium(II) complex immobilized in a silicone-rubber film for oxygen measurement. *Analyst*, 1993, **118**(3), 289-292.
 18. MacCraith, B. D., O'Keeffe, G., McEvoy, A. K. and McDonagh, C. Development of a LED-based fibre optic oxygen sensor using a sol-gel-derived coating. *Proceedings of SPIE - The International Society for Optical Engineering*, 1994, **2293**, 110-120.
 19. McEvoy, A. K., McDonagh, C. M. and MacCraith, B. D. Dissolved oxygen sensor based on fluorescence quenching of oxygen-sensitive ruthenium complexes immobilized in sol-gel-derived porous silica coatings. *Analyst*, 1996, **121**(6), 785-788.
 20. Amao, Y., Asai, K., Miyashita, T. and Okura, I. Novel optical oxygen sensing material: Platinum porphyrin-fluoropolymer film. *Polymers for Advanced Technologies*, 2000, **11**(8-12), 705-709.
 21. Vasil'ev, V. V. and Borisov, S. M. Optical oxygen sensors based on

- phosphorescent water-soluble platinum metals porphyrins immobilized in perfluorinated ion-exchange membrane. *Sensors and Actuators B-Chemical*, 2002, **82**(2-3), 272-276.
22. Tang, Y., Tehan, E. C., Tao, Z. Y. and Bright, F. V. Sol-gel-derived sensor materials that yield linear calibration plots, high sensitivity, and long-term stability. *Analytical Chemistry*, 2003, **75**(10), 2407-2413.
23. Koo, Y. E. L., Cao, Y. F., Kopelman, R., Koo, S. M., Brasuel, M. and Philbert, M. A. Real-time measurements of dissolved oxygen inside live cells by organically modified silicate fluorescent nanosensors. *Analytical Chemistry*, 2004, **76**(9), 2498-2505.
24. Bukowski, R. M., Ciriminna, R., Pagliaro, M. and Bright, F. V. High-performance quenchometric oxygen sensors based on fluorinated xerogels doped with $[\text{Ru}(\text{dpp})_3]^{2+}$. *Analytical Chemistry*, 2005, **77**(8), 2670-2672.
25. Stern, O. and Volmer, M. Uber die abklingungszeit der fluoreszenz. *Physikalische Zeitschrift*, 1919, **20**, 183-188.
26. Kautsky, H., Hirsch, A. and Davidshofer, F. Energie-umwandlungen an grenzflachen. *Berichte Deutsche Chemische Gesellschaft*, 1932, **65**, 1762-1770.

27. Kautsky, H. Quenching of luminescence by oxygen. *Transactions of the Faraday Society*, 1939, **35**, 216-219.
28. Vaugham, W. M. and Weber, G. Oxygen quenching of pyrenebutyric acid fluorescence in water . A dynamic probe of microenvironment. *Biochemistry*, 1970, **9**(3), 464-473.
29. Wolfbeis, O. S., Posch, H. E. and Kroneis, H. W. Fiber optical fluorosensor for determination of halothane and/or oxygen. *Analytical Chemistry*, 1985, **57**(13), 2556-2561.
30. Lee, E. D., Werner, T. C. and Seitz, W. R. Luminescence ratio indicators for oxygen. *Analytical Chemistry*, 1987, **59**(2), 279-283.
31. Wolfbeis, O. S., Fiber optical fluorosensors in analytical and clinical chemistry, in *Molecular luminescence spectroscopy. Methods and applications: Part 2*, Schulman, S. G., ed. New York:John Wiley & Sons, Inc., 1988
32. Diaz Garcia, M. E., Pereirogarcia, R. and Velascogarcia, N. Optical oxygen sensing materials based on the room-temperature phosphorescence intensity quenching of immobilized Erythrosin-B. *Analyst*, 1995, **120**(2), 457-461.
33. Gouterman, M. Oxygen quenching of luminescence of pressure sensitive paint for wind tunnel research. *Journal of Chemical Education*, 1997, **74**(6),

697-702.

34. Demas, J. N. and DeGraff, B. A. Applications of luminescent transition metal complexes to sensor technology and molecular probes. *Journal of Chemical Education*, 1997, **74**(6), 690-695.
35. Peterson, J. R. and Kalyanasundaram, K. Energy-transfer and electron-transfer processes of the lowest triplet excited-state of tetrakis(diphosphito)diplatinate(II). *Journal of Physical Chemistry*, 1985, **89**(12), 2486-2492.
36. Li, X. M. and Wong, K. Y. Luminescent platinum complex in solid films for optical sensing of oxygen. *Analytica Chimica Acta*, 1992, **262**(1), 27-32.
37. Lee, W. S., Wong, K. Y. and Li, X. M. Luminescent dicyanoplatinum(II) complexes as sensors for the optical measurement of oxygen concentrations. *Analytical Chemistry*, 1993, **65**(3), 255-258.
38. Rumsey, W. L., Vanderkooi, J. M. and Wilson, D. F. Imaging of phosphorescence - a novel method for measuring oxygen distribution in perfused tissue. *Science*, 1988, **241**(4873), 1649-1651.
39. Kavandi, J., Callis, J., Gouterman, M., Khalil, G., Wright, D., Green, E., Burns, D. and Mclachlan, B. Luminescent barometry in wind tunnels. *Review of Scientific Instruments*, 1990, **61**(11), 3340-3347.

40. Papkovskii, D. B., Yaropolov, A. I., Savitskii, A. P., Olah, J., Rumyantseva, V. D., Mironov, A. F., Troyanovsky, I. V. and Sadovsky, N. A. Fibre-optic oxygen sensor based on phosphorescence quenching. *Biomedical Science*, 1991, **2**, 536-539.
41. Papkovsky, D. B., Olah, J., Troyanovsky, I. V., Sadovsky, N. A., Rumyantseva, V. D., Mironov, A. F., Yaropolov, A. I. and Savitsky, A. P. Phosphorescent polymer films for optical oxygen sensors. *Biosensors & Bioelectronics*, 1992, **7**(3), 199-206.
42. Papkovsky, D. B. Luminescent porphyrins as probes for optical (bio)sensors. *Sensors and Actuators B-Chemical*, 1993, **11**(1-3), 293-300.
43. Lee, W. W. S., Wong, K. Y., Li, X. M., Leung, Y. B., Chan, C. S. and Chan, K. S. Halogenated platinum porphyrins as sensing materials for luminescence-based oxygen sensors. *Journal of Materials Chemistry*, 1993, **3**(10), 1031-1035.
44. Papkovsky, D. B. New oxygen sensors and their application to biosensing. *Sensors and Actuators B-Chemical*, 1995, **29**(1-3), 213-218.
45. Hartmann, P. and Trettnak, W. Effects of polymer matrices on calibration functions of luminescent oxygen sensors based on porphyrin ketone complexes. *Analytical Chemistry*, 1996, **68**(15), 2615-2620.

46. Lee, S. K. and Okura, I. Porphyrin-doped sol-gel glass as a probe for oxygen sensing. *Analytica Chimica Acta*, 1997, **342**(2-3), 181-188.
47. Mills, A. and Lepre, A. Controlling the response characteristics of luminescent porphyrin plastic film sensors for oxygen. *Analytical Chemistry*, 1997, **69**(22), 4653-4659.
48. Papkovsky, D. B., O'Riordan, T. and Soini, A. Phosphorescent porphyrin probes in biosensors and sensitive bioassays. *Biochemical Society Transactions*, 2000, **28**, 74-77.
49. Tsukada, K., Sakai, S., Hase, K. and Minamitani, H. Development of catheter-type optical oxygen sensor and applications to bioinstrumentation. *Biosensors & Bioelectronics*, 2003, **18**(12), 1439-1445.
50. Khalil, G. E., Gounterman, M. P. and Green, E., Method of measuring oxygen concentration, *U.S. Patent* 480655, 1989.
51. Demas, J. N. and Degraff, B. A. Design and applications of highly luminescent transition-metal complexes. *Analytical Chemistry*, 1991, **63**(17), A829-A837.
52. Wolfbeis, O. S., Leiner, M. J. P. and Posch, H. E. A new sensing material for optical oxygen measurement, with the indicator embedded in an aqueous phase. *Mikrochimica Acta*, 1986, **3**(5-6), 359-366.

53. Kaneko, M. and Hayakawa, S. Application of polymer-embedded tris(2,2'bipyridine)ruthenium(II) to photodetection of oxygen. *Journal of Macromolecular Science-Chemistry*, 1988, **A25**(10-11), 1255-1261.
54. Moreno Bondi, M. C., Wolfbeis, O. S., Leiner, M. J. P. and Schaffar, B. P. H. Oxygen optrode for use in a fiberoptic glucose biosensor. *Analytical Chemistry*, 1990, **62**(21), 2377-2380.
55. Carraway, E. R., Demas, J. N., Degraff, B. A. and Bacon, J. R. Photophysics and photochemistry of oxygen sensors based on luminescent transition-metal complexes. *Analytical Chemistry*, 1991, **63**(4), 337-342.
56. Carraway, E. R., Demas, J. N. and Degraff, B. A. Photophysics and oxygen quenching of transition-metal complexes on fumed silica. *Langmuir*, 1991, **7**(12), 2991-2998.
57. MacCraith, B. D., McDonagh, C. M., O'keefe, G., Keyes, E. T., Vos, J. G., O'Kelly, B. and McGilp, J. F. Fiber optic sensor based on fluorescence quenching of evanescent-wave excited ruthenium complexes in sol-gel derived porous coatings. *Analyst*, 1993, **118**(4), 385-388.
58. Sacksteder, L. A., Demas, J. N. and Degraff, B. A. Design of oxygen sensors based on quenching of luminescent metal complexes: Effect of ligand size on heterogeneity. *Analytical Chemistry*, 1993, **65**(23), 3480-3483.

59. Klimant, I., Belser, P. and Wolfbeis, O. S. Novel metal-organic ruthenium(II) diimine complexes for use as longwave excitable luminescent oxygen probes. *Talanta*, 1994, **41**(6), 985-991.
60. Li, X. M., Ruan, F. C., Ng, W. Y. and Wong, K. Y. Scanning optical sensor for the measurement of dissolved oxygen and BOD. *Sensors and Actuators B-Chemical*, 1994, **21**(2), 143-149.
61. MacCraith, B. D., O'Keeffe, G., McEvoy, A. K., McDonagh, C. M., McGilp, J. F., OKelly, B., Omahony, J. D. and Cavanagh, M. Light-emitting-diode based oxygen sensing using evanescent-wave excitation of a dye-doped sol-gel coating. *Optical Engineering*, 1994, **33**(12), 3861-3866.
62. MacCraith, B. D., Okeeffe, G., McDonagh, C. and McEvoy, A. K. LED-based fiber optic oxygen sensor using sol-gel coating. *Electronics Letters*, 1994, **30**(11), 888-889.
63. McMurray, H. N., Douglas, P., Busa, C. and Garley, M. S. Oxygen quenching of tris(2,2'-bipyridine) ruthenium(II) complexes in thin organic films. *Journal of Photochemistry and Photobiology A-Chemistry*, 1994, **80**(1-3), 283-288.
64. Xu, W. Y., Mcdonough, R. C., Langsdorf, B., Demas, J. N. and Degraff, B. A. Oxygen sensors based on luminescence quenching - interactions of metal-complexes with the polymer supports. *Analytical Chemistry*, 1994,

- 66**(23), 4133-4141.
65. Draxler, S., Lippitsch, M. E., Klimant, I., Kraus, H. and Wolfbeis, O. S. Effects of polymer matrices on the time-resolved luminescence of a ruthenium complex quenched by oxygen. *Journal of Physical Chemistry*, 1995, **99**(10), 3162-3167.
66. Hartmann, P., Leiner, M. J. P. and Lippitsch, M. E. Luminescence quenching behavior of an oxygen sensor-based on a Ru(II) complex dissolved in polystyrene. *Analytical Chemistry*, 1995, **67**(1), 88-93.
67. Klimant, I. and Wolfbeis, O. S. Oxygen-sensitive luminescent materials based on silicone-soluble ruthenium diimine complexes. *Analytical Chemistry*, 1995, **67**(18), 3160-3166.
68. Meier, B., Werner, T., Klimant, I. and Wolfbeis, O. S. Novel oxygen sensor material based on a ruthenium bipyridyl complex encapsulated in zeolite-Y-dramatic differences in the efficiency of luminescence quenching by oxygen on going, from surface-adsorbed to zeolite-encapsulated fluorophores. *Sensors and Actuators B-Chemical*, 1995, **29**(1-3), 240-245.
69. O'Keeffe, G., MacCraith, B. D., McEvoy, A. K., McDonagh, C. M. and McGilp, J. F. Development of a led-based phase fluorometric oxygen sensor using evanescent-wave excitation of a sol-gel immobilized dye. *Sensors and*

- Actuators B-Chemical*, 1995, **29**(1-3), 226-230.
70. Wolfbeis, O. S. and Kilmant, I. Oxygen-sensitive luminescent materials based on silicone - soluble ruthenium diimine complexes. *Analytical Chemistry*, 1995, **67**(18), 3160 - 3166.
71. Zemskii, V. I., Kolesnikov, Y. L. and Veresov, A. V. The study of luminescence characteristics of Ru complexes immobilized on porous glass. *Proceedings of SPIE - The International Society for Optical Engineering*, 1995, **2388**, 423-428.
72. Kneas, K. A., Xu, W. Y., Demas, J. N. and DeGraff, B. A. Oxygen sensors based on luminescence quenching: Interactions of tris(4,7-diphenyl-1,10-phenanthroline)ruthenium(II) chloride and pyrene with polymer supports. *Applied Spectroscopy*, 1997, **51**(9), 1346-1351.
73. Mongey, K. F., Vos, J. G., MacCraith, B. D., McDonagh, C. M., Coates, C. and McGarvey, J. J. Photophysics of mixed-ligand polypyridyl ruthenium(II) complexes immobilised in silica sol-gel monoliths. *Journal of Materials Chemistry*, 1997, **7**(8), 1473-1479.
74. Mongey, K., Vos, J. G., MacCraith, B. D. and McDonagh, C. M. The photophysical properties of ruthenium polypyridyl complexes within a sol-gel matrix. *Journal of Sol-Gel Science and Technology*, 1997, **8**(1-3), 979-983.

75. Murtagh, M. T., Shahriari, M. R. and Krihak, M. A study of the effects of organic modification and processing technique on the luminescence quenching behavior of sol-gel oxygen sensors based on a Ru(II) complex. *Chemistry of Materials*, 1998, **10**(12), 3862-3869.
76. Chan, C. M., Chan, M. Y., Zhang, M., Lo, W. and Wong, K. Y. The performance of oxygen sensing films with ruthenium-adsorbed fumed silica dispersed in silicone rubber. *Analyst*, 1999, **124**(5), 691-694.
77. Chan, C. M., Lo, W. H., Wong, K. Y. and Chung, W. F. Monitoring the toxicity of phenolic chemicals to activated sludge using a novel optical scanning respirometer. *Chemosphere*, 1999, **39**(9), 1421-1432.
78. Choi, M. M. F. and Xiao, D. Oxygen-sensitive reverse-phase optode membrane using silica gel-adsorbed ruthenium(II) complex embedded in gelatin film. *Analytica Chimica Acta*, 1999, **387**(2), 197-205.
79. Choi, M. M. F. and Xiao, D. Linear calibration function of luminescence quenching-based optical sensor for trace oxygen analysis. *Analyst*, 1999, **124**(5), 695-698.
80. Garcia-Fresnadillo, D., Marazuela, M. D., Moreno-Bondi, M. C. and Orellana, G. Luminescent nafion membranes dyed with ruthenium(II) complexes as sensing materials for dissolved oxygen. *Langmuir*, 1999, **15**(19), 6451-6459.

81. Maruszewski, K., Jasiorski, M., Salamon, M. and Streck, W. Physicochemical properties of $[\text{Ru}(\text{bpy})_3]^{2+}$ entrapped in silicate bulks and fiber thin films prepared by the sol-gel method. *Chemical Physics Letters*, 1999, **314**(1-2), 83-90.
82. Klimant, I., Ruckruh, F., Liebsch, G., Stangelmayer, C. and Wolfbeis, O. S. Fast response oxygen micro-optodes based on novel soluble ormosil glasses. *Mikrochimica Acta*, 1999, **131**(1-2), 35-46.
83. Baker, G. A., Wenner, B. R., Watkins, A. N. and Bright, F. V. Effects of processing temperature on the oxygen quenching behavior of tris(4,7'-diphenyl-1,10'-phenanthroline)ruthenium(II) sequestered within sol-gel-derived xerogel films. *Journal of Sol-Gel Science and Technology*, 2000, **17**(1), 71-82.
84. Ahmad, M., Mohammad, N. and Abdullah, J. Sensing material for oxygen gas prepared by doping sol-gel film with tris(2,2-bipyridyl)dichlororuthenium complex. *Journal of Non-Crystalline Solids*, 2001, **290**(1), 86-91.
85. Cho, E. J. and Bright, F. V. Optical sensor array and integrated light source. *Analytical Chemistry*, 2001, **73**(14), 3289-3293.
86. McDonagh, C., Kolle, C., McEvoy, A. K., Dowling, D. L., Cafolla, A. A.,

- Cullen, S. J. and MacCraith, B. D. Phase fluorometric dissolved oxygen sensor. *Sensors and Actuators B-Chemical*, 2001, **74**(1-3), 124-130.
87. Lee, S. K., Shin, Y. B., Pyo, H. B. and Park, S. H. Highly sensitive optical oxygen sensing material: Thin silica xerogel doped with tris(4,7-diphenyl-1,10-phenanthroline)ruthenium. *Chemistry Letters*, 2001, (4), 310-311.
88. Chen, X., Zhong, Z. M., Li, Z., Jiang, Y. Q., Wang, X. R. and Wong, K. Y. Characterization of ormosil film for dissolved oxygen-sensing. *Sensors and Actuators B-Chemical*, 2002, **87**(2), 233-238.
89. Zhang, P., Guo, J. H., Wang, Y. and Pang, W. Q. Incorporation of luminescent tris(bipyridine)ruthenium(II) complex in mesoporous silica spheres and their spectroscopic and oxygen-sensing properties. *Materials Letters*, 2002, **53**(6), 400-405.
90. John, G. T., Klimant, I., Wittmann, C. and Heinzle, E. Integrated optical sensing of dissolved oxygen in microtiter plates: A novel tool for microbial cultivation. *Biotechnology and Bioengineering*, 2003, **81**(7), 829-836.
91. Amao, Y. and Okura, I. Optical oxygen sensing materials: Chemisorption film of ruthenium(II) polypyridyl complexes attached to anionic polymer. *Sensors and Actuators B-Chemical*, 2003, **88**(2), 162-167.

92. Chang-Yen, D. A. and Gale, B. K. An integrated optical oxygen sensor fabricated using rapid-prototyping techniques. *Lab on a Chip*, 2003, **3**(4), 297-301.
93. Jorge, P. A. S., Caldas, P., Rosa, C. C., Oliva, A. G. and Santos, J. L. Optical fiber probes for fluorescence based oxygen sensing. *Sensors and Actuators B-Chemical*, 2004, **103**(1-2), 290-299.
94. Garcia, E. A., Fernandez, R. G. and Diaz-Garcia, M. E. Tris(bipyridine)ruthenium(II) doped sol-gel materials for oxygen recognition in organic solvents. *Microporous and Mesoporous Materials*, 2005, **77**(2-3), 235-239.
95. Carraway, E. R., Demas, J. N. and Degraff, B. A. Luminescence quenching mechanism for microheterogeneous systems. *Analytical Chemistry*, 1991, **63**(4), 332-336.
96. Fuller, Z. J., Bare, W. D., Kneas, K. A., Xu, W. Y., Demas, J. N. and DeGraff, B. A. Photostability of luminescent ruthenium(II) complexes in polymers and in solution. *Analytical Chemistry*, 2003, **75**(11), 2670-2677.
97. Watkins, A. N., Wenner, B. R., Jordan, J. D., Xu, W. Y., Demas, J. N. and Bright, F. V. Portable, low-cost, solid-state luminescence-based O₂ sensor. *Applied Spectroscopy*, 1998, **52**(5), 750-754.

98. Zhao, Y. D., Richman, A., Storey, C., Radford, N. B. and Pantano, P. In situ fiber-optic oxygen consumption measurements from a working mouse heart. *Analytical Chemistry*, 1999, **71**(17), 3887-3893.
99. Xiao, D., Mo, Y. Y. and Choi, M. M. F. A hand-held optical sensor for dissolved oxygen measurement. *Measurement Science & Technology*, 2003, **14**(6), 862-867.
100. Brook, T. E. and Narayanaswamy, R. Polymeric films in optical gas sensors. *Sensors and Actuators B-Chemical*, 1998, **51**(1-3), 77-83.
101. Hartmann, P., Leiner, M. J. P. and Lippitsch, M. E. Response characteristics of luminescent oxygen sensors. *Sensors and Actuators B-Chemical*, 1995, **29**(1-3), 251-257.
102. Lee, S. K. and Okura, I. Photoluminescent determination of oxygen using metalloporphyrin-polymer sensing systems. *Spectrochimica Acta Part A-Molecular and Biomolecular Spectroscopy*, 1998, **54**(1), 91-100.
103. Amao, Y., Asai, K. and Okura, I. Fluorescence quenching oxygen sensor using an aluminum phthalocyanine-polystyrene film. *Analytica Chimica Acta*, 2000, **407**(1-2), 41-44.
104. Gewehr, P. M. and Delpy, D. T. Optical oxygen sensor based on phosphorescence lifetime quenching and employing a polymer immobilized

- metalloporphyrin probe. 2. Sensor membranes and results. *Medical & Biological Engineering & Computing*, 1993, **31**(1), 11-21.
105. Mills, A. and Thomas, M. Fluorescence-based thin plastic film ion-pair sensors for oxygen. *Analyst*, 1997, **122**(1), 63-68.
106. Mills, A. and Thomas, M. D. Effect of plasticizer viscosity on the sensitivity of an $[\text{Ru}(\text{bpy})_3]^{2+}(\text{Ph}_4\text{B}^-)_2$ -based optical oxygen sensor. *Analyst*, 1998, **123**(5), 1135-1140.
107. Amao, Y., Miyashita, T. and Okura, I. Optical oxygen detection based on luminescence change of metalloporphyrins immobilized in poly(isobutylmethacrylate-co-trifluoroethylmethacrylate) film. *Analytica Chimica Acta*, 2000, **421**(2), 167-174.
108. Amao, Y., Okura, I. and Miyashita, T. Thenoyltrifluoroacetate 1,10-phenanthroline europium(III) complex immobilized in fluoropolymer film as optical oxygen sensing material. *Chemistry Letters*, 2000, (8), 934-935.
109. Amao, Y., Ishikawa, Y. and Okura, I. Green luminescent iridium(III) complex immobilized in fluoropolymer film as optical oxygen-sensing material. *Analytica Chimica Acta*, 2001, **445**(2), 177-182.
110. Amao, Y., Miyashita, T. and Okura, I. Metalloporphyrins immobilized in

- styrene-trifluoroethylmethacrylate copolymer film as an optical oxygen sensing probe. *Journal of Porphyrins and Phthalocyanines*, 2001, **5**(5), 433-438.
111. Amao, Y., Miyashita, T. and Okura, I. Novel optical oxygen sensing material: Platinum octaethylporphyrin immobilized in a copolymer film of isobutyl methacrylate and tetrafluoropropyl methacrylate. *Reactive & Functional Polymers*, 2001, **47**(1), 49-54.
112. Gillanders, R. N., Tedford, M. C., Crilly, P. J. and Bailey, R. T. A composite thin film optical sensor for dissolved oxygen in contaminated aqueous environments. *Analytica Chimica Acta*, 2005, **545**(2), 189-194.
113. McEvoy, A. K., McDonagh, C. and MacCraith, B. D. Optimisation of sol-gel-derived silica films for optical oxygen sensing. *Journal of Sol-Gel Science and Technology*, 1997, **8**(1-3), 1121-1125.
114. Lee, S. K. and Okura, I. Optical sensor for oxygen using a porphyrin-doped sol-gel glass. *Analyst*, 1997, **122**(1), 81-84.
115. Costa-Fernandez, J. M., Diaz-Garcia, M. E. and Sanz-Medel, A. Sol-gel immobilized room-temperature phosphorescent metal-chelate as luminescent oxygen sensing material. *Analytica Chimica Acta*, 1998, **360**(1-3), 17-26.
116. McDonagh, C., MacCraith, B. D. and McEvoy, A. K. Tailoring of sol-gel

- films for optical sensing of oxygen in gas and aqueous phase. *Analytical Chemistry*, 1998, **70**(1), 45-50.
117. Murtagh, M. T., Kwon, H. C., Shahriari, M. R., Krihak, M. and Ackley, D. E. Luminescence probing of various sol-gel hosts with a Ru(II) complex and the practical ramifications for oxygen-sensing applications. *Journal of Materials Research*, 1998, **13**(11), 3326-3331.
118. McCulloch, S. and Uttamchandani, D. Fibre optic micro-optrode for dissolved oxygen measurements. *IEE Proceedings-Science Measurement and Technology*, 1999, **146**(3), 123-127.
119. Wolfbeis, O. S., Oehme, I., Papkovskaya, N. and Klimant, I. Sol-gel based glucose biosensors employing optical oxygen transducers, and a method for compensating for variable oxygen background. *Biosensors & Bioelectronics*, 2000, **15**(1-2), 69-76.
120. Diaz-Garcia, J., Costa-Fernandez, J. M., Bordel-Garcia, N. and Sanz-Medel, A. Room-temperature phosphorescence fiber-optic instrumentation for simultaneous multiposition analysis of dissolved oxygen. *Analytica Chimica Acta*, 2001, **429**(1), 55-64.
121. Xu, H., Aylott, J. W., Kopelman, R., Miller, T. J. and Philbert, M. A. A real-time ratiometric method for the determination of molecular oxygen

- inside living cells using sol-gel-based spherical optical nanosensors with applications to rat C6 glioma. *Analytical Chemistry*, 2001, **73**(17), 4124-4133.
122. McDonagh, C., Bowe, P., Mongey, K. and MacCraith, B. D. Characterisation of porosity and sensor response times of sol-gel-derived thin films for oxygen sensor applications. *Journal of Non-Crystalline Solids*, 2002, **306**(2), 138-148.
123. Lev, O., Tsionsky, M., Rabinovich, L., Glezer, V., Sampath, S., Pankratov, I. and Gun, J. Organically modified sol-gel sensors. *Analytical Chemistry*, 1995, **67**(1), A22-A30.
124. Ingersoll, C. M. and Bright, F. V. Using sol-gel-based platforms for chemical sensors. *Chemtech*, 1997, **27**(1), 26-31.
125. Lechna, M., Holowacz, I., Ulatowska, A. and Podbielska, H. Optical properties of sol-gel coatings for fiberoptic sensors. *Surface & Coatings Technology*, 2002, **151**, 299-302.
126. Collinson, M. M. Recent trends in analytical applications of organically modified silicate materials. *Trac-Trends in Analytical Chemistry*, 2002, **21**(1), 30-38.
127. Vorotilov, K. A., Vasiljev, V. A., Sobolevsky, M. V. and Sigov, A. S. Thin

- ORMOSIL films with different organics. *Journal of Sol-Gel Science and Technology*, 1998, **13**, 467-472.
128. Yang, L., Saavedra, S. S. and Armstrong, N. R. Sol-gel-based, planar waveguide sensor for gaseous iodine. *Analytical Chemistry*, 1996, **68**(11), 1834-1841.
129. Lavin, P., McDonagh, C. M. and MacCraith, B. D. Optimization of ormosil films for optical sensor applications. *Journal of Sol-Gel Science and Technology*, 1998, **13**(1-3), 641-645.
130. Butler, T. M., MacCraith, B. D. and McDonagh, C. Leaching in sol-gel-derived silica films for optical pH sensing. *Journal of Non-Crystalline Solids*, 1998, **224**(3), 249-258.
131. Lobnik, A. and Wolfbeis, O. S. Polarity studies on ormosils using a solvatochromic fluorescent probe. *Analyst*, 1998, **123**(11), 2247-2250.
132. Makote, R. and Collinson, M. M. Template recognition in inorganic-organic hybrid films prepared by the sol-gel process. *Chemistry of Materials*, 1998, **10**(9), 2440-2445.
133. Makote, R. and Collinson, M. M. Dopamine recognition in templated silicate films. *Chemical Communications*, 1998, (3), 425-426.
134. Makote, R. and Collinson, M. M. Organically modified silicate films for

- stable pH sensors. *Analytica Chimica Acta*, 1999, **394**(2-3), 195-200.
135. Wei, H. J. and Collinson, M. M. Functional-group effects on the ion-exchange properties of organically modified silicates. *Analytica Chimica Acta*, 1999, **397**(1-3), 113-121.
136. Kimura, K., Yajima, S., Okamoto, K. and Yokoyama, M. Supported sol-gel-derived membranes for neutral carrier-type ion-selective electrodes. *Journal of Materials Chemistry*, 2000, **10**(8), 1819-1824.
137. Kimura, K., Yajima, S., Takase, H., Yokoyama, M. and Sakurai, Y. Sol-gel modification of pH electrode glass membranes for sensing anions and metal ions. *Analytical Chemistry*, 2001, **73**(7), 1605-1609.
138. Avnir, D. Organic-chemistry within ceramic matrices-doped sol-gel materials. *Accounts of Chemical Research*, 1995, **28**(8), 328-334.
139. Collinson, M. M. and Howells, A. R. Sol-gels and electrochemistry: Research at the intersection. *Analytical Chemistry*, 2000, **72**(21), 702a-709a.
140. Liu, H. Y., Switalski, S. C., Coltrain, B. K. and Merkel, P. B. Oxygen permeability of sol-gel coatings. *Applied Spectroscopy*, 1992, **46**(8), 1266-1272.
141. Chung, K. E., Lan, E. H., Davidson, M. S., Dunn, B. S., Valentine, J. S. and Zink, J. I. Measurement of dissolved-oxygen in water using

- glass-encapsulated myoglobin. *Analytical Chemistry*, 1995, **67**(9), 1505-1509.
142. MacCraith, B. D., McDonagh, C. M., O'Keeffe, G., McEvoy, A. K., Butler, T. and Sheridan, F. R. Sol-gel coatings for optical chemical sensors and biosensors. *Sensors and Actuators B-Chemical*, 1995, **29**(1-3), 51-57.
143. Ma, Y. G., Cheung, T. C., Che, C. M. and Shen, J. C. New sol-gel oxygen sensor based on luminescence cyclometallated platinum complexes. *Thin Solid Films*, 1998, **333**(1-2), 224-227.
144. Malins, C., Fanni, S., Glever, H. G., Vos, J. G. and MacCraith, B. D. The preparation of a sol-gel glass oxygen sensor incorporating a covalently bound fluorescent dye. *Analytical Communications*, 1999, **36**(1), 3-4.
145. Chan, M. A., Lawless, J. L., Lam, S. K. and Lo, D. Fiber optic oxygen sensor based on phosphorescence quenching of erythrosin B trapped in silica-gel glasses. *Analytica Chimica Acta*, 2000, **408**(1-2), 33-37.
146. Lam, S. K., Chan, M. A. and Lo, D. Characterization of phosphorescence oxygen sensor based on erythrosin B in sol-gel silica in wide pressure and temperature ranges. *Sensors and Actuators B-Chemical*, 2001, **73**(2-3), 135-141.
147. Blair, S., Katakya, R. and Parker, D. Sol gel-immobilised terbium complexes

- for luminescent sensing of dissolved oxygen by analysis of emission decay. *New Journal of Chemistry*, 2002, **26**(5), 530-535.
148. Chen, X., Li, Z., Jiang, Y. Q., Zhong, Z. M., Wang, X. R. and Wong, K. Y. Oxygen sensing film based on organically modified sol-gel with ruthenium complexes and their fluorescent spectra studies. *Spectroscopy and Spectral Analysis*, 2002, **22**(5), 796-799.
149. Bailey, R. T., Cruickshank, F. R., Deans, G., Gillanders, R. N. and Tedford, M. C. Characterization of a fluorescent sol-gel encapsulated erythrosin B dissolved oxygen sensor. *Analytica Chimica Acta*, 2003, **487**(1), 101-108.
150. Holthoff, W. G., Tehan, E. C., Bukowski, R. M., Kent, N., MacCraith, B. D. and Bright, F. V. Radioluminescent light source for the development of optical sensor arrays. *Analytical Chemistry*, 2005, **77**(2), 718-723.
151. Demas, J. N., Degraff, B. A. and Xu, W. Y. Modeling of luminescence quenching-based sensors - comparison of multisite and nonlinear gas solubility models. *Analytical Chemistry*, 1995, **67**(8), 1377-1380.
152. McDonagh, C. M., Shields, A. M., McEvoy, A. K., MacCraith, B. D. and Gouin, J. F. Optical sol-gel-based dissolved oxygen sensor: Progress towards a commercial instrument. *Journal of Sol-Gel Science and Technology*, 1998, **13**(1-3), 207-211.

153. Mongey, K. F., Vos, J. G., MacCraith, B. D. and McDonagh, C. M. The photophysical properties of monomeric and dimeric ruthenium polypyridyl complexes immobilized in sol-gel matrices. *Coordination Chemistry Reviews*, 1999, **186**, 417-429.
154. Lakowicz, J. R., Gryczynski, I. and Gryczynski, Z. Novel fluorescence sensing methods for high throughput screening. *Journal of Biomolecular Screening*, 2000, **5**(3), 123-131.
155. Wodnicka, M., Guarino, R. D., Hemperly, J. J., Timmins, M. R., Stitt, D. and Pitner, J. B. Novel fluorescent technology platform for high throughput cytotoxicity and proliferation assays. *Journal of Biomolecular Screening*, 2000, **5**(3), 141-152.
156. Pitner, J. B., Hemperly, J. J., Guarino, R. D., Wodnicka, M., Stitt, D. T., Burrell, G. J., Foley, T. G. J. and Beaty, P. S., Device for monitoring cells, *U.S. Patent* 6395506, 2002.
157. Liebsch, G., Klimant, I., Frank, B., Holst, G. and Wolfbeis, O. S. Luminescence lifetime imaging of oxygen, pH, and carbon dioxide distribution using optical sensors. *Applied Spectroscopy*, 2000, **54**(4), 548-559.
158. Papkovsky, D. B. Respirometric screening technology (RST). *Screening -*

Trends in Drug Discovery, 2005, **6**, 46-47.

159. Rosenzweig, Z. and Kopelman, R. Analytical properties and sensor size effects of a micrometer-sized optical fiber glucose biosensor. *Analytical Chemistry*, 1996, **68**(8), 1408-1413.
160. Rosenzweig, Z. and Kopelman, R. Analytical properties of miniaturized oxygen and glucose fiber optic sensors. *Sensors and Actuators B-Chemical*, 1996, **36**(1-3), 475-483.
161. Li, L. and Walt, D. R. Dual-analyte fiberoptic sensor for the simultaneous and continuous measurement of glucose and oxygen. *Analytical Chemistry*, 1995, **67**(20), 3746-3752.
162. Ovchinnikov, A. N., Ogurtsov, V. I., Trettnak, W. and Papkovsky, D. B. Enzymatic flow-injection analysis of metabolites using new type of oxygen sensor membranes and phosphorescence phase measurements. *Analytical Letters*, 1999, **32**(4), 701-716.
163. Wang, W. J., Upshaw, L., Strong, D. M., Robertson, R. P. and Reems, J. A. Increased oxygen consumption rates in response to high glucose detected by a novel oxygen biosensor system in non-human primate and human islets. *Journal of Endocrinology*, 2005, **185**(3), 445-455.
164. Nomura, Y., Chee, G. J. and Karube, I. Biosensor technology for

- determination of BOD. *Field Analytical Chemistry and Technology*, 1998, **2**(6), 333-340.
165. APHA, AWWA and WEF, *Standard methods for the examination of water and wastewater, 19th ed.*, Washington, DC: American Public Health Association, 1995.
166. Kwok, N. Y., Dong, S., Lo, W. and Wong, K. Y. An optical biosensor for multi-sample determination of biochemical oxygen demand (BOD). *Sensors and Actuators B-Chemical*, 2005, **110**(2), 289-298.
167. Preininger, C., Klimant, I. and Wolfbeis, O. S. Optical fiber sensor for biological oxygen demand. *Analytical Chemistry*, 1994, **66**(11), 1841-1846.
168. Chee, G. J., Nomura, Y., Ikebukuro, K. and Karube, I. Optical fiber biosensor for the determination of low biochemical oxygen demand. *Biosensors & Bioelectronics*, 2000, **15**(7-8), 371-376.
169. Dai, Y. J., Lin, L., Li, P. W., Chen, X., Wang, X. R. and Wong, K. Y. Comparison of BOD optical fiber biosensors based on different microorganisms immobilized in ormosil matrixes. *International Journal of Environmental Analytical Chemistry*, 2004, **84**(8), 607-617.
170. Stitt, D. T., Nagar, M. S., Haq, T. A. and Timmins, M. R. Determination of growth rate of microorganisms in broth from oxygen-sensitive fluorescence

- plate reader measurements. *Biotechniques*, 2002, **32**(3), 684-689.
171. Guarino, R. D., Dike, L. E., Haq, T. A., Rowley, J. A., Pitner, J. B. and Timmins, M. R. Method for determining oxygen consumption rates of static cultures from microplate measurements of pericellular dissolved oxygen concentration. *Biotechnology and Bioengineering*, 2004, **86**(7), 775-787.
172. Hutter, B. and John, G. T. Evaluation of OxoPlate for real-time assessment of antibacterial activities. *Current Microbiology*, 2004, **48**(1), 57-61.
173. Wittmann, C., Kim, H. M. and Heinzle, E. Metabolic network analysis of lysine producing corynebacterium glutamicum at a miniaturized scale. *Biotechnology and Bioengineering*, 2004, **87**(1), 1-6.
174. Deshpande, R. R. and Heinzle, E. On-line oxygen uptake rate and culture viability measurement of animal cell culture using microplates with integrated oxygen sensors. *Biotechnology Letters*, 2004, **26**(9), 763-767.
175. Deshpande, R. R., Wittmann, C. and Heinzle, E. Microplates with integrated oxygen sensing for medium optimization in animal cell culture. *Cytotechnology*, 2004, **46**(1), 1-8.
176. Deshpande, R. R., Koch-Kirsch, Y., Maas, R., John, G. T., Krause, C. and Heinzle, E. Microplates with integrated oxygen sensors for kinetic cell respiration measurement and cytotoxicity testing in primary and secondary

- cell lines. *Assay and Drug Development Technologies*, 2005, **3**(3), 299-307.
177. O'Riordan, T. C., Buckley, D., Ogurtsov, V., O'Connor, R. and Papkovsky, D. B. A cell viability assay based on monitoring respiration by optical oxygen sensing. *Analytical Biochemistry*, 2000, **278**(2), 221-227.
178. Hynes, J., Floyd, S., Soini, A. E., O'Connor, R. and Papkovsky, D. B. Fluorescence-based cell viability screening assays using water-soluble oxygen probes. *Journal of Biomolecular Screening*, 2003, **8**(3), 264-272.
179. Feizi, T., Fazio, F., Chai, W. C. and Wong, C. H. Carbohydrate microarrays - a new set of technologies at the frontiers of glycomics. *Current Opinion in Structural Biology*, 2003, **13**(5), 637-645.
180. Schena, M., Shalon, D., Davis, R. W. and Brown, P. O. Quantitative monitoring of gene-expression patterns with a complementary-DNA microarray. *Science*, 1995, **270**(5235), 467-470.
181. Mitchell, P. A perspective on protein microarrays. *Nature Biotechnology*, 2002, **20**(3), 225-229.
182. Kocourek, J. and Horejsi, V. Defining a lectin. *Nature*, 1981, **290**(5803), 188-188.
183. Sharon, N. and Lis, H., *Lectins, 2nd ed.*, Dordrecht: Kluwer Academic Publishers, 2003.

184. Sharon, N. and Lis, H. Lectins: Cell-agglutinating and sugar-specific proteins. *Science*, 1972, **177**(4053), 949-959.
185. Kocourek, J., Historical background, in *The lectins: Properties, functions and applications in biology and medicine*, Liener, I. E., Sharon, N. and Glodstein, I. J., ed. New York:Academic Press, pp. 1-32, 1986
186. Jelinek, R. and Kolusheva, S. Carbohydrate biosensors. *Chemical Reviews*, 2004, **104**(12), 5987-6015.
187. Lis, H. and Sharon, N. Lectin-carbohydrate interactions. *Current Opinion in Structural Biology*, 1991, **1**(5), 741-749.
188. Osborn, H. M. I., Evans, P. G., Gemmell, N. and Osborne, S. D. Carbohydrate-based therapeutics. *Journal of Pharmacy and Pharmacology*, 2004, **56**(6), 691-702.
189. Sharon, N. Carbohydrate-lectin interactions in infectious disease. *Advances in Experimental Medicine and Biology*, 1996, **408**(Toward Anti-Adhesion Therapy for Microbial Diseases), 1-8.
190. Sharon, N. and Lis, H. Lectins as cell recognition molecules. *Science*, 1989, **246**(4927), 227-234.
191. Bies, C., Lehr, C. M. and Woodley, J. F. Lectin-mediated drug targeting: History and applications. *Advanced Drug Delivery Reviews*, 2004, **56**(4),

425-435.

192. Gabor, F., Bogner, E., Weissenboeck, A. and Wirth, M. The lectin-cell interaction and its implications to intestinal lectin-mediated drug delivery. *Advanced Drug Delivery Reviews*, 2004, **56**(4), 459-480.
193. Borman, S. Carbohydrate advances. *Chemical & Engineering News*, 2005, **83**(32), 41-50.
194. Wang, D. N. Carbohydrate microarrays. *Proteomics*, 2003, **3**(11), 2167-2175.
195. Wang, D. N., Liu, S. Y., Trummer, B. J., Deng, C. and Wang, A. L. Carbohydrate microarrays for the recognition of cross-reactive molecular markers of microbes and host cells. *Nature Biotechnology*, 2002, **20**(3), 275-281.
196. Fukui, S., Feizi, T., Galustian, C., Lawson, A. M. and Chai, W. G. Oligosaccharide microarrays for high-throughput detection and specificity assignments of carbohydrate-protein interactions. *Nature Biotechnology*, 2002, **20**(10), 1011-1017.
197. Bryan, M. C., Plettenburg, O., Sears, P., Rabuka, D., Wacowich-Sgarbi, S. and Wong, C. H. Saccharide display on microtiter plates. *Chemistry & Biology*, 2002, **9**(6), 713-720.
198. Fazio, F., Bryan, M. C., Blixt, O., Paulson, J. C. and Wong, C. H. Synthesis of

- sugar arrays in microtiter plate. *Journal of the American Chemical Society*, 2002, **124**(48), 14397-14402.
199. Fazio, F., Bryan, M. C., Lee, H. K., Chang, A. and Wong, C. H. Assembly of sugars on polystyrene plates: A new facile microarray fabrication technique. *Tetrahedron Letters*, 2004, **45**(12), 2689-2692.
200. Langenhan, J. M. and Thorson, J. S. Recent carbohydrate-based chemoselective ligation applications. *Current Organic Synthesis*, 2005, **2**(1), 59-81.
201. Houseman, B. T. and Mrksich, M. Carbohydrate arrays for the evaluation of protein binding and enzymatic modification. *Chemistry & Biology*, 2002, **9**(4), 443-454.
202. Houseman, B. T., Gawalt, E. S. and Mrksich, M. Maleimide-functionalized self-assembled monolayers for the preparation of peptide and carbohydrate biochips. *Langmuir*, 2003, **19**(5), 1522-1531.
203. Adams, E. W., Ratner, D. M., Bokesch, H. R., McMahon, J. B., O'Keefe, B. R. and Seeberger, P. H. Oligosaccharide and glycoprotein microarrays as tools in hiv glycobiology: Glycan-dependent gp120/protein interactions. *Chemistry & Biology*, 2004, **11**(6), 875-881.
204. Disney, M. D., Magnet, S., Blanchard, J. S. and Seeberger, P. H.

- Aminoglycoside microarrays to study antibiotic resistance. *Angewandte Chemie-International Edition*, 2004, **43**(12), 1591-1594.
205. Disney, M. D. and Seeberger, P. H. The use of carbohydrate microarrays to study carbohydrate-cell interactions and to detect pathogens. *Chemistry & Biology*, 2004, **11**(12), 1701-1707.
206. Ratner, D. M., Adams, E. W., Su, J., O'Keefe, B. R., Mrksich, M. and Seeberger, P. H. Probing protein-carbohydrate interactions with microarrays of synthetic oligosaccharides. *ChemBiochem*, 2004, **5**(3), 379-382.
207. Park, S. J. and Shin, I. J. Fabrication of carbohydrate chips for studying protein-carbohydrate interactions. *Angewandte Chemie-International Edition*, 2002, **41**(17), 3180-3182.
208. Park, S., Lee, M. R., Pyo, S. J. and Shin, I. Carbohydrate chips for studying high-throughput carbohydrate-protein interactions. *Journal of the American Chemical Society*, 2004, **126**(15), 4812-4819.
209. Bryan, M. C., Fazio, F., Lee, H. K., Huang, C. Y., Chang, A., Best, M. D., Calarese, D. A., Blixt, C., Paulson, J. C., Burton, D., Wilson, I. A. and Wong, C. H. Covalent display of oligosaccharide arrays in microtiter plates. *Journal of the American Chemical Society*, 2004, **126**(28), 8640-8641.
210. Demas, J. N., DeGraff, B. A. and Coleman, P. B. Oxygen sensors based on

- luminescence quenching. *Analytical Chemistry*, 1999, **71**(23), 793A-800A.
211. Papkovsky, D. B., Method in optical oxygen sensing: Protocols and critical analyses, in *Methods in enzymology*, Sen, C. K. and Semenza, G. L., ed. San Diego:Academic Press, pp. 715-735, 2004
212. Alderman, J., Hynes, J., Floyd, S. M., Kruger, J., O'Connor, R. and Papkovsky, D. B. A low-volume platform for cell-respirometric screening based on quenched-luminescence oxygen sensing. *Biosensors & Bioelectronics*, 2004, **19**(11), 1529-1535.
213. Douglas, P. and Eaton, K. Response characteristics of thin film oxygen sensors, Pt and Pd octaethylporphyrins in polymer films. *Sensors and Actuators B-Chemical*, 2002, **82**(2-3), 200-208.
214. Lin, C. T., Bottcher, W., Chou, M., Creutz, C. and Sutin, N. Mechanism of quenching of emission of substituted polypyridineruthenium(II) complexes by iron(III), chromium(III), and europium(III) ions. *Journal of the American Chemical Society*, 1976, **98**(21), 6536-6544.
215. Hermann, R., Walther, N., Maier, U. and Buchs, J. Optical method for the determination of the oxygen-transfer capacity of small bioreactors based on sulfite oxidation. *Biotechnology and Bioengineering*, 2001, **74**(5), 355-363.
216. Hermann, R., Lehmann, M. and Buchs, J. Characterization of gas-liquid mass

- transfer phenomena in microtiter plates. *Biotechnology and Bioengineering*, 2003, **81**(2), 178-186.
217. Winkler, L. W. The determination of dissolved oxygen in water. *Berlin Deutsch Chem Gellsch*, 1888, **21**, 2843-2854.
218. Bryans, T. R., Brawner, V. L. and Quitevis, E. L. Microstructure and porosity of silica xerogel monoliths prepared by the fast sol-gel method. *Journal of Sol-Gel Science and Technology*, 2000, **17**(3), 211-217.
219. Onyiriuka, E. C., Hersh, L. S. and Hertl, W. Solubilization of corona discharge-treated and plasma-treated polystyrene. *Journal of Colloid and Interface Science*, 1991, **144**(1), 98-102.
220. Dislich, H., Thin films from the sol-gel process, in *Sol-gel technology for thin films, fibers, preforms, electronics, and specialty shapes*, Klein, L. C., ed. Park Ridge:Noyes Publications, pp. 55, 1988
221. Lakowicz, J. R., *Principles of fluorescence spectroscopy, 2nd ed.*, New York: Kluwer Academic/Plenum, 1999.
222. Nau, M. E., Emerson, L. R., Martin, R. K., Kyle, D. E., Wirth, D. F. and Vahey, M. Technical assessment of the affymetrix yeast expression GeneChip YE6100 platform in a heterologous model of genes that confer resistance to antimalarial drugs in yeast. *Journal of Clinical Microbiology*, 2000, **38**(5),

1901-1908.

223. Qbiogene BIO 101[®] system.
<http://www.qbiogene.com/products/media/ymedia/YGM.shtml>
224. Peavy, H. S., Rowe, D. R. and Tchobanoglous, G., *Environmental engineering, ed.*, New York: McGraw-Hill, 1985.
225. Kwok, N. Y., *Development of high-throughput biosensors for multi-sample determination of biochemical oxygen demand (BOD) based on optical detection of oxygen*, Ph.D. Thesis, in Department of Applied Biology and Chemical Technology, The Hong Kong Polytechnic University, Hong Kong, 2005.
226. Karube, I., Matsunaga, T., Mitsuda, S. and Suzuki, S. Microbial electrode BOD sensors. *Biotechnology and Bioengineering*, 1977, **19**(10), 1535-1547.
227. Tan, T. C., Li, F., Neoh, K. G. and Lee, Y. K. Microbial membrane-modified dissolved-oxygen probe for rapid biochemical oxygen demand measurement. *Sensors and Actuators B-Chemical*, 1992, **8**(2), 167-172.
228. Hikuma, M., Suzuki, H., Yasuda, T., Karube, I. and Suzuki, S. Amperometric estimation of BOD by using living immobilized yeasts. *European Journal of Applied Microbiology and Biotechnology*, 1979, **8**(4), 289-297.
229. Karube, I., Mitsuda, S., Matsunaga, T. and Suzuki, S. Rapid method for

- estimation of BOD by using immobilized microbial cells. *Journal of Fermentation Technology*, 1977, **55**(3), 243-248.
230. Japanese Industrial Standard Committee (JIS), *Japanese industrial standard committee. Apparatus for the estimation of biochemical oxygen demand (BOD) with microbial sensor*, pp. JIS K 3602 Tokyo, 1990
231. Organization for Economic Cooperation and Development (OECD), Activated sludge, respiration inhibition test, in *OECD guideline for testing of chemicals*, 1981
232. Yoshida, N., McNiven, S. J., Yoshida, A., Morita, T., Nakamura, H. and Karube, I. A compact optical system for multi-determination of biochemical oxygen demand using disposable strips. *Field Analytical Chemistry and Technology*, 2001, **5**(5), 222-227.
233. Li, Y. R. and Chu, J. Study of BOD microbial sensors for waste-water treatment control. *Applied Biochemistry and Biotechnology*, 1991, **28/29**, 855-863.
234. Ohki, A., Shinohara, K., Ito, O., Naka, K., Maeda, S., Sato, T., Akano, H., Kato, N. and Kawamura, Y. A BOD sensor using *Klebsiella oxytoca* ASI. *International Journal of Environmental Analytical Chemistry*, 1994, **56**(4), 261-269.

235. Riedel, K., Renneberg, R., Kuhn, M. and Scheller, F. A fast estimation of biochemical oxygen demand using microbial sensors. *Applied Microbiological Biotechnology*, 1988, **28**(3), 316-318.
236. Karube, I., Yokoyama, K., Sode, K. and Tamiya, E. Microbial BOD sensor utilizing thermophilic bacteria. *Analytical Letters*, 1989, **22**(4), 791-801.
237. Galindo, E., Garcia, J. L., Torres, L. G. and Quintero, R. Characterization of microbial membranes used for the estimation of biochemical oxygen demand with a biosensor. *Biotechnology Techniques*, 1992, **6**(5), 399-404.
238. Tan, T. C. and Wu, C. H. BOD sensors using multi-species living or thermally killed cells of a BODSEED microbial culture. *Sensors and Actuators B-Chemical*, 1999, **54**(3), 252-260.
239. Li, F. and Tan, T. C. Effect of heavy metal ions on the efficacy of a mixed *bacilli* BOD sensor. *Biosensors & Bioelectronics*, 1994, **9**(4-5), 315-324.
240. Wong, K. Y., Zhang, M. Q., Li, X. M. and Lo, W. H. A luminescence-based scanning respirometer for heavy metal toxicity monitoring. *Biosensors & Bioelectronics*, 1997, **12**(2), 125-133.
241. Chee, G. J., Nomura, Y. and Karube, I. Biosensor for the estimation of low biochemical oxygen demand. *Analytica Chimica Acta*, 1999, **379**(1-2), 185-191.

242. Shin, I. J., Cho, J. W. and Boo, D. W. Carbohydrate arrays for functional studies of carbohydrates. *Combinatorial Chemistry & High Throughput Screening*, 2004, **7**(6), 565-574.
243. Lubineau, A., Auge, J. and Drouillat, B. Improved synthesis of glycosylamines and a straightforward preparation of N-acylglycosylamines as carbohydrate-based detergents. *Carbohydrate Research*, 1995, **266**(2), 211-219.
244. Wang, J. Y., Chen, W., Liu, A. H., Lu, G., Zhang, G., Zhang, J. H. and Yang, B. Controlled fabrication of cross-linked nanoparticles/polymer composite thin films through the combined use of surface-initiated atom transfer radical polymerization and gas/solid reaction. *Journal of the American Chemical Society*, 2002, **124**(45), 13358-13359.
245. Lobnik, A., Oehme, I., Murkovic, I. and Wolfbeis, O. S. pH optical sensors based on sol-gels: Chemical doping versus covalent immobilization. *Analytica Chimica Acta*, 1998, **367**(1-3), 159-165.
246. Savel'ev, Y. V., Khranovskii, V. A., Veselov, V. Y., Grekov, A. P. and Savel'eva, O. A. Specificity of the reaction of 1,1-dimethylhydrazine with phenyl isocyanate. *Russian Journal of Organic Chemistry*, 2003, **39**(1), 96-98.
247. Thomson, T., *Polyurethanes as specialty chemicals: Principles and*

applications, ed., Boca Raton, Fla.: CRC Press, 2005.

248. Goldstein, I. J. and Poretz, R. D., Isolation, physicochemical characterization, and carbohydrate-binding specificity of lectins, in *The lectins: Properties, functions, and applications in biology and medicine*, Liener, I. E., Sharon, N. and Goldstein, I. J., ed. Orlando:Academic Press, Inc., pp. 33-244, 1986
249. Lis, H. and Sharon, N. Lectins: Carbohydrate-specific proteins that mediate cellular recognition. *Chemical Reviews*, 1998, **98**(2), 637-674.